Bio-catalytic upgrading of phenolic components present in waste water of a hydrothermal liquefaction plant

E. Chimbazaza

orcid.org 0000-0002-9752-1237

Dissertation accepted in fulfilment of the requirements for the degree *Master of Engineering in Chemical Engineering* at the North-West University

Supervisor:	Prof. S. Marx
Co-supervisor:	Dr. R. van der Sluis
Graduation	August 2021
Student number	33479542

ACKNOWLEDGEMENTS

I would like to thank my supervisor, Prof. Sanette Marx, for being not only the study leader but a mother to me, with all her guidance and contributions throughout this study. I also want to express my sincere gratitude to my co-supervisor Dr. Rencia van der Sluis, Mr. Strauss van Graan and all the collegues in the Biochemistry molecular and mitochondria laboratories for their help throughout the research project. A special thanks to Dr. Roelf Venter and Miss Rene Bekker for all the help they provided each time I needed assistance, both with the experimental work and writing up during the study.

I am extremely grateful to my parents, Ester Musariri (mom), and brothers, Farai Maimba and wife, Takudzwa Maimba, Lewis Mutasa and wife, Hammond Motsi, for all their love, support and for always encouraging and believing in me throughout my studies. With great thanks to my school mates, Lungie, Clement, Yaneh, Jonedine and others for their help in the laboratory and on writing up my thesis. Also not forgetting my friends Thabile, Samuel, Simba, Victor, Ruda, Tarsy, Ushe, Patrick, Tatenda and others for their encouragements and advices. I would also want to thank all the staff from the department of Biochemistry for their assistance with laboratory equipment and access to the department at any given time. To the staff members from the School of Chemical and Minerals Engineering and the North-West University as a whole I really appreciate our time together. Lastly the National Research Foundation (NRF), for providing financial assistance.

ABSTRACT

Vanillyl alcohol oxidase is a flavoenzyme naturally sourced from *Penicillium simplicissimum*. It is a potential candidate in the commercial production of vanillin, an expensive natural flavourant in the cosmetic, food, beverages and pharmaceutical industries. During hydrothermal liquefaction of biomass, only the oil and the char phases are considered as essential while the aqueous phase is discarded. However, the aqueous phase is rich in phenolic compounds like guaiacol and vanillyl alcohol that can be upgraded to vanillin. A method channeled towards the production of vanillin from the phenolic components of the aqueous phase using vanillyl alcohol oxidase was investigated. The vanillyl alcohol oxidase enzyme was expressed in *Escherichia coli* BL21(DE3) bacteria cells and purified in order to characterize the production of vanillin from vanillyl alcohol. The expression and purification of the recombinant expressed vanillyl alcohol oxidase was preliminary detected by sodium dodecyl sulfate polyacrylamide gel electrophoresis (SDS-PAGE) and a band of 65 kDa was observed. The total yield of purified protein after purification from a 50 ml bacterial culture was 17.6 mg (w/v).

The effect of the aqueous phase components of HTL on the enzyme reaction was investigated. High Performance Liquid Chromatography (HPLC) analysis was done to detect the phenolic and sugar composition of the aqueous phase of biomass sourced from municipality sewage waste, then used as a reference in making the synthetic aqueous phase. Vanillic acid increased the reaction rate while guaiacol inhibited the reaction rate at 95% confidence. However, in the presence of acetic acid, there was a noticeable and statistically significant difference from 15 minutes onwards, where acetic acid containing reactions were slower than all the other reactions. Conclusively, active vanillyl alcohol oxidase can be expressed and purified using BL21(DE3) cells. The enzyme reaction is affected by other phenolic compounds in the hydrothermal liquefaction aqueous phase, but a component of the HTL, acetic acid can slow down the rate of this reaction with a greater margin.

Key terms: Vanillyl alcohol oxidase, vanillin, vanillyl alcohol, hydrothermal liquefaction, aqueous phase, phenolic compounds.

Table of Contents

List of figures

List of tables

List of Abbreviations

PCMH	p-Cresol methyl hydroxylase
Abs	Absorbance
Asp	Asparagine
Arg	Arginine
BLAST	Basic Local Alignment Search Tool algorithm
BCA	Bicinchoninic Acid Assay
BSA	Bovine Serum Albumin
DNA	Deoxyribonucleic acid
DTT	Dithiothreitol
EC	Enzyme Commission
FAD	Flavin Adenine Dinucleotide
GC-MS	Gas Chromatography Mass Spectrometry
His	Histidine
HPLC	High Performance Liquid Chromatography
HTL	Hydrothermal Liquefaction
Ile	Isoleucine
ICP	Inductively Coupled Plasma
LB	Lysogeny Broth
m-VA	meta Vanillyl Alcohol (3-Hydroxy-4-methoxybenzyl alcohol)
NCBI	National Center for Biotechnology Information

o-VA	ortho Vanillyl Alcohol (2-Hydroxy-3-methoxybenzyl alcohol)
OD	Optical Density
*Ps*VAO	*Penicillium simplicissimum* Vanillyl Alcohol Oxidase gene
p-VA	para Vanillyl Alcohol (4-Hydroxy-3-methoxybenzyl alcohol)
SDS-PAGE	Sodium Dodecyl Sulfate Polyacrylamide Gel Electrophoresis.
SOC	Super Optimal broth with Catabolites repression
Std	`Standard
Thr	Threonine
Tyr	Tyrosine
VAO	Vanillyl alcohol oxidase

List of symbols

°C	Degrees Celsius
α	alpha
β	beta
bp	base pair
CO_2	carbon dioxide
g	grams
H^+	hydronium ion; Proton
H_2	hydrogen
H_2O	water molecule
H_2S	hydrogen sulphide
IU	enzyme units
µg	microgram
µl	microliter
kDa	kilodaltons
mM	millimolar
rpm	revolutions per minute
xg	times gravity (a measure of relative centrifugal force)

CHAPTER ONE

INTRODUCTION

This chapter outlines the introduction and gives a brief overview of the topic, aim, and objectives of the study, and the thesis framework.

1.1. General introduction

The detrimental environmental effect of fossil fuel use in different industries can be minimized by replacing fossil fuel based products with renewable alternatives (Ratshomo & Nembahe, 2018). Renewable biomass is one such alternative sustainable source that can be used to replace many carbon-rich fossil fuel products (Handayani *et al.*, 2019). Although renewable, the effect of growing energy crops for biofuels and chemicals production has already been realized (Koçar & Civaş, 2013; Stafford *et al.*, 2019). Non-food and non-feed biomass resources, such as sewage sludge, waste lignin, algae and municipal solid waste are thus preferred to enable a sustainable industry (Anastasakis *et al.*, 2018; Chen *et al.*, 2020; Lin, Ma, *et al.*, 2017; Midgett & Theegala, 2007; Shamaei *et al.*, 2020; Theegala & Midgett, 2012; Wielligh *et al.*, 2018).

Vanillin is used in the pharmaceutical, food, beverage and fragrance industries. Natural vanillin is commercially produced from vanilla beans (Ramachandra Rao & Ravishankar, 2000). However, currently the available natural vanillin cannot meet the market demand due to limited confined areas worldwide that are suitable for the production of the beans (Arya, 2019). Artificial vanillin for the commercial market (Karakhanov *et al.*, 2010) are thus mostly synthesized from lignin (Evstigneyev & Shevchenko, 2020; Fache *et al.*, 2016a) and through the benzene, toluene and xylene (BTX) processing (Sweeney & Bryan, 2007) that uses hazardous fossil fuel–based chemicals (Zhao *et al.*, 2017). In the BTX process, benzene is used as starting material which is upgraded to phenol, guaiacol and finally vanillin using different chemical treatments and catalysts (Schmidt, 2005). Many processes have been developed from this route to try and maximize vanillin production at a lower cost.

Consumers still prefer natural flavors due to their health benefits i.e. helps to treat infection, antioxidant activity, antimicrobial activity, anti-inflammatory activity and anti-nociceptive effect as compared to synthetic vanillin (Bloom, 2017). The latter results in a large margin in price difference between natural and synthetic vanillin. Pathways to produce natural vanillin from biomass through

biochemical processes has thus become of interest to the research society (Luziatelli *et al.*, 2019) Biochemical conversion methods involve the use of enzymes and/or micro-organisms to produce vanillin from aromatic-rich biomass. Most biochemical approaches can use natural phenol from biomass feedstock (ETC Group, 2013; Goswami *et al.*, 2013; Huang *et al.*, 1993; Kaprasob *et al.*, 2017; Li *et al.*, 2019; Van Rooyen, 2012; Zamzuri & Abd-Aziz, 2012).

Several publications have reported on laboratory scale biochemical synthesis of vanillin from different phenolic building blocks (Havkin-Frenkel & Belanger, 2011). However, biochemical processes for vanillin synthesis have not yet received commercial or industrial acceptance because of several process limitations. Some of the limitations include, production of side products, microbial spoilage, very low yield and substrate and end-product inhibition of the enzymes (Converti *et al.*, 2010). These limitations need to be addressed for biochemical processes to be commercially accepted for vanillin production as an alternative for replacement of fossil fuels in the fuel industry as "conventional fuel sector". Currently, the fermentation of raw biomass (e.g. rice bran and clove) is one of the only biochemical methods that has received some industrial implications in the European Union (EU) and the United States (US) for vanillin production (Gallage & Møller, 2015).

Lignin is a complex polymer of phenolic components and could be a source of phenol and phenolic components to produce vanillin through biochemical processes (Fache *et al.*, 2016a,b; Franco *et al.*, 2017; Kumar *et al.*, 2012; Li *et al.*, 2019; Wong, 2012). However, the production of monomeric phenolic derivatives is not easily gifted, but under hydrothermal liquefaction conditions, lignin can be degraded to polyphenols and monomeric phenolic components (Kang *et al.*, 2013). The biomass feedstock which is the source of the lignin plays a very important role because lignin from some biomass contains less of the β-O-4 bonds between successive monomers and more of the 5'-5' bonds that are more difficult to break (Rutherford *et al.*, 2012). Suitable biomass feedstock should contain a high concentration of the β-O-4 lignin bonds (Bunzel & Ralph, 2006; Jegers & Klein, 1985) to yield guaiacol or vanillyl alcohol in the HTL aqueous phase that can be biochemically converted to vanillin.

Hydrothermal liquefaction (HTL) is a thermochemical process of biomass conversion into solids, bio-crude and an aqueous phase containing various organic compounds (Gai *et al.*, 2015). The initial goal of using HTL was to produce bio-oil (Akhtar & Amin, 2011; Demirbas, 2009; Mathimani & Mallick, 2019; Saber *et al.*, 2016; Toor *et al.*, 2011; Zhang *et al.*, 2019) and upgrade it to biodiesel or bio-crude fuels (Chen *et al.*, 2019; Gollakota *et al.*, 2018; Graca *et al.*, 2013; Toor *et*

al., 2019) as an alternative for replacement of fossil fuels in the fuel industry (Elliott, 2016). Apart from hydrochar and bio-oil utilization, the aqueous phase can also be considered. The aqueous phase contains phenolic building blocks that includes guaiacol, p-cresol catechol, vanillin, vanillyl alcohol etc. (Marais *et al.*, 2019; Omar, 2021; Watson *et al.*, 2020). The phenolic components vary depending on the biomass type. Several biomass types, rice husks, municipal sewage sludge, Kraft lignin, sugarcane bagasse and micro algae yielded different compositions of these phenolic compounds in the aqueous phase (Funkenbusch *et al.*, 2019; Gai *et al.*, 2015; Posmanik *et al.*, 2017; Rensburg *et al.*, 2018; Yang, He, *et al.*, 2018; Yang, Xu, *et al.*, 2018; Zhu *et al.*, 2015a).

In hydrothermal liquefaction of lignin biomass, guaiacol and vanillin are part of the products in the aqueous and the oil phase (Gai *et al.*, 2015; Marais *et al.*, 2019). Guaiacol is derived from coniferyl alcohol, a monomer of lignin. Vanillin's structure has no relationship to the degradation of lignin with reference to the monomer makeup of lignin (Schuler *et al.*, 2017). However, reports concluded that vanillin can be formed from different reactions of products (Arun *et al.*, 2021) and/or from the components added (Isola *et al.*, 2018) to the reactor to facilitate the HTL process. One suggested possibility is the rearrangement of glucose rings (Catallo *et al.*, 2010). The concentration ratios of guaiacol to vanillin in HTL aqueous products showed vanillin to be a minor product with negligible percentage yield compared to guaiacol (Lyu *et al.*, 2015; Marais *et al.*, 2019).

Guaiacol can be converted to vanillyl alcohol via the formylation of guaiacol, thus directing the CH_2OH group to the *para* position of guaiacol (Ji & Schäffer, 2004; Ardizzi *et al*., 2005). This reaction can be achieved in an acidic medium using a proton donated by the acid as the catalyst (Cavani., *et al.*, 2002). Several authors have reported this reaction to be challenging, but feasible (Cavani, Corrado, *et al.*, 2002; Cavani *et al.*, 2002; M. Ardizzi, F. Cavani *et al*., 2005; Mezzogori & Cavani, 2002). One of the challenges is the selectivity of the para and ortho products. The hydroxyl group of guaiacol has a higher priority of directing the CH_2OH group to the para and ortho positions compared to the methoxy group (Neuman, 2013). The main product of interest for biochemical synthesis of vanillin is para-vanillyl alcohol (p-VA), but the challenge of maximizing p-VA selectivity during the reaction has not yet been addressed in literature.

Vanillyl alcohol oxidase (VAO) is a flavoenzyme sourced from fungal *Penicillium simplicissimum* (Gygli *et al.*, 2018). In several experiments, VAO contributed to the oxidation of different phenolic precursors to different compounds. p-Creosol is converted to vanillyl alcohol, eugenol yields

coniferyl alcohol, 4-ethylphenol is converted to (*R*)-1-(4-hydroxyphenyl) ethanol and 4-(methoxymethyl)phenol is oxidatively demethylated to 4-hydroxybenzaldehyde. All these reactions occurred through the para-addition of oxygen atoms to each precursor. The reaction of vanillyl alcohol to vanillin showed a different product where oxidation occurred by dehydrogenation to yield an aldehyde (Gygli *et al.*, 2018). Vanillyl alcohol oxidase belongs to the vanillyl alcohol oxidase p-Quinone methide family as reported by the phylogenetic analysis of different flavoenzymes (Gygli *et al.*, 2017)). In this family, VAO is a member of sub-group 4-phenol oxidizing enzymes. 4-Phenol oxidizing enzymes catalyze the oxidation of para-substituted phenols at the α-Carbon atom of the para substituent (Goswami *et al.*, 2013). This property links VAO to its ability to oxidize vanillyl alcohol to vanillin.

1.2. Research problem and purpose

Phenol derivatives are present in relatively low concentration in the aqueous product from HTL (Marais *et al.*, 2019; Rensburg *et al.*, 2018). Phenolic components are mostly toxic to the environment but could be valuable building blocks for bio-based chemicals if recoverable. Recovery of the phenolics from the aqueous product will result in the wastewater meeting environmental limits for recycle and re-use. Separation of components present in low concentrations is however expensive and complete recovery can more easily be achieved if the phenolic component concentration in the aqueous product can be concentrated. A possible solution to this challenge is to convert some of the components to vanillin to increase the vanillin concentration and lower downstream separation costs.

1.3. Aim

The aim of this study is to investigate the feasibility of utilizing vanillyl alcohol oxidase to biochemically convert phenolic components in the aqueous product from HTL to vanillin.

1.4. Objectives

- Determine feasible oxidases for the production of vanillin from phenolic components;
- Determine the yield and para vanillyl alcohol selectivity during the hydroxyalkylation of guaiacol to vanillyl alcohol;

- Determine the feasibility of synthesizing and purifying vanillyl alcohol oxidase using a bacterial expression system for use in the biochemical conversion of vanillyl alcohol to vanillin;
- Determine the yield and selectivity towards vanillin during the enzymatic conversion of vanillyl alcohol to vanillin;
- Compare vanillin yields obtained from enzymatic conversion of pure vanillyl alcohol to that of vanillin using the aqueous product of HTL as the source of vanillyl alcohol;
- Determine the inhibitory effects of selected HTL aqueous product components on vanillin yield during enzymatic conversion of vanillyl alcohol.

1.5. Thesis outline

This dissertation contains five chapters. Chapter 1 gives an introduction to the study and the aim and objectives to be achieved. In chapter 2, a review of the literature pertaining to the subject matter of this dissertation is given.

In chapter 3, materials used and experimental and analysis methods developed and used in the experimental work are described. Chapter 3 is divided into three subsections. In section 3.1, the reaction methods for the production of vanillyl alcohol from guaiacol is described. Guaiacol is carboxylated with formaldehyde under acidic conditions. The aim of this reaction is to maximize the para vanillyl alcohol production. Therefore, the optimum temperature and pH to maximize yield and selectivity was determined and reported. Section 3.2 describes the methods and steps used in the synthesis and purification of vanillyl alcohol oxidase. The enzyme synthesis involved DNA transformation of the pET28a(+) vector ligated with PsVAO gene, protein expression in *E. coli* BL21(DE3), protein expression, protein purification, quantification and activity assay of the protein. Section 3.3 describes how the protein was used in the HTL aqueous phase to synthesise vanillin. Methods of analysis and the approach used in the design of the reaction medium are also described.

Chapter 4 contains detailed results and a discussion of the results of the three experimental phases of the project described in Chapter 3. In chapter 5 conclusions and recommendations for the study are drawn based on the results discussed in chapter 4.

CHAPTER TWO

LITERATURE REVIEW

2.1. Introduction

This chapter presents a critical review on how vanillin is formed via biological and chemical processes. The sourcing of natural vanillin is described in Section 2.2.1, as a way to relate the enzymes involved in the formation of vanillin in vanilla pods during the curing process. The discovery of these enzymes, their chemical pathways and precursors led to vanillin formation. This shed light on which enzymes to use to produce natural vanillin through biochemical processes.

Vanillin is often found as a phenolic degradation product of lignin, which highlighted the question of producing phenolic components through lignin degradation for enzymatic conversion to vanillin. Therefore, a detailed structure and the bond energies of lignin have been described in Section 2.4.4. Some of the most promising and currently used techniques for lignin degradation include pyrolysis, gasification and hydrothermal liquefaction. All these processes still have some challenges in degrading lignin to yield a higher percentage of lignin monomers. In this chapter, the discussion on lignin degradation is limited to the hydrothermal liquefaction process since it is known that this process yields higher monomeric phenolic component concentrations compared to pyrolysis and gasification.

A summary of reaction pathway and enzymatic pathways involved in the conversion of phenolic compounds to vanillin is discussed. The focus in this section is mainly on suitable substrates, enzymes and optimum parameters for enzymatic conversion. Vanillyl alcohol oxidase (VAO) is discussed in greater detail since it is believed to be the most promising enzyme for synthesis of vanillin from phenolic components (Van Rooyen, 2012). However, the specific pathway by which vanilla pods produce vanillin through the action of enzymes is still not well understood.

Guaiacol is reported to be the main lignin sourced monomer that has a higher likelihood to be converted to vanillin. Because of the complex reaction of carboxylation of guaiacol under biological means, a chemical method is involved as the first step to vanillin formation. This step involves the formation of vanillyl alcohol, a para-substituted 4-hydroxy-3-methoxy (vanillyl alcohol), which is a good substrate for vanillyl alcohol oxidase (Gygli, *et al.,* 2018). Therefore, the chemical conversion of guaiacol to vanillyl alcohol is described in more detail in Section 2.5.

2.2. Vanillin

Vanillin is a white crystalline powder, an aromatic aldehyde, having a pleasant, sweet and intense aroma offering a vanilla-like flavor. It is more soluble in alcohol and ether than in water (Gallage & Møller, 2015), but its solubility in water increases with temperature. Vanillin is a flavoring agent in food, beverages and fragrances and is used as a precursor in polymer and fine chemical synthesis (Krings & Berger, 1998). Vanillin on the market falls under different categories depending on the source, though some sources are still limited to laboratory scale (Figure 2.1).

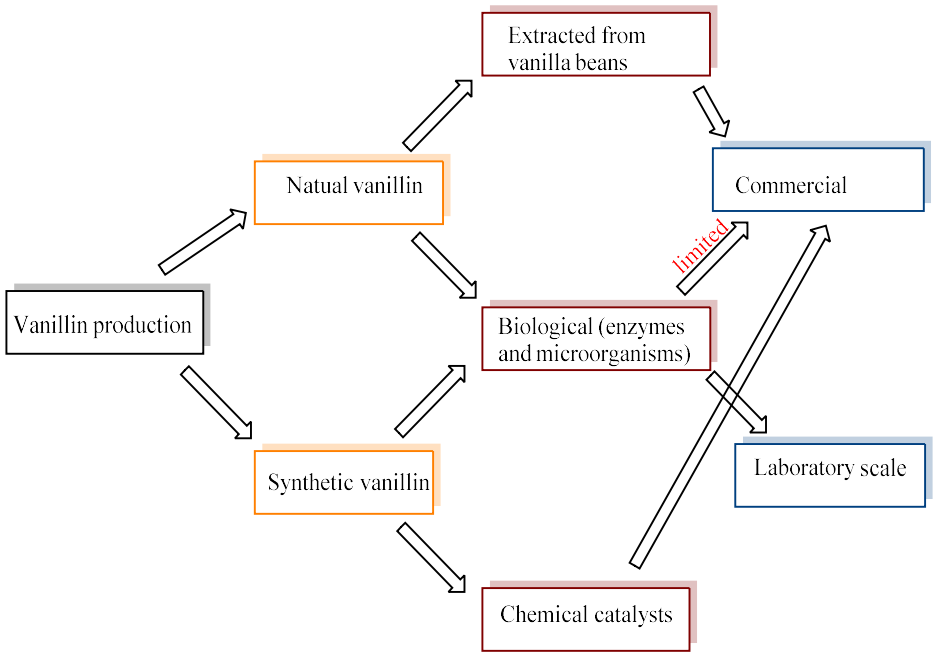

Figure 2.1. Two categories of vanillin production (natural and synthetic) coupled with the three methods used to obtain each vanillin type and the extent of utilization of each method (commercial and/or laboratory).

Vanillin is characterized by three functional groups attached to the aromatic ring, a hydroxyl group(–OH), a methoxyl group (-OCH_3) and a carbonyl group (–CHO) (Figure 2.2).

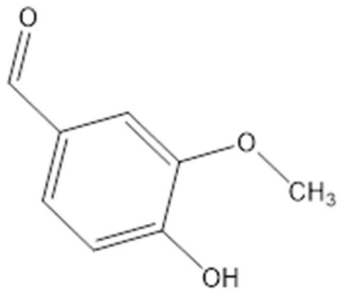

Figure 2.2. The structure of vanillin adapted from Gallage & Møller (2015)

Vanillin is obtained through both chemical and natural synthesis (Gallage & Møller, 2015). Natural vanillin is categorized as vanillin extracted from vanilla pods and/or synthesis through biochemical pathways (Havkin-Frenkel & Belanger, 2011). The natural biochemical synthesis methods have not yet been commercialized due to several limiting factors such as the formation of side products, end-product inhibition and spoilage of microorganisms (Converti *et al.*, 2010). The biochemical method is the most promising and environmentally friendly pathway for the synthesis of vanillin to meet the increased in consumer demand for natural vanillin (Banerjee & Chattopadhyay, 2019).

The major phenol derivatives that can be upgraded to vanillin are ferulic acid, phenol, guaiacol, syringol, and eugenol. However, the difference in the market value, demand and availability highlighted the value in upgrading the low-value phenols to those with a higher market value. In a review by Varanasi *et al.* (2013) it was reported that natural vanillin has a very high market value compared to all other phenols. Eugenol, guaiacol and syringol are used as feedstock to produce vanillin. Benzene is a by-product from liquid fuel production (Zhang *et al.*, 2005) and is industrially upgraded to phenol via the cumene process (Schmidt, 2005). Phenol is also a fossil based chemical that can be naturally obtained from coal tar (Zhao *et al.*, 2017). Phenol is further converted to catechol via the hydroxylation of phenol using hydrogen peroxide (Karakhanov *et al.*, 2010). The formed catechol is upgraded to guaiacol and finally to vanillin. This series of reactions from benzene to vanillin is the most used pathway in industry to produce synthetic vanillin. Eugenol is commercially synthesized from coniferyl alcohol, a monomer from lignin degradation Eugenol is almost as valuable as natural vanillin, but the demand is low, because there is not yet a viable pathway for vanillin production from eugenol at commercial scale, although many successful laboratory-scale experiments have been reported (Havkin-Frenkel & Belanger, 2011).

Guaiacol upgrade to vanillin is a commercially viable process through the glyoxylic pathway (the Reimer reaction) (Wynberg, 1954). Consumers have more interest in natural than synthetic vanillin (Bloom, 2017). The use of microorganisms is the only natural way in which vanillin can be synthesized apart from the vanilla beans according to the European Union report (European Directive 88/388/CEE, JO No. L184, 22 June 1988) and US food legislation (Krings & Berger, 1998).

2.2.1. Natural Vanillin from vanilla pods.

Vanillin extracted from cured vanilla beans is in high demand and therefore have a very high market value (De Guzman & Zara, 2012). One kilogram of 100% natural vanillin has a market value of around R370000 (Green, 2019). The climatic conditions necessary for successful cultivation of vanilla bean is the greatest limiting factor on the availability of natural vanillin. Madagascar is the leading producer of vanillin from vanilla bean, supplying 80-85% of the world's natural vanillin with an annual worth of approximately R59 billion (Tridge, 2020).

Many researchers have investigated the chemical and biochemical processes of vanilla plant growth and the steps involved in the curing and growing process (Table 2.1). A study of the chemical changes at each stage helped to identify the chemical composition and changes in the bean in an effort to use this data to synthetically produce natural vanillin through both biochemical and chemical pathways (Havkin-Frenkel & Belanger, 2011). *Vanilla planifolia* and *Vanilla tahitensis* are the two vanilla orchids species that are sourced from vanilla bean cured pods and the complex flavor assortment is referred to as natural vanilla (Ramachandra Rao & Ravishankar, 2000). Vanilla extract from these plants contains more than 200 components that contribute to the flavor profile. Guaiacol is one of the major components with an average concentration of 1.5 wt. % in cured vanilla pods (Sinha *et al.*, 2008).

Table 2.1. A timeline for the development of concepts related to vanillin biosynthesis *(Adapted from Handbook of Vanilla Science and Technology, 2018).*

System and approach	Concept	Reference
Radiolabeling of *V. planifola* pods	Vanillin is formed directly from ferulic acid	Zenk (1965)
Radiolabeling of *V. planifolia* tissue cultures	Isoferulic acid as an intermediate (followed by demethylation)	(Funk & Brodelius, 1990 a,b)
Enzyme assay in cell free extracts from *Lithospermum erythrorhizon*	Coumaric acid to 4-hydroxybenzaldehyde (non-oxidative chain shortening)	(Yazaki *et al*.,1991)
Measuring metabolite levels in *V. planifolia* pods	Tartrate esters as intermediates	(Kanisawa *et al*., 1994)
Enzyme isolation and assay from cell cultures of Hypericum androaemum	non-oxidative chain shortening involvement of a cinnamoyl CoA hydratase/lyase	(El-Mawla *et al*., 2002)
Enzyme isolation from *V. planifolia* cell cultures	Thiol-dependent non-oxidative conversion of 4-coumarate to benzaldehyde	(Podstolski *et al*., 2002)
Gene cloned from *V. planifolia* embryo cultures	A cysteine-protease like protein catalyzing weak thiol-dependent non-oxidative conversion of 4-coumarate to benzaldehyde	(Havkin-Frenkel *et al*., 2013)
Partial purification of an enzyme from pods of *V. planifolia*.	Iron-dependent dioxygenase for thiol-dependent chain-shortening of 4-coumaric and ferulic acids	(Negishi and Negishi, 2014, 2015, 2017)
Gene cloned from *V. planifolia* pods.	Vanillin synthase, converting ferulic acid to vanillin.	(Gallage *et al*., 2014)

2.2.2. Biochemical pathways for production of natural vanillin

Some biochemical methods for natural vanillin production involve fermentation and biotransformation of raw biomass (Figure 2.3) and have already been considered for commercial

production of vanillin mainly in the EU and US. However, some of the biomass types, for example corn and clove are also used as food. This will lead to food in-securities as producers will now choose to produce their crops for energy supply (Paschalidou *et al.*, 2016). The biomass sources are mostly from land utilization, therefore this might pose pressure of land competition with the agriculture industry (Popp *et al.*, 2014). The other disadvantage is the environmental effects that will lead to water scarcity and climate change (Cintas *et al.*, 2016; Popp *et al.*, 2014). The most basic alternative route of natural vanillin production without affecting other industries can be the use of enzymes on waste biomass (Kapdan & Kargi, 2006). Enzymatic conversion from phenols produced from waste materials would be an environmentally more acceptable route for sustainable production of vanillin (Soares-Castro *et al.*, 2021). Enzyme reaction does not need energy to occur and also enzymes can be synthesized from different expression systems (Hawkins & Smolke, 2008; Kumar *et al.*, 2005; Lee *et al.*, 2013; Sadhu, S and Maiti, 2013; Shraddha *et al.*, 2011).

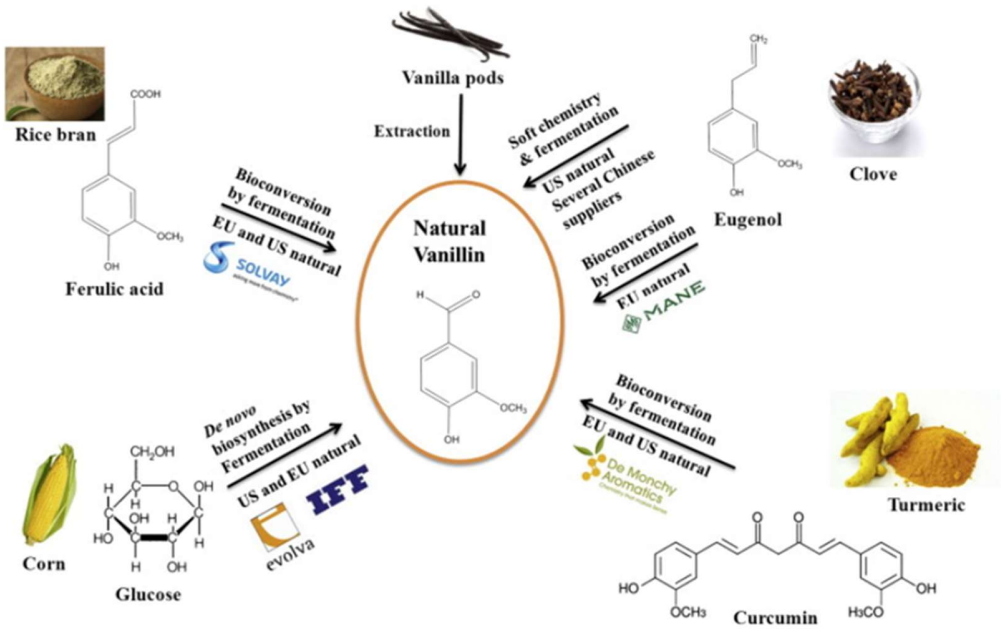

Figure 2.3. Vanillin production, four different starting materials that are available on market in the US using biological methods (adapted from Gallage & Møller (2015).

Biosynthesis yield a new completely different compound from the original starting material, while bioconversion only changes certain functional groups of the starting compound. Fermentation involves the activity of bacteria on a certain compound, using the latter as a carbon source thus changing its structure and resulting in a different product. Fermentation is involved in a

biosynthesis reaction of glucose, a component of maize corn to vanillin (Figure 2.3). The main nutrient from corn is carbohydrates that is in the form of starch and the monomer units of starch is glucose (Loy & Lundy, 2018). The bioconversion reactions from ferulic acid, eugenol and curcumin to vanillin are also reported (Figure 2.3). Ferulic acid, eugenol and curcumin are building blocks of rice bran, clove and turmeric respectively. Therefore the compounds are utilized by the microorganisms in a fermentation reaction to form vanillin (Gallage & Møller, 2015).

Biochemical synthesis, involving bioengineering through the use of genes that are transformed to express enzymes in different host microorganisms (Table 2.2), are still suffering from some challenges and are therefore generally limited to laboratory-scale production. Many genomes from different microorganisms have been sequenced and engineered through the introduction of some mutations to favor vanillin production (Table 2.2).

Table 2.2. Laboratory scale methods of Vanillin production using microorganisms and enzymes.

Precursors	Intermediates	Enzyme and/or microorganism	Reaction Conditions	Vanillin Yield %	References
	β-Hydroxy ferulic acid	*S. stoneii* ATCC39116	pH 7, glucose 17 hrs	68	(Muheim & Lerch, 1999)
Ferulic acid	Vanillic acid	*A. niger* 1-1472	Continous,		(Lesage-Meessen *et al.*, 1996)
		P. cinnabarius MUCL 38467	360hr, Phospholipids celloboise	82	
		E. coli BL21 pETDfdc, pETDcso$_2$ pGro7	pH 9.5, 10.5 24 hrs	40	(Furuya *et al.*, 2015)
Vanillic acid	nill	*Micrococcus isabellinus* Zyl849	pH 3.8; 20 hrs continuous process	80	(Cheetham *et al.*, 2005)
Eugenol	nill	*Pseudomonas sp.* HR199		89	(Overhage *et al.*, 2003)
		Lipoxygenase	36 hrs, charcoal	1.1	(Wu *et al.*, 2008)
Isoeugenol	nill	*Pseodomonas putida* IE27	60% Isoeugenol 24 hrs	75	(Yamada *et al.*, 2008)
		Bacillus fusiformis CGMCC1347	pH 7.0; 72 hrs resin H103	17.5	(Zhao *et al.*, 2006)
		Lipoxygenase	H_2O_2; Charcoal	13.3	(Li *et al.*, 2005)

2.2.3. Pathways for producing synthetic vanillin

Chemically synthesized vanillin is relatively inexpensive compared to natural vanillin. The lower price for synthetic vanillin has made it the dominant vanillin sold in the market since most consumers can afford it. A summary of the different methods used for the industrial synthesis of vanillin in different countries are shown in figure 2.4.

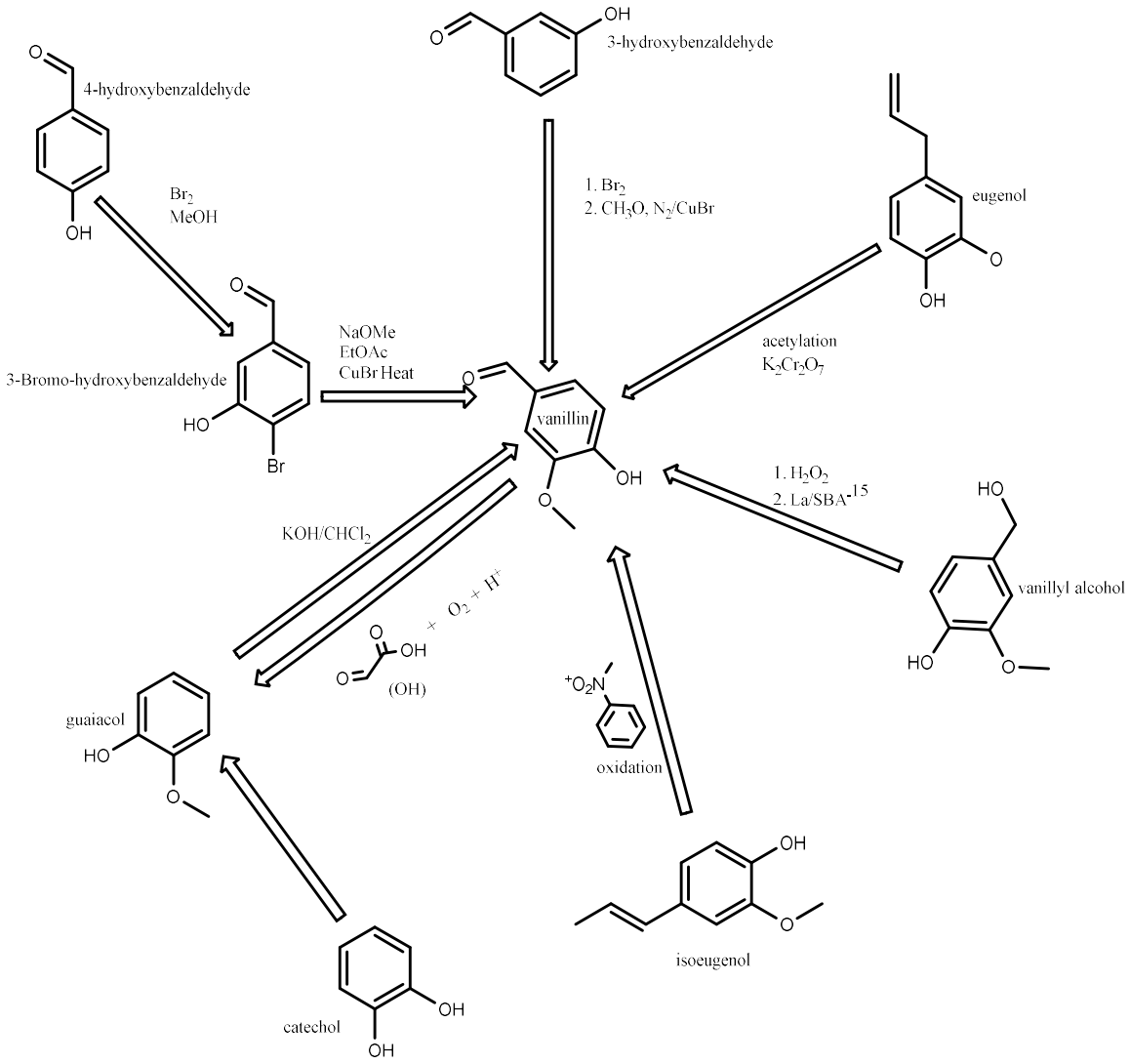

Figure 2.4. A summary of methods of production of synthetic vanillin from different phenolic components.

2.3. Lignin as source of monomeric phenols

Next to cellulose, lignin is the most abundant plant-derived polymer (Haider & Guggenberger, 2005). It is found in almost all dry-land plant wall cells (Calvo-Flores *et al.*, 2015). Lignin is a complex three-dimensional phenylpropanoid polyphenol linked by ether bonds or carbon-carbon linkages as well as different functional groups (Figure 2.5). It is the second most abundant natural compound that composes a significant portion of lignocellulosic biomass amongst cellulose and hemicellulose (Xing *et al.*, 2013). Softwood contain 28–30 % lignin content (Gîlcă *et al.*, 2011), hardwood 20–28 % (Pinkert *et al.*, 2011), and most annual plants 15–21 % (Day *et al.*, 2001; Del Río *et al.*, 2011).

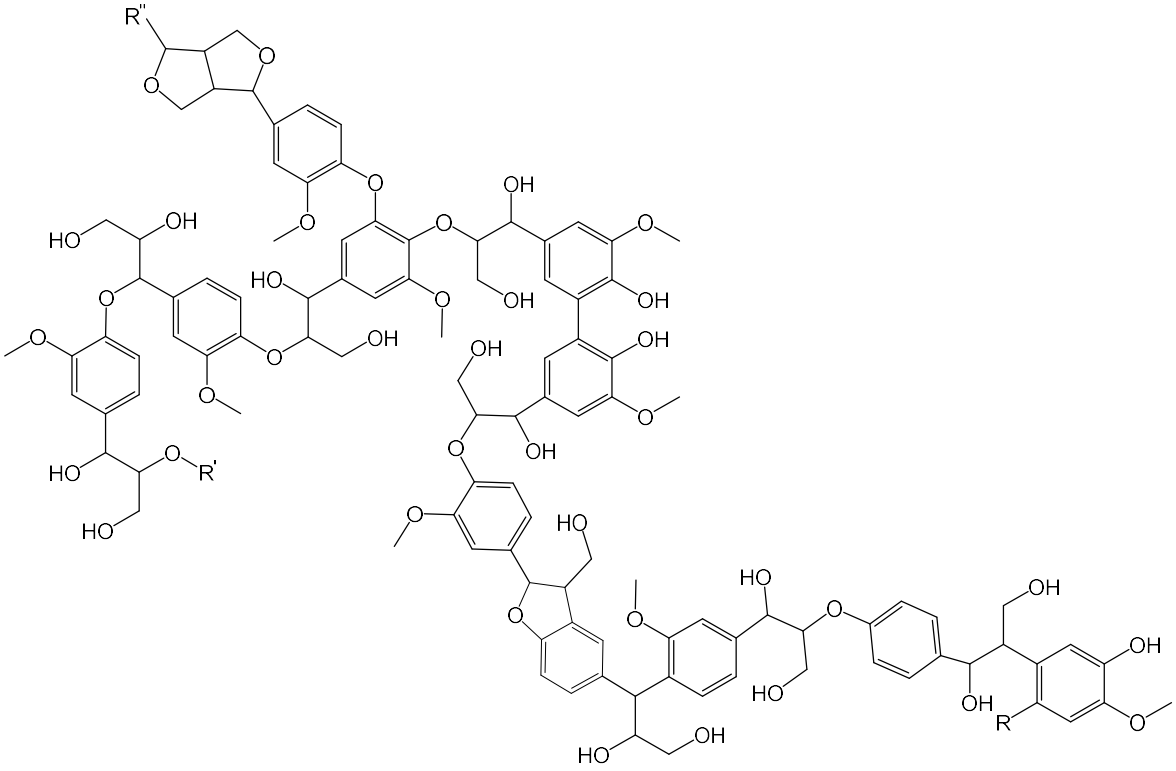

Figure 2.5. Complex structure of lignin (Schuler *et al.*, 2019).

The structure includes three monomeric units namely, sinapyl, p-cumaryl and coniferyl alcohols (Figure 2.6). The distribution of these monomers differ depending on the lignin source, i.e., plant or algae (Gellerstedt & Henriksson, 2008; Haghdan *et al.*, 2016). Sinapyl alcohol leads to syringol and coniferyl alcohol leads to guaiacyl units from a theoretical point of view according to the lignin structure.

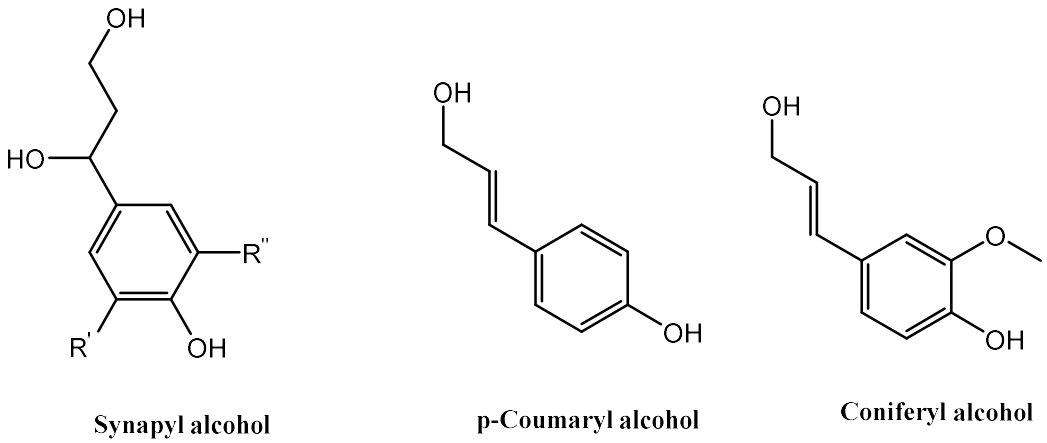

Figure 2.6. Monomer units of lignin (Schuler et al., 2019).

2.3.1. Degradation of lignin

Lignin can be used in different applications either as raw lignin or through a stage of depolymerisation into different monomers (José Borges Gomes *et al.*, 2020). In a review according to Schutyser *et al.* (2018) lignin depolymerisation has been done through acidic and alkaline depolymerisation (Pineda & Lee, 2016), reductive and oxidative depolymerisation (Das & König, 2018), solvolytic (Li, Greenchem, *et al.*, 2018; Renders *et al.*, 2019, 2018) and thermal depolymerisation (Li, Wang, *et al.*, 2017; Naron *et al.*, 2019a,b; Trejo-Machin *et al.*, 2020). All these depolymerisation methods uses transition metal catalysts (Cesari *et al.*, 2019; Chen, Korányi, *et al.*, 2016; Das & König, 2018). The reaction temperatures of range 180-320ºC promotes the formation of phenolic compounds through the degradation of the β-O-4 bonds (Bosque *et al.*, 2017; van Parijs *et al.*, 2010; Sun *et al.*, 2005). Above 320ºC, the product of the depolymerisation is mostly fused ring structures (Schutyser *et al.*, 2018). Apart from only the formation of aromatic compounds, lignin yields a number of straight chain and cycle aliphatic compounds (Demirel, 2017; Karnjanakom *et al.*, 2017; Lin, Zhang, *et al.*, 2017; Růžičková *et al.*, 2019; Zabeti *et al.*, 2016). Lignin is used in a number of applications as raw or after degradation, fertilizer and herbicide production for agriculture (Du *et al.*, 2014; Mulder *et al.*, 2011), bioplastic production (Wang & Zhao, 2013), adsorbents in solution (He *et al.*, 2013, 2012) and in electro-chemical applications (Nagaraju *et al.*, 2014; Naylor *et al.*, 2012).

2.4. Hydrothermal liquefaction of lignocellulos biomass

Hydrothermal liquefaction (HTL) is a thermochemical process that can convert wet biomass into solids, bio-crude oil and gas (Brindhadevi *et al.*, 2021; Das *et al.*, 2021; Nagappan *et al.*, 2021; Paul *et al.*, 2021; Sangjan *et al.*, 2020; Scarsella *et al.*, 2020; Wang *et al.*, 2021). HTL takes place in the presence of a solvent (Cui *et al.*, 2020; Han, Hoekman, Jena, *et al.*, 2019; Ramola *et al.*, 2019), usually water, and is thus the only thermochemical process that produces an aqueous product as one of the product streams (Cha *et al.*, 2016; Djandja *et al.*, 2021; Gai *et al.*, 2015; Goyal *et al.*, 2008; Song *et al.*, 2020; Zhu *et al.*, 2015b)) (Figure 2.7). The aqueous product contains an abundance of organic components such as phenolic derivatives, organic acids, aldehydes and ketones that are degradation products of the biomass used during HTL (Marais *et al.*, 2019)

HTL has gained more attention in recent years as a viable method for treatment of wet waste because of its mild operating temperatures (200–350°C), high energy efficiency (despite operating pressures of between 10 and 25 MPa) and relatively low oxygen content of the bio-crude oil and hydrochar products (Matsumura *et al.*, 2005; Peterson *et al.*, 2008). Many different feedstock have been used for production of liquid and solid fuels, including, agricultural and forestry residues, herbaceous crops, aquatic and marine plants, and organic wastes (Asadullah *et al.*, 2013; Li, Sun, *et al.*, 2018; Zhang, Yang, *et al.*, 2018). Many of these crops have also been investigated for the production of bio-oil, hydrochar, biogas and aqueous products using HTL to assess product quality and applicability for various applications (Goleta *et al*., 2018).

Literature reports on the effect of subcritical HTL operating parameters such as temperature (Nagappan *et al.*, 2021; Xu & Savage, 2017), initial inert pressure (Carpio *et al.*, 2018; Yu *et al.*, 2011a), biomass to solvent ratio (Baloch *et al.*, 2018; Biswas *et al.*, 2019; Han, Hoekman, Cui, *et al.*, 2019; Matayeva *et al.*, 2019), solvent type (López Barreiro *et al.*, 2015; Zhang *et al.*, 2013), biomass feedstock (Baloch *et al.*, 2018; Li, Leow, *et al.*, 2017; Watson *et al.*, 2020; Yu *et al.*, 2011b), operating atmosphere (Matayeva *et al.*, 2019; Pirwitz *et al.*, 2016) and catalysts (Han, Hoekman, Cui, *et al.*, 2019; López Barreiro *et al.*, 2015; Matayeva *et al.*, 2019; Muppaneni *et al.*, 2017; Posmanik *et al.*, 2018; Villadsen *et al.*, 2012; Yu *et al.*, 2011a) on product distribution and quality. Products and steps in HTL process are shown in figure 2.7.

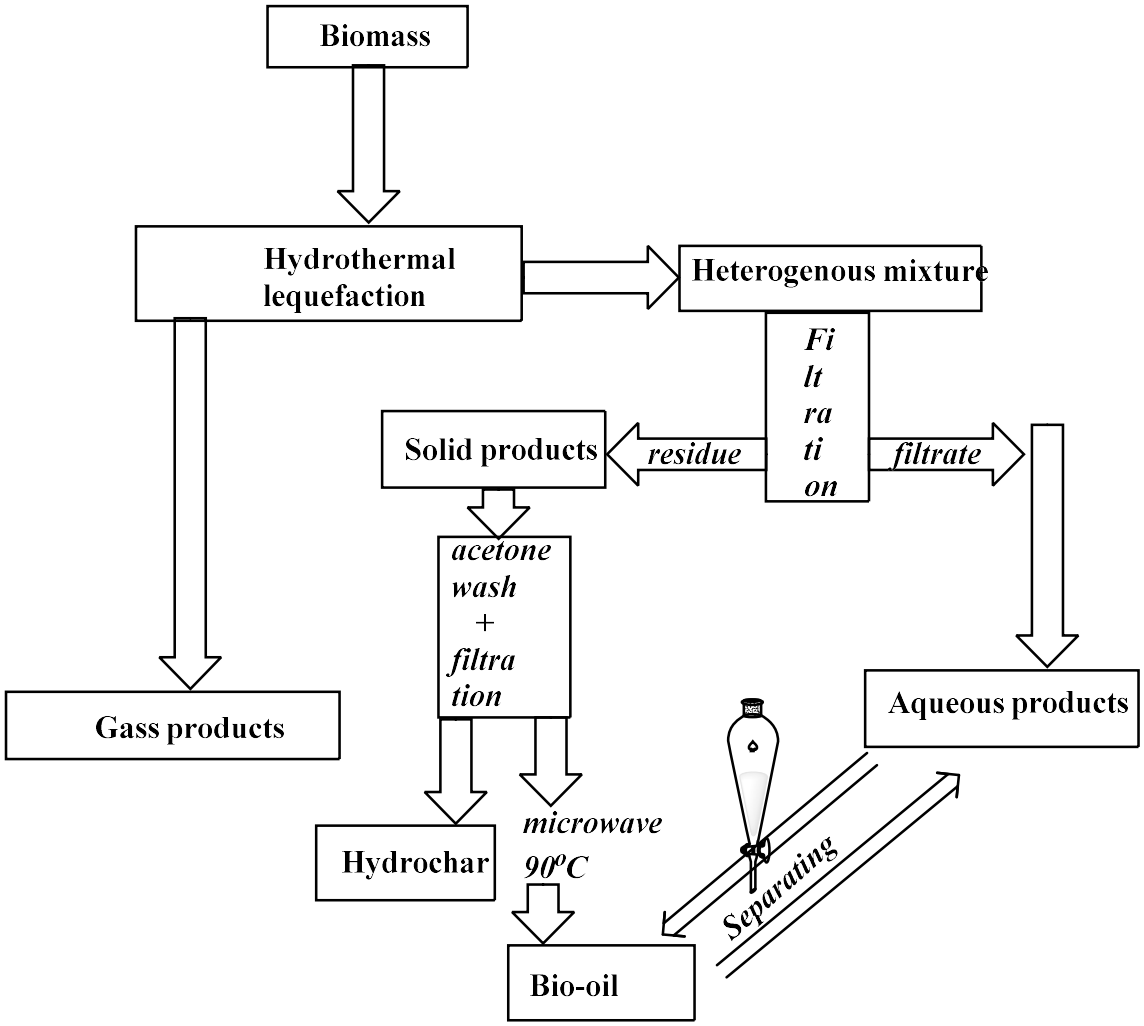

Figure 2.7. Sketch diagram to show the steps involved in HTL.

2.4.1. Gas-phase

The gaseous product obtained from HTL of different biomass types usually contains some hydrogen (H_2), carbon monoxide (CO), methane (CH_4) and trace amounts of hydrogen sulfide (H_2S) with carbon dioxide (CO_2) making up the bulk of the composition (> 90%) (Arun *et al.*, 2018; Madsen *et al.*, 2015). The quantity and quality of liquid, solid and gaseous products from HTL were reported to be determined by operating parameters like temperature, biomass loading, heating rate, and feedstock source (Stephenson *et al*., 2010).

2.4.2. Hydrochar

Hydrochar is a carbon-rich solid residue from hydrothermal liquefaction of biomass (Lehmann and Joseph, 2009). A variety of biomass feedstocks from wastes from dairy industries (manure and

yogurt whey), municipal waste-water treatment plants, fruit and alcohol manufacturing and olive oil production can yield hydrochar (Cantero-Tubilla *et al.*, 2018). If the chemistry and functionalities of the hydrochar are known, then alternative niches of applications can be revealed. According to Cantero-Tubilla *et al*. (2018), based on elemental analysis, it was revealed that different pH of feedstocks yields different compositions of chemicals in each hydrochar, the major elements being carbon, hydrogen, nitrogen and oxygen. There is also a higher yield of hydrochar from alkaline biomass compared to acidic biomass feedstocks (Cantero-Tubilla *et al.*, 2018). Hydrochar is one such product that has limited amounts of heavy metals thus making it cleaner to be used in different applications (Cao *et al.*, 2017). Hydrochar can be utilized in different applications for example, carbon sequestration (Jain *et al.*, 2016), activated to work as adsorbent (Zhu, Liu, *et al.*, 2014), magnetic carbon composite (Zhu *et al*., 2016), carbon catalyst (Reza *et al.*, 2014) and in addition the carbon material of hydrochar can be used in increasing the efficiency of fuel cells (Li *et al.*, 2014; Wang *et al.*, 2013).

2.4.2. Bio-oil

Bio-oil is one of the products of HTL that is of main attention so far (Chang, 2014; Demirbas, 2009; Marx, 2016; Xiu & Shahbazi, 2012; Zastrow & Jennings, 2013). Bio-oil can be converted to transportation biofuels such as renewable diesel (Shelke., 2016) and jet fuel (Tzanetis *et al*., 2017) by upgrading processes such as hydro treatment. Several upgrading processes of bio-oil have been reported in literature, including separation by distillation and solvent extraction, dehydrogenation, cracking (thermal and catalytic cracking) and esterification (Baloch *et al.*, 2018). Taghipour *et al*. (2019) outlined the positive and negative features of each of these upgrading processes. HTL bio-oil is still not applied neither in industry nor beyond the laboratory stage due to several issues. These issues includes low heating value, high viscosity, density and acidity, high undesirable content of heteroatoms and its instability, immiscibility with petro crude (Taghipour *et al*., 2019).

Bio-oil contains various chemical compounds such as acetic acid, hydroxy acetaldehyde, laevoglucose, levoglucosenone and maltol (Rosendahl, 2017). It is also a source of phenolic derivatives that are valuable platform chemicals that can be extracted to produce specialty chemicals such as preservatives, liquid smoke, resin precursors, additives in fertilizers and pharmaceutical industries and, flavoring agents (such as glycolaldehyde) for food industries (Kang *et al.*, 2013; Marais *et al.*, 2019; Remón *et al.*, 2019; Rosendahl, 2017)). Some of the organic components found in HTL-derived bio-oil from different feedstock include acids, furans,

ketones, aldehydes, esters, alcohols, phenolic compounds, aromatics and heterocyclic compounds, alkanes and alkenes, alcohols, nitrogen containing compounds and fatty acid as determined by gas chromatography-mass spectrometry (GC-MS) analysis (Chen *et al.*, 2015; Taghipour *et al.*, 2019). In addition to this, insoluble lignin and anhydrous sugars are also reported (Brigwater *et al*., 2001). In a further investigation on the differences in the distribution of all of these compounds from different types of biomass (softwood and pine), a large quantity of lignin guaiacyl units was reported (Lyn *et al*., 2001).

2.4.3. Aqueous product

Little attention has been given to the product from HTL due to several factors even though a significant fraction (20-50% of the organics in the biomass) are converted to valuable water-soluble products that are found in the aqueous product (Tommaso *et al.*, 2015). The components of the aqueous phase vary according to biomass type and reaction parameters. Water and light-soluble organic solvents are the main components (Beims *et al.*, 2020). Acetic acid, formic acid, glycolic acid, phenol, ethanol, methanol, ethylene glycol, and lactone are some of the organic compounds identified in the aqueous phase (Beims *et al.*, 2020). Several phenolic compounds in the aqueous product from HTL of rice straw detected includes a total guaiacol concentration of about 152 mg/L (Lyu *et al.*, 2015). In a different investigation by Chen, Lyu, *et al.* (2015) the compounds and impurities, including organic acids, ketones and 5-hydroxymethylfurfural in the aqueous phase product were quantified by high-performance liquid chromatography (HPLC) and include phenol and 2-methoxy phenol (15% of the total product).

Considering the composition of an HTL aqueous product, several ways to recover chemical components or otherwise utilize the product stream has been considered. One application is recycling of the aqueous product to the HTL reactor as solvent to minimize external water use. It has been reported that aqueous product recycle improved the overall bio-oil yield and quality (Das *et al.*, 2020; Edmundson *et al.*, 2017; Leng *et al.*, 2018). However, utilizing the aqueous phase only on the recycle processes and in algal growth can mimic the utilization of some components of the aqueous phase. The aqueous phase when used for algal growth, it is only the nutrients (Biller *et al.*, 2012; Das *et al*., 2020) and the trace metals (Edmundson *et al*., 2017) that is used by the algae. There are many other phenolic and organic compounds that are not retained. Therefore, a need for more routes to recover some or all of these compounds for a 100% energy recovery.

The aqueous product from HTL can also be used as a growth medium for cultivation of algae biomass because of the presence of both phosphorous and nitrogen which are essential nutrients for algae growth (Trivedi *et al.*, 2015). Algae oil is a promising non-edible source for biodiesel production compared to energy crops, but require water as growth medium. Use of the aqueous phase for this purpose can considerably reduce the cost and resource requirement for algae cultivation (Demirbas & Fatih Demirbas, 2011). However, studies on algae growth in HTL aqueous products obtained from various feedstock have shown low growth rates compared to other media currently used (Cherad *et al.*, 2016). The latter was suspected to be due to inhibitors present in the aqueous phase. This was confirmed by increased growth rates after 400 times dilution of the aqueous phase from microalgae biomass (Cherad *et al.*, 2016). Possible inhibitors from algae biomass includes phenolics, heterocyclic nitrogenous compounds, and heavy metals, among others, such as dibutylphthalate (Fernandez *et al.*, 2018; Leng *et al.*, 2020) Removal of inhibitors prior to aqueous phase recycle is a better way of utilizing the aqueous for algal growth. This may be achieved using adsorbents (Shanmugam *et al.*, 2017; Zhang *et al.*, 2018), solvent extraction (Chen, Wan, *et al.*, 2016) or microbial degradation of inhibitors (Si *et al.*, 2018). The other solution to the inhibitors is through genetic engineering. The algae strains are robust to tolerate aqueous phased inhibitions by genomic modification of the strains (Leng *et al.*, 2020)

Some studies (Li, Wang, *et al.*, 2018; Naqi, 2018 Seyedi *et al.*, 2020; Zhou *et al.*, 2015) have investigated the use of the HTL aqueous product as a feedstock for biogas production through anaerobic digestion. However, the presence of less biodegradable organics is a challenge to increase the efficiency of HTL aqueous phase anaerobic digestion (Seyedi *et al.*, 2020).. Anaerobic biogas production when using granular activated carbon yields as high as 259 ml CH_4/g COD from the aqueous phase of HTL of sewage sludge compared to 202 ml/g when granular activated carbon was absent (Usman *et al.*, 2019). Additionally, degradation of heterocyclic acids and aromatic compounds in the presence of the granular activated carbon was observed in the HTL aqueous phase (Usman *et al.*, 2019). In a similar investigation (Zhou *et al.*, 2015), granular activated carbon promoted anaerobic digestion at relatively low concentrations of HTL aqueous phase, giving ~53% energy recovery efficiency. Higher concentrations of the waste water had an inhibitory effect on the anaerobic digestion process indicated by delayed, slower, or no biogas production (Zhou *et al.*, 2015). Successful use of aqueous product from HTL require many additional purification steps (Cherad *et al.*, 2016; Maag *et al.*, 2018; Zhu, Biddy, *et al.*, 2014) or organisms (Cherad *et al.*, 2016; Egerland Bueno *et al.*, 2020; Naqi, 2018; Vardon *et al.*, 2011; Zhou *et al.*, 2015) and this can increase the efficiency to a point where it is economically feasible.

2.4.4. Hydrothermal degradation of lignin

The aqueous phase from HTL of black liquor was found to contain many phenolic components, including phenol, guaiacol, 4-ethylphenol, p-creosol; 2,3-dihydrobenzofuran, 1,2-benzenediol, 3-methoxy- 4-ethylguaiacol, 2-methoxy-4-vinylphenol, syringol, vanillin, 1,2,3-trimethoxybenzene, eugenol, acetoguaiacone,1,2,3-trimethoxy-5-methylbenzene, syringaldehyde, methoxyeugenol, acetosyringone, p-hydroxycinnamic acid, ethyl ester, ferulic acid ethyl ester, hexadecanoic acid and ethyl (Huet *et al.*, 2016; Schuler *et al.*, 2017).

The extent of lignin degradation to different monomer units under different HTL operating conditions has been reported (Dunn & Hobson, 2016; Kang *et al.*, 2013; Schuler *et al.*, 2017). The name of each bond in the lignin molecule is done according to the carbon numbering on the three monomers of lignin (see Figure 2.8). The knowledge of the bond strength among the various linkages allowed for the interference of the conditions on which they cleave (Kang *et al.*, 2013). The presence of more C-C bonds (Figure 2.8) between the aromatic and the aliphatic chain, for instance in the formation of guaiacol leads to a reduced yield as the bond strength is too high and requires a lot of energy (470 kJ/mol) to cleave (Schuler *et al.*, 2017). Depending on the heat capacity, the energy absorbed to break a certain bond is directly proportional to the increase in temperature (Luo, 2007). The bond most commonly broken during lignin degradation is β-O-4 (Hossain *et al.*, 2019). The β-O-4 bond has relatively low bond energy and is therefore one of the first bonds which are cleaved during the liquefaction process (Bunzel & Ralph, 2006; Jegers & Klein, 1985). In many instances, the monomer units can be attached to different bond types i.e. the β-O-4 and the 5-5 bond (Figure 2.8). This means that the monomer unit will be broken on one side and remain attached on the other side. In the product analysis, only completely separate monomers are detected. Thus, different lignin types give different monomer yields as the incomplete broken down bonds will be channeled to char formation (Rutherford *et al.*, 2012).

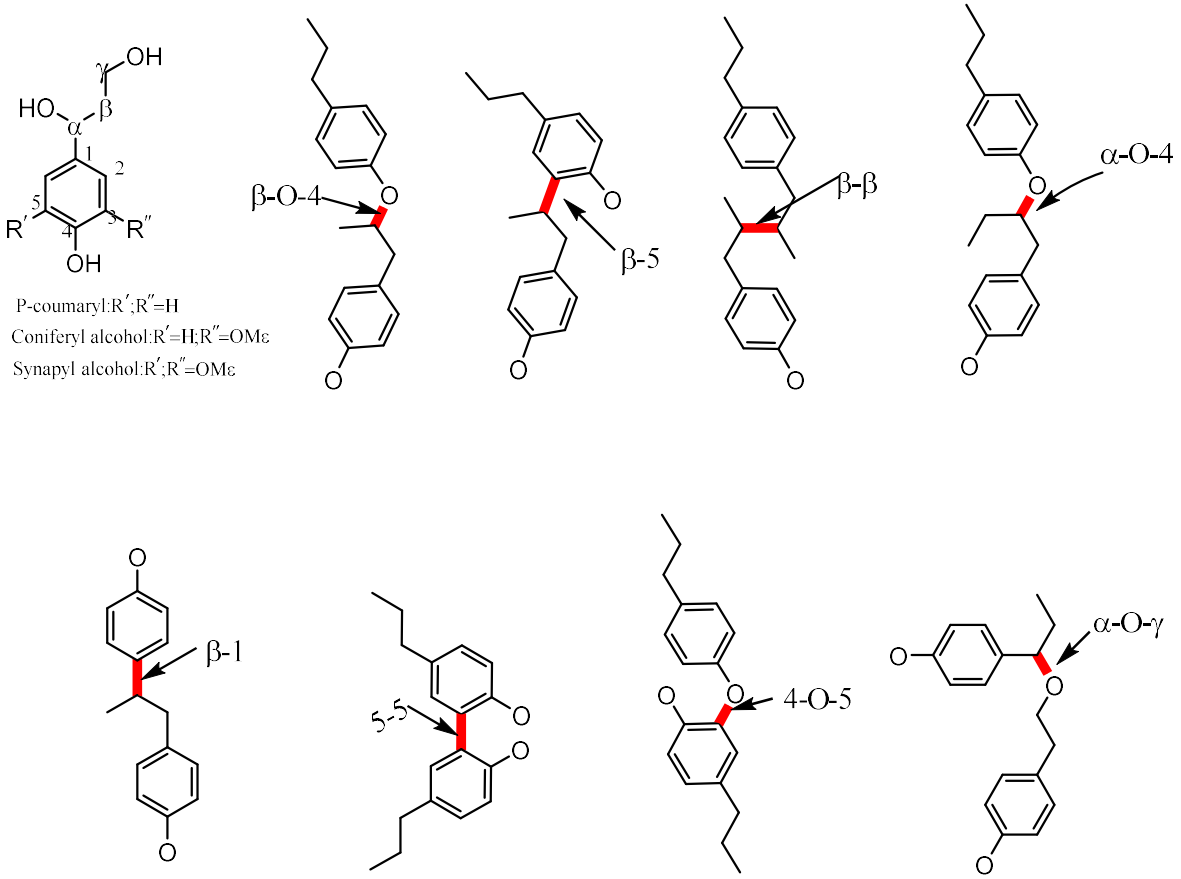

Figure 2.8. Lignin structure units and the important linkages (adapted from Kang et al. (2013)).

Schuler *et al*. (2019) reported on the degradation of Kraft lignin from pulping through HTL and found guaiacol and catechol as main products at HTL conditions of 300-350°C. The Indulin AT Kraft lignin used contained no sinapyl alcohol but only p-coumaryl alcohol and coniferyl alcohol of 2.5% and 97.5% respectively. Although guaiacol was the most abundant product, the same authors also reported the conversion of guaiacol to catechol under conditions of prolonged HTL residence times. The latter was shown by the rate of formation of catechol that was directly proportional to the decrease in guaiacol (Schuler *et al.*, 2017).

A coupled-system of two batch reactors at a temperature range from 203–303°C was used to liquify biomass derived from Japanese cedar bark (Watanabe *et al.,* 2018). The results showed that 65% (w/w) of lignin was obtained in the first 10 minutes. From a calculation using simple proportion, it highlighted the possibility of getting about 0.3 kg-lignin per kilogram of Japanese cedar bark biomass. From the characterization, it was revealed that the hydrothermal-soluble lignin had a simple structure with a molecular mass of about 1 kDa. However, the yield of lignin

decreased at temperatures higher than 248°C due to degradation of lignin at elevated temperatures (Watanabe *et al.,* 2018).

Many other sources stress the point that guaiacol is the main product in lignin degradation under hydrothermal conditions (Bunzel & Ralph, 2006; Bunzel *et al.*, 2007) with 19-78% reporting to the bio-oil product (Zhou, 2014). An investigation to determine the monolignol content of lignin fractions from kiwi, pear, rhubarb and wheat bran fibers showed comparable guaiacyl and syringyl contributions with kiwi lignins being guaiacyl-rich, and rhubarb lignins, being syringyl-rich (Bunzel and Ralph, 2006; Bunzel *et al*., 2017).

2.5. Vanillyl alcohol from guaiacol: The formaldehyde reaction

One promising reaction pathway is the conversion of guaiacol to vanillin through vanillyl alcohol. Guaiacol can be converted to vanillyl alcohol through a formylation reaction (Cavani, Corrado, *et al.*, 2002; Cavani., *et al.*, 2002; M. Ardizzi, F. Cavani.,, 2005; Mezzogori & Cavani, 2002). Several parameters have been reported to have a significant influence on both the conversion and selectivity of products during the formylation of guaiacol, i.e., methanol, reaction time, pH and temperature. The effect of methanol on guaiacol conversion to vanillyl alcohol (Cavani *et al.*, 2002; Cavani; Mezzogori and Cavani, 2002) under both homogeneous and heterogeneous acid-catalyzed conditions for the hydro-methylation of guaiacol with formalin was investigated. The percentage of methanol added influences the product distribution. At higher methanol loadings (10-15%), many diaryl and monoaryl products are formed as unwanted by-products compared to vanillyl alcohols (Cavani, Corrado, *et al.*, 2002). At lower methanol loadings (1%) more vanillyl alcohols are produced.

A further study was done on this reaction mainly focusing on the reaction pH (Cavani *et al*., 2002; Ardizzi *et al.*, 2005). In homogenous catalysis, the pH of the reaction solution plays a role in the activation of formaldehyde. At pH 2, it was reported that there is higher selectivity towards para-carboxylation whereas at pH 1 the ratio of the ortho to para vanillols are the same. Apart from selectivity towards vanillols, pH also has a contribution towards the total conversion of guaiacol. At pH ranges from 2 to 6, there was zero conversion of guaiacol even towards diaryl or mono aryl products (Ardizzi *et al*., 2005). Heterogeneous catalysis using H-mordenite zeolite as catalyst at a pH of 2 and a homogenous acid catalyst were compared. With the mordenite catalyst, the guaiacol conversion increased from 3% in homogenous catalysis to 20%, however, the product yield remains constant. This leads to a conclusion that most of the guaiacol is converted to by-

products (Bolognini *et al.*, 2004). The Si/Al ratio of the zeolite was also reported to play a role as it causes an increase in pH with an increase in Si/Al ratio and vice versa (Asghari *et al.*, 2019).

2.6. Vanillyl alcohol oxidase

2.6.1. Structure of vanillyl alcohol oxidase

Vanillyl alcohol oxidase (VAO, **EC** 1.1. 3.38), exists as an octameric flavoenzyme that is made up of two chains of 560 amino acids each. The two chains are referred to as chain A and B. Therefore, the octameric structure of VAO is made up of 8 chains, 4As and 4Bs (Figure 2.9).

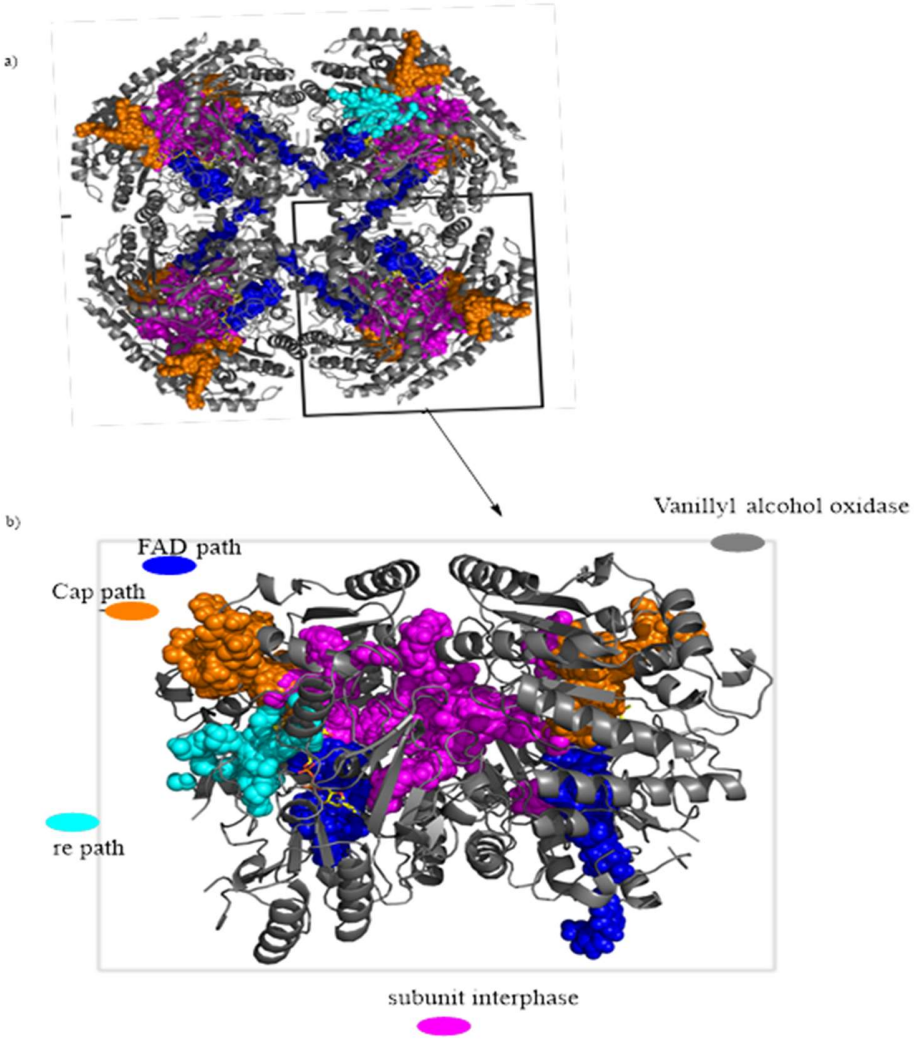

Figure 2.9. (a) The octameric structure of VAO made up of 8 subunits (b) Pathways through one subunit of the dimeric VAO (adapted from Gygli *et al.*, 2017).

According to (Gygli *et al.*, 2017), the substrate and enzyme interaction for vanillyl alcohol oxidase involves four pathways. These pathways allow the entrance of substrate and exist of products. The substrate entrance and product exit are through the cap path of the protein. The Flavin adenine dinucleotide (FAD) path (in blue) is where ligands traverse the protein through the FAD-binding domain. The subunit interface path (in magenta), corresponds to a path connecting the subunits. Only one of the three paths, the cap path, is exclusively connecting the active site to the solvent. Paths leading to the interface of subunits or dimers allow the enzyme to connect the different active sites of the subunits.

2.6.2. Mechanism of action of Vanillyl alcohol oxidase

The active site of VAO is made up of 10 critical amino acids (Figure 2.10). Each amino acid of the active site has its function with relation to the transfer of electrons and protons leading to product formation (Figure 2.10). The binding of the FAD co-factor to the enzyme molecule has a very crucial role in the activity of the enzyme.

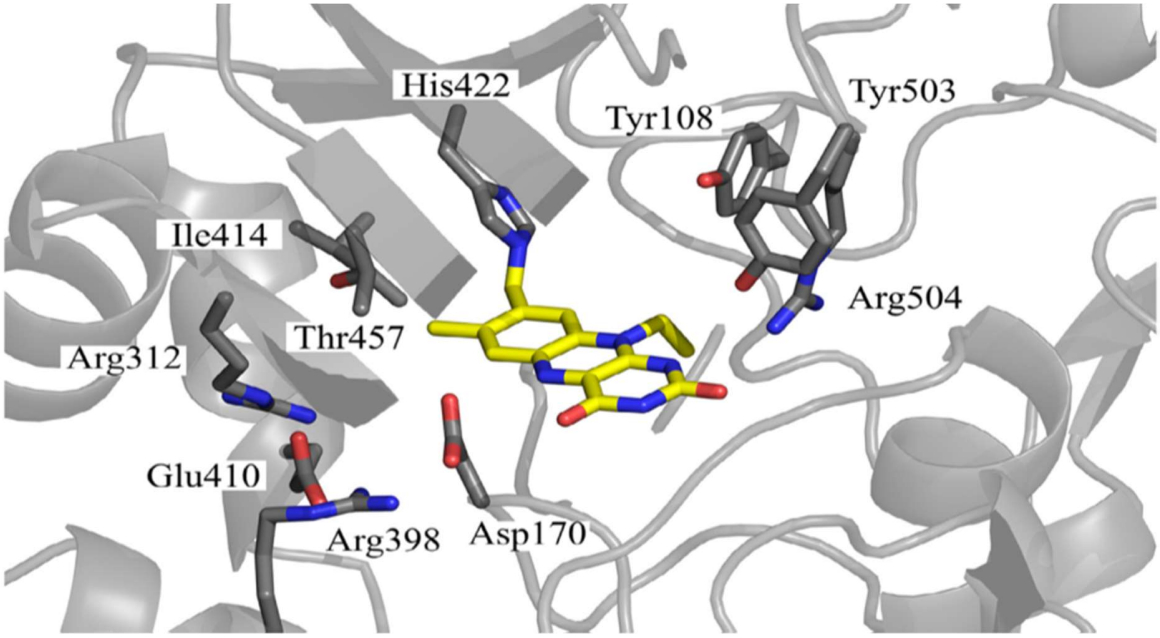

Figure 2.10. The active site amino acids of vanillyl alcohol oxidase as per single chain out of the eight chains. The cofactor FAD (shown with three rings in yellow and blue at the center of the picture) is bound to His422 (adapted from Gygli *et al*. (2018))

The mechanism below shows how the active site amino acids interact with the substrate during the conversion of vanillyl alcohol to vanillin. Certain amino acids promote deprotonation of the

ligand to create a negative charge which then allow a change in conformation. The H^+ ion of the position one hydroxyl group on the ring of the substrate is critical for the first deprotonation of the substrate by Asp170. FAD promotes the first deprotonation of the major functional alcohol group (CH_2OH), removing the carbon attached H^+. This deprotonation promotes the formation of a partial negative carbocation. Later on, the water molecule promotes an addition-elimination reaction on the ^-CHOH group and resulting in a ring rearrangement with the help of Asp170, thus forming an aldehyde, vanillin (Figure 2.11).

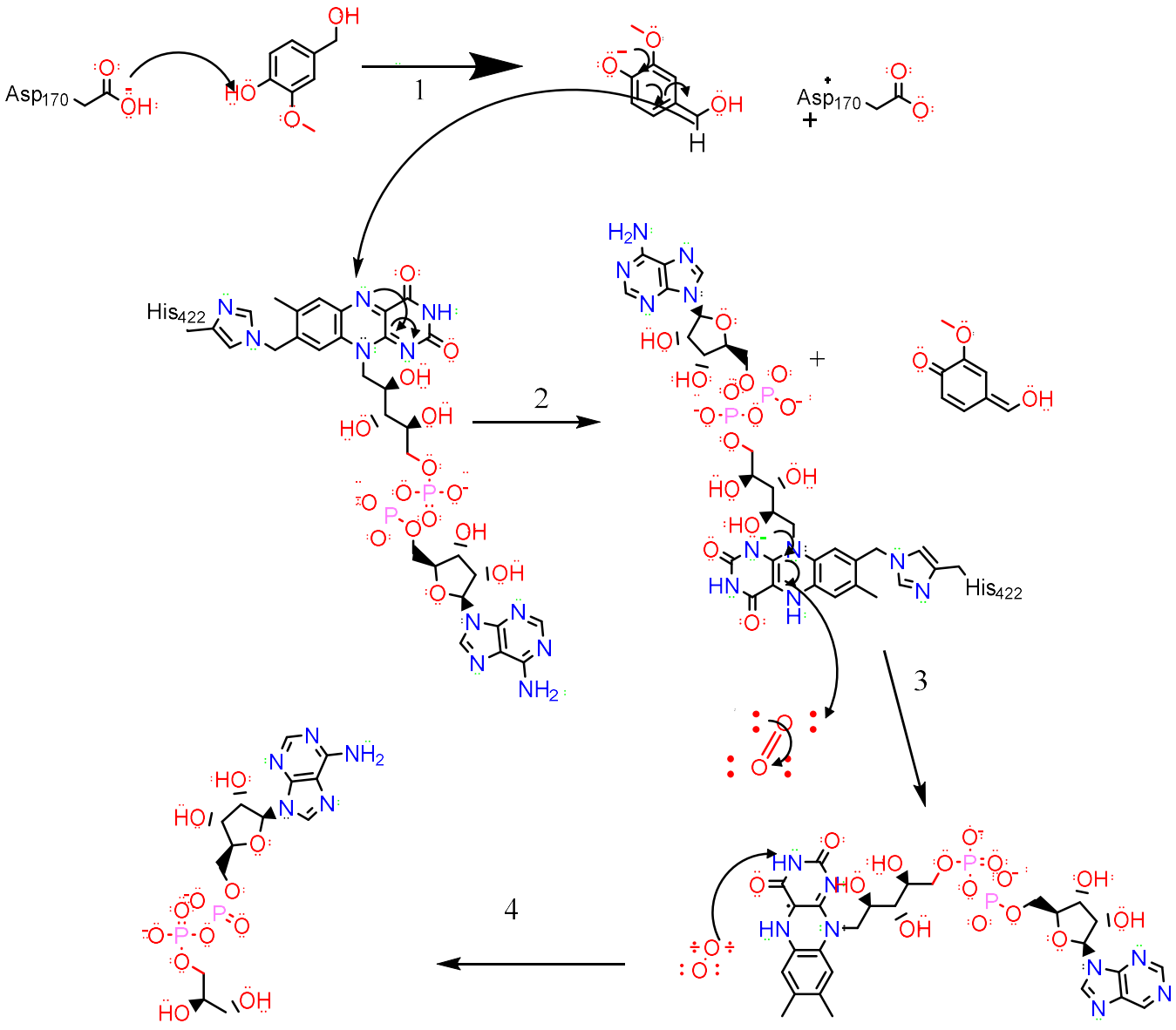

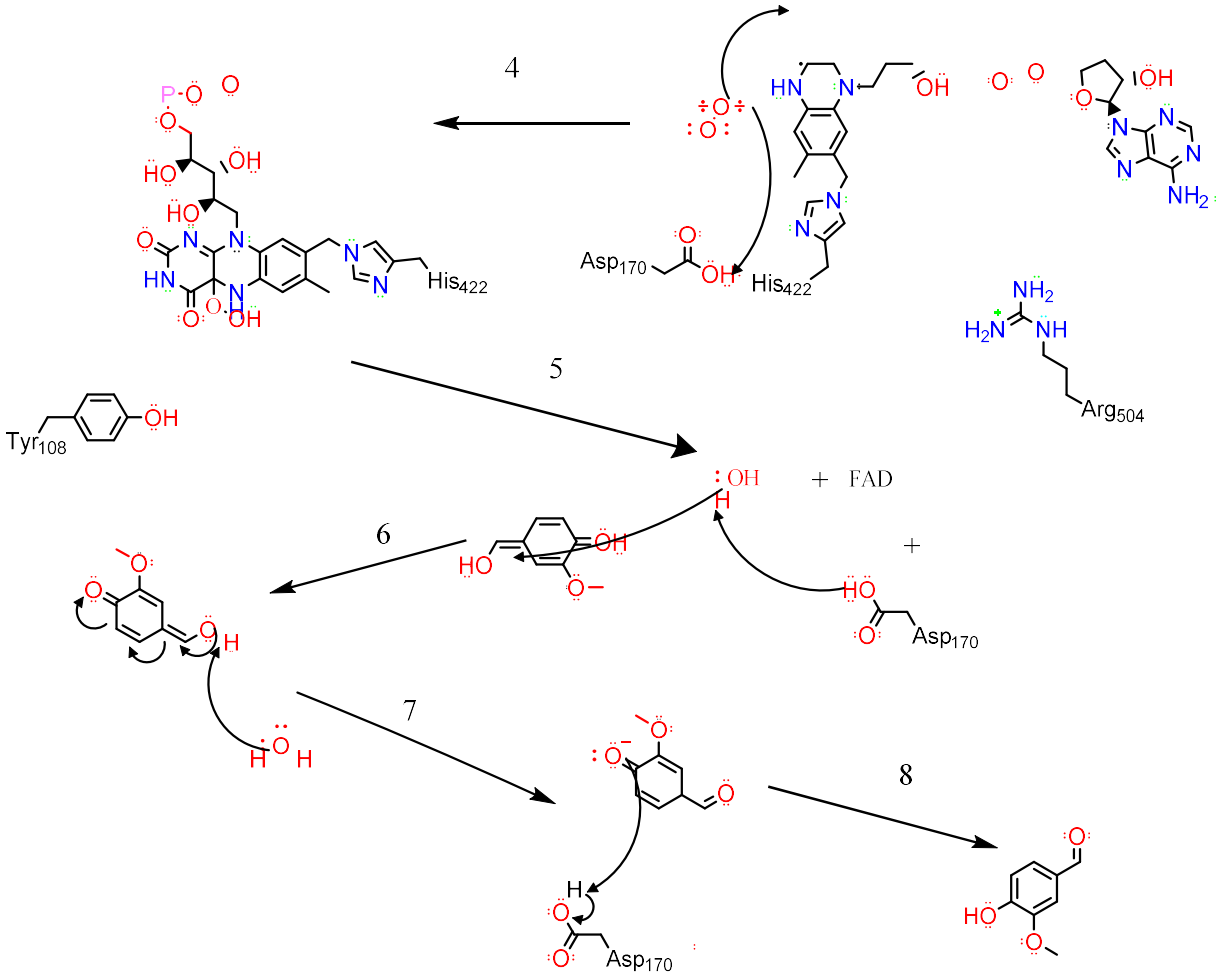

Figure 2.11. The steps involved in the reaction pathway from the point of interaction of VAO with the substrate (1) Vanillyl alcohol deprotonation of the OH group directly attached to the ring by active site amino acid Asp170. (2) Deprotonation of the alcohol group of vanillyl alcohol by FAD. (3) O_2 molecule oxidases the $FADH_2$ and itself becomes H_2O_2. (4) O_2 detaches the proton from Asp_{170} the same proton is at the same time released to FAD. (5) FADH releases the proton. (6) Proton addition and ring rearrangement of the vanillyl alcohol. (7) Proton loss and ring rearrangement forming an aldehyde group in place of the alcohol.(8) Reformation of the OH group by deprotonating Asp170 resulting in vanillin; up to the formation of product (Mattevi *et al.*, 1997).

From the mechanism above, Asp170 and His422 are the only two active site amino acids involved, where His422 is a FAD binding site. The rest of the catalytic triad amino acids are involved in stabilizing both the substrate and the FAD molecule during the reaction. Tyr108, Tyr503 and

Arg504 are involved in substrate binding and also in protonation like Asp170 (Ewing *et al.*, 2017; van den Heuvel *et al.*, 2002; Mattevi *et al.*, 1997). The function of Ile414 of VAO is involved in covalent bonding catalysis of FAD to the enzyme molecule, (Mattevi *et al.*, 1997). Thr457 was reported for stereoselectivity (Drijfhout *et al.*, 1998; Fraaije *et al.*, 2000).

2.7.3. Review of the action vanillyl alcohol oxidase on phenol derivatives as substrates

In an investigation according to Van Den Heuvel *et al*. (2004a), *E. coli* strain TG2 was transformed with vector plasmid pUC19 carrying VAO gene for vanillyl alcohol oxidase expression. In this study, the effect of random mutations in the VAO gene on the conversion rate to vanillin, was investigated comparing to the wild type (no mutation) using different substrates creosol, p-cresol and vanillyl alcohol. The enzyme reaction was setup for 48 hours at 37°C, pH 8 and 10 in a phosphate buffer (Van Den Heuvel *et al.*, 2004). Creosol was converted to vanillin in a two-step reaction with vanillyl alcohol as an intermediate (Figure 2.12). Assays of products at 340nm showed a 40-fold increased product turnover in the mutated versions of the gene when creosol was used as a substrate. However, using vanillyl alcohol as the starting material showed that the highest vanillin yield is achieved using the wild type (Van Den Heuvel *et al.*,2004).

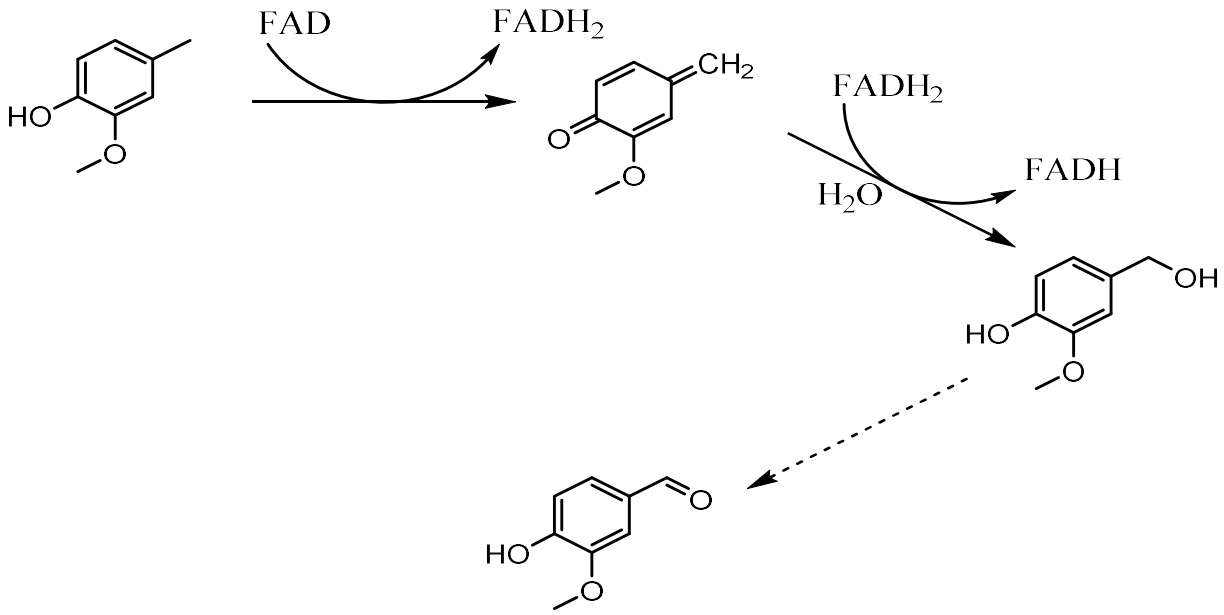

Figure 2.12. A redox reaction in the vanillyl alcohol oxidase active site showing the importance of FAD in the conversion of creosol to vanillin (Van Den Heuvel *et al.*, 2004).

The first step to the formation of vanillin from eugenol via coniferyl alcohol and ferulic acid was reported (Figure 2.13*a*). The reaction is catalyzed by vanillyl alcohol oxidase. In this reaction the plasmid carrying vanillyl alcohol oxidase gene from *Penicillium simplicissimum* was transformed into *E. coli* XL1-Blue cells and the genome was used to express the vanillyl alcohol oxidase enzyme. A conversion of 91% of eugenol to ferulic acid in 15 hours was reported and a concentration of 8.6 g/l ferulic acid was obtained (Overhage *et al.*, 2003).

Single mutants and double mutants were investigated in an enantiomeric conversion of 4-ethylphenol to 1-(4-hydroxyphenyl) ethanol (Figure 2.13*d*). The double mutants gave a greater and maximum conversion of product of 80% (S)-isomer while the single mutants resulted in 26% and 55% respectively of the (*R*)-isomer. This was lower compared to the wild type that produced 94% (*R*)-isomer. This in turn showed the importance of the critical amino acids of the active site. The reaction was performed by using *Escherichia coli* strain DH5aF9 ligated with the vector plasmids pUCBM20 and pEMBL19 respectively for the vanillyl alcohol oxidase gene expression (Van Den Heuvel *et al.*, 2000). Ewing *et al.*, 2000, reported a 97% yield of the same reaction stressing that Asp170 amino acid is critical for the stereospecific hydroxylation of phenolic substrates.

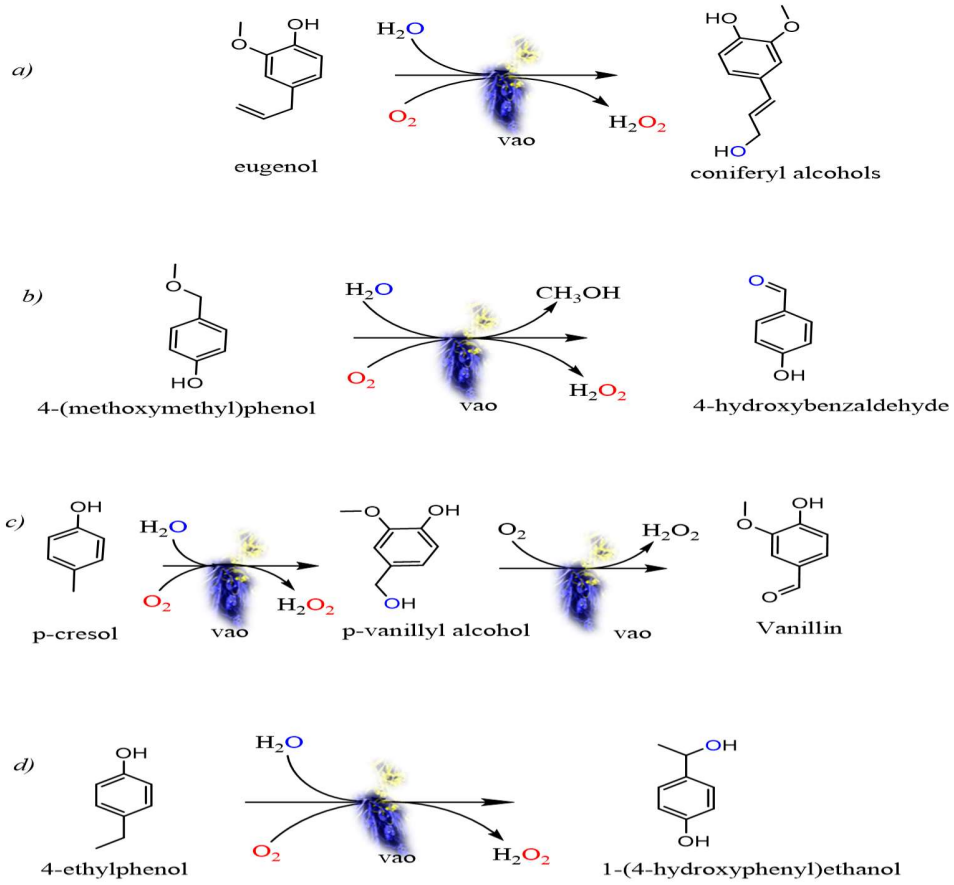

Figure 2.13. An outline of some of the reactions catalyzed by vanillyl alcohol oxidase adapted from (Gygli *et al.*, 2018)

2.7. Concluding remarks

In summary, there is an understanding of the compositions of HTL aqueous phase from different biomass types. This also identifies suitable compounds which can be upgraded to vanillin an expensive natural compound using an enzyme. All the other phases of HTL have been explained so as to express their value compared to aqueous phase utilization. The literature study shows that a biochemical process of vanillin is deemed natural and can therefore help increase the natural vanillin supply to the global market. Phenolic compounds form a greater portion in most HTL aqueous phases. The literature summarizes different ways by which vanillin is produced from different enzymes but these processes still have some obstacles to overcome before they can be commercialized. Also, other synthetic methods using chemicals have been reported. This opened a discussion on the pros and cons of these methods' implementation in different industries. In

addition, the literature report leads to a visualization of research gap of more advanced methods that are environmentally friendly, which can be the use of enzymes. A detailed report of vanillyl alcohol oxidase structure, mechanism of action and some known catalyzed reactions was reported. In enzyme production the structure should be confirmed in order to be sure that the right enzyme is being used. The mechanism of action brings understanding on how the enzyme interacts with the substrate.

CHAPTER THREE

MATERIALS AND METHODS

In this chapter, detailed materials and methods of the experiment are reported. The chapter is divided into three major sections. The first section (3.1) describes the conversion of guaiacol to vanillyl alcohol. Two parameters (temperature and pH) were optimised and their effect on the guaiacol to vanillyl alcohol reaction was described in detail. Optimised reaction conditions were used to deduce the yield of the para vanillyl alcohol from guaiacol. However, in this investigation the reaction was limited only to commercial guaiacol use instead of guaiacol in the aqueous phase. This was because a different biomass rich in vanillyl alcohol (compared to most biomass types rich in guaiacol) was available at a later stage for further experiments with the enzyme. Therefore, the enzyme reactions were done using the biomass containing vanillyl alcohol as the major aqueous phase phenolic.

Section 3.2 describes how the vanillyl alcohol oxidase was produced, purified and quantified. The same enzyme was used for the production of vanillin with detailed materials and methods in section 3.3. Section 3.3 is compiled with details of how the HTL aqueous phase was utilized in an enzyme reaction, the resulting yields and the effect of other components in the medium to the enzyme reaction.

3.1. Chemical conversion of guaiacol to p-vanillyl alcohol

This section gives a detailed description of the materials and methods used in the guaiacol formaldehyde reaction.

3.1.1. Materials

The list of instruments/equipment used for the investigation included; Incubator, Oven, Centrifuge, Vortex, Analysis instruments (HPLC, GC-MS, FTIR), Balance, Spectrophotometer, Beakers, Conical flasks, Cuvettes, Vials, Eppendorf tubes, reagent bottles, Micropipettes.

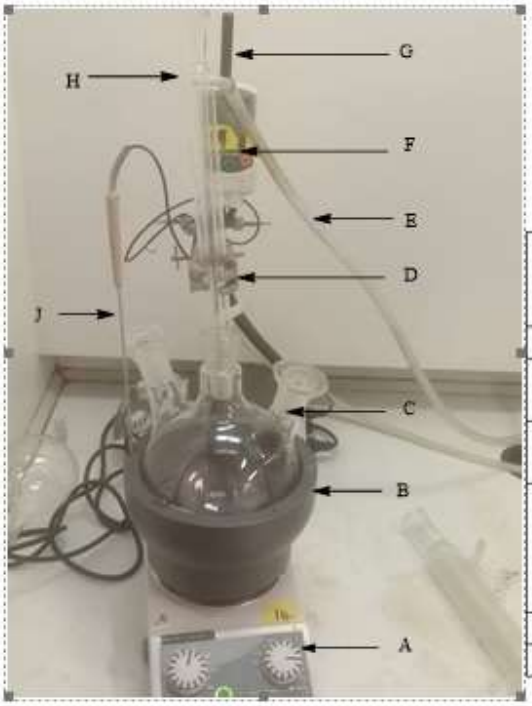

Name of equipment	Letter presentation for fig 3.1
IKA dry block heater	A
IKA 500ML flask heating block series	B
3 opening round bottomed flask	C
Clamp Water outlet Temperature monitor Stand	D E F G
Condenser	H
Thermocouple	J

Figure 3.1. The experimental setup used in the formylation of guaiacol prepared in a round bottomed flask fitted with a condenser sitting on dry block heater fitted with flask heating block.

Experimental procedure

3.1.2. Reaction mixture preparation.

The reaction mixture was prepared to total volume of 50 ml containing 29% (v/v) formaldehyde, 8% (v/v) guaiacol, 1,5% (v/v) methanol and water (Cavani, Corrado, *et al.*, 2002). Each component volume was prepared from their stock solutions using the following equation,

$$stock\ solution(\%) \times final\ volume\ (ml)/concentration\ of\ each\ reagent(\%)$$

The volume was added up to 50 ml using deionized water.

3.1.3. Overall reaction procedure

The apparatus of the experiment was set up as shown in Figure 3.1. The temperature was adjusted considering the displayed value by the temperature monitor connected via the thermocouple. Running water was opened through the condenser throughout the experiment. A total concentration of 29% formaldehyde (37%) was measured into the round-bottomed flask A concentration of up to 1.5% methanol (99%) was made in formaldehyde solution. The mixture

was placed in the heating mantle maintained at +/-2°C for the respective temperatures below. The mixture was stirred at approximately 320 rpm using a stirrer bar. The reaction solution was removed from the heating mantle and the pH was adjusted. The pH of the solution was measured using a pH meter through one of the openings of the flask. Aliquots of 10 µl concentrated sulphuric acid solution was added until the desired pH was accomplished. The formaldehyde solution was re-heated to the adjusted temperature, following the addition of 4 ml of guaiacol using. The first aliquot was taken soon after the addition of guaiacol and at 10 minutes' intervals thereafter.

Determination of optimum pH

Using the overall procedure described in the subsequent section, experiments were done according to guidelines by Ardizzi *et al.*, (2005) and Sheldon and Van Bekkum., (2007) to determine the optimum pH for the reaction. Reactions were performed at different pH values of 1.0; 1.3; 1.5; and 2.0 at temperature 80 °C. A total volume of 50 ml reaction mixture was used.

Determination of optimum temperature

At an optimum pH of 1.3, experiments were done to determine the optimum temperature according to Ardizzi *et al.* (2005) and Sheldon and Van Bekkum. (2007). Temperatures 55, 70, 80 and 90°C were investigated as described in the overall procedure above. In this case, the volume of the reaction was adjusted to 200 ml, with the same concentration of components.

3.1.5. Analytical Method-High performance liquid chromatography

High performance liquid chromatography (HPLC) (Alignment Technologies 1260 Infinity II: Infinity Lab Pros hell 120 EC-18 column) was used to determine the total phenol concentration. The equipment conditions (Temperature 65°C, mobile phase 0.1% formic acid in water, flow rate 0.7 $ml.min^{-1}$, 2 µL sample injection volume) were set on analysis. Sample was prepared for HPLC trough filtering the 5 ml aliquots into a clean Eppendorf tube using 0.22 µl syringe filters. Each filtered sample (100 µl), was transferred to a vial. A volume of 100 µl internal standard (garlic acid) was added, followed by 800 µl of the HPLC mobile phase. The results were given out in form of printed chromatograms and the concentration of vanillyl alcohol was calculated by using **Equation 1.**

Vanillyl alcohol concentration (g/L) = (Peak area / k-value) * dilution factor…….**Equation 1**

3.2. Enzyme production

This section gives details on how the enzyme, vanillyl alcohol oxidase was synthesized, purified and quantified.

3.2.1. Preparation of stock solutions

All stock solutions were prepared with molecular biology grade water. Glycerol stock (80%, v/v) was prepared by adding glycerol to deionized water. The stock was sterilized by autoclaving at 121ºC at 101 kilopascals for 15 minutes. The stock solution was stored at room temperature.

Buffers, Media and Solutions

A stock solution of 2.5 M $CaCl_2$ solution was prepared from $CaCl_2.2H_2O$ (Sambrook & Russell, 2001), filter sterilized using a 22 µL syringe filter, aliquoted into 1.5 ml Eppendorf tubes and stored at 4°C. A volume of 1 L Lysogeny Broth media (LB) (1% tryptone (w/v), 0.5% yeast extract, (w/v), 1% NaCl (w/v)) was prepared. Thereafter, the media was autoclaved for 15 minutes then stored at room temperature on a benchtop (Sambrook & Russell, 2001).

Nutrient agar plates (agar, 1,5% w/v) were prepared from 500 ml LB media and agar capsules and autoclaved for 15 minutes. A concentration of 50 µg/ml kanamycin antibiotic was added when the media had cooled to 60 ºC, poured into plates, paraffilmed and stored at 4ºC.

3.2.2. Plasmids and bacterial strains used in this study.

*To allow for long term storage, glycerol stocks of the BL21(DE3) cells were prepared by mixing 800 µl of the cells with 200 µl sterile 80% (v/v) glycerol in a micro centrifuge tube. The stocks were stored at -80 °C.

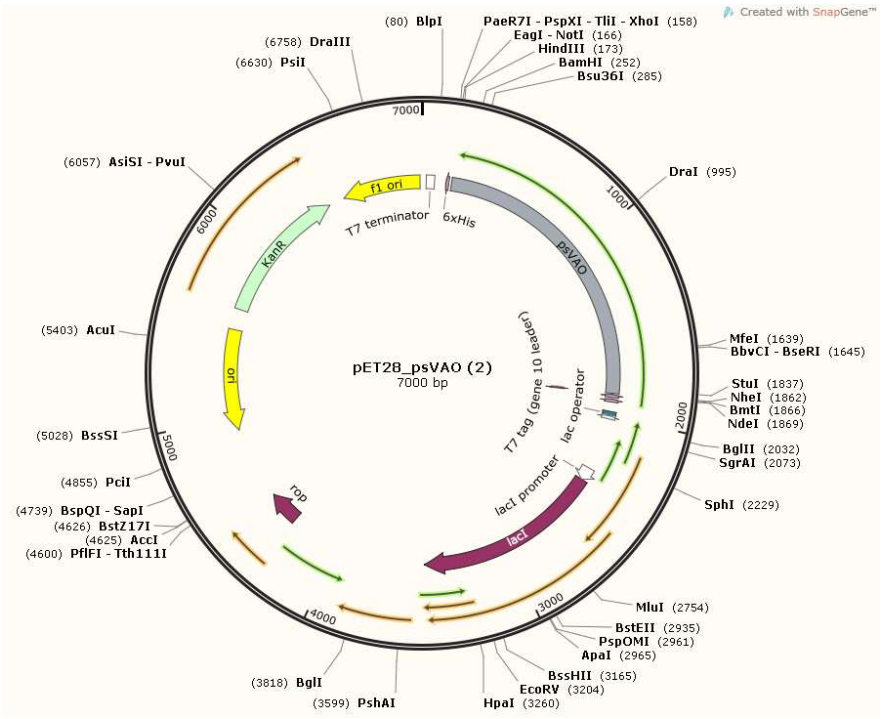

Figure 3.2. Recombinant pET28a(+)/PsVAO plasmid map which was transformed into *E. coli* BL21(DE3) bacteria cells.

3.2.3. DNA quantification and purity determination

Upon receiving the plasmids and the bacterial cells, the first step was to determine the concentration of the DNA in the stock solution obtained from UFS. This was to make sure the right concentration is send for DNA sequencing. The concentration was determined using the Nano-drop one (Thermo-Fischer Scientific, Madison, USA) with 1.3.1 Software.

This method relies on the principle of the Beer Lambert Law in which the concentration of a molecule can be calculated from the amount of light it absorbs (Swinehart, 1962). For double-stranded DNA, a change of one absorbance unit at 260 nm corresponds to a concentration of 50 µg/ml (Sambrook *et al.*, 1989). The DNA purity was also determined with the above mentioned system by assessing the A260/A280 ratio (Oliveira *et al.*, 2014).

DNA has maximum absorption at 260 nm and protein at 280 nm. For a pure DNA sample, an A260/A280 value of approximately 1.8 is expected. This ratio can reveal whether a sample is contaminated with proteins, as the proteins will absorb strongly at 280 nm, thus causing the ratio to fall below the desired 1.8 value (Oliveira *et al.*, 2014).

3.2.4. Sanger sequencing and data analyses for PsVAO

Plasmid DNA concentrations of more than 100 ng/µl as required by the sequencing facility (Central Analytical Facility (CAF), Stellenbosch) were sent for Sanger sequencing. To achieve a minimum concentration for the sequencing facility, the sample was concentrated using the SpeedVac (Cat. No. ISS110FS-115) (Thermo Scientific, Waltham, MA, USA). The SpeedVac creates a vacuum within the sample container so that centrifugal force holds the sample in place. The liquid is evaporated resulting in a concentrated sample. After concentration the sample was sent for Sanger sequencing at the Central Analytical Facility (CAF), Stellenbosch.

The DNA sequencing chromatograms provided by CAF were analyzed using FinchTV (version 1.40) (www.geospiza.com/finchtv). ClustalX was used for the alignment of the sequences to VAO: EC 1:1:3:38 (Accession: 5MXU_A, NCBI). To check the similarity organisms, nucleotide blastn NCBI was used for both the reverse and forward primer sequences. The pET28a(+)/PsVAO was made from the ligation of the PsVAO made from two forward (**cctatagtgagtcgtatta-5'-3')** and reverse **(caaaaaacccctcaagacc-5'-3')** primers with additional sticky ends restriction enzyme sites for *HindIII* and *NheI*.

3.2.5. Transformation of DNA into bacterial cells.

Before transformation, the bacterial cells were made competent to allow the plasmid into the cells

3.2.5.1. Preparation of competent *E. coli* BL21(DE3)

Competent bacteria cells were prepared using the $MgCl_2$-$CaCl_2$ method (Sambrook & Russell, 2001). Cells from a glycerol stock were streaked on LB agar plates without antibiotics and grown in an incubator overnight at 37°C. After overnight growth at 37°C, a single colony was inoculated in 100 ml of LB broth in a 1-liter conical flask covered with foil at the top. The cells were grown to the early log phase (OD_{600} = 0.5) for 3 hours. The resulting culture was transferred into sterile, disposable, ice-cold 50ml polythene tubes (CELLSTAR by greiner bio one). The cultures were cooled down for 10 min on ice. The cells were collected by centrifugation at 4000 xg, 4°C for 10 minutes. The supernatant was removed and the cells were suspended in 30 ml ice-cold $MgCl_2$-$CaCl_2$ solution (80 mM $MgCl_2$, 20 mM $CaCl_2$). The cells were again collected by centrifugation at 4000 xg, 4°C for 10 minutes. The medium was decanted from the cell pellets. The cells were resuspended in 2 ml ice-cold 0.1 M $CaCl_2$ solution each. The cells were stored at 4°C for 22 hours to improve the transformation efficiency. Glycerol was added to a final concentration of 15%. Aliquots of 200 µl cells were collected into ice-cold Eppendorf tubes (CELLSTAR by greiner bio one) and snap-frozen in liquid N_2. The cells were stored at -80°C.

3.2.5.2. Transformation

A tube of competent *E. coli* BL21(DE3) cells was thawed on ice until the last ice crystals disappear. The thawed solution was gently mixed then 50 µl of cells was carefully pipetted into a transformation tube on ice. A solution of 2 µl containing 1 ng–100 ng of plasmid DNA was added to the cell mixture. The tube was carefully flicked five times to mix cells and DNA. The mixture was placed on ice for 30 minutes without mixing. The resulting sample was heat-shocked at 42°C for 90 seconds. This was placed on ice for five minutes. A volume of 800 µl of room temperature commercial Super optimal broth (SOC) media was pipetted into the mixture. The mixture was vigorously shaken (250 rpm) for 60 minutes at 37°C. Selection plates containing kanamycin antibiotics (50 µg/ml) were warmed to 37°C. The cells were thoroughly mixed by flicking the tube and inverting, then several 10-fold serial dilutions were performed using SOC medium. A volume of 100 µl of each dilution was spread onto the warmed LB plates and incubated overnight at 37°C. A single colony from the overnight plates was inoculated in 5 ml (LB) medium fortified with 50 µg/ml kanamycin, and incubated overnight, shaking at 37°C, 200 rpm. To allow for long term storage, glycerol stocks of the *E. coli* BL21(DE3) cells containing the pET28a(+)/PsVAO plasmid were prepared by mixing 800 µl of the cells with 200 µl sterile 80% (v/v) glycerol in a micro centrifuge tube. The stocks were then stored at -80 °C.

3.2.5.3. Plasmid extraction.

After transformation of pET28a(+)/PsVAO into bacterial cells, to confirm if the bacteria cells were successfully transformed with the right plasmid, a positive growth test (shown by colonies) on the kanamycin containing agar plate was done. The plasmid was extracted from the bacteria cells to test if it is the right plasmid.

A volume of 100 µl of the transformed cells was spread on a kanamycin (50 µg/ml) selection plate for overnight growth. A single colony from transformation plate was grown overnight in a kanamycin antibiotic (50 µg/ml) containing LB-broth. The cell culture was harvested by centrifugation at 5000 xg. The resulting pellet was resuspended in 1,2 ml of resuspension buffer. A GenElute plasmid Midiprep kit (Sigma Aldrich) containing lysis and neutralizing buffers 1.2 ml and 1.6 ml each respectively was used for cell lysis and neutralization. The DNA was bound to the column that comes with the kit, through successive steps of column wash and preparation. The DNA was eluted using 8 ml of elution buffer and quantified by Nano-drop technology (Thermo-Fischer Scientific, Madison, USA) with 1.3.1 Software.

3.2.5.4. Restriction endonuclease digests of plasmids

From section 3.2.5.3, following the confirmation of plasmid integrity and successful transformation, shown by colonies forming on the kanamycin plate there was a need to determine if the DNA for VAO on the plasmid is of the right size and intact. Therefore, recombinant DNA restriction digestion was necessary followed by agarose gel electrophoresis analysis. Restriction enzymes that cuts at specific sites of the DNA are used to separate the DNA from the plasmid.

Two restriction enzyme sites (*HindIII* and *NheI*) were chosen according to the pET28a(+) plasmid map (see Figure 3.1). The pET28(+)/PsVAO plasmids were digested using *HindIII* and *NheI* (Table 3.1). Four reaction mixtures were setup containing two control reactions without the enzymes and two reactions with the enzyme (Table 3.1).The isolated DNA plasmids were digested with *HindIII* and *NheI* according to Sambrook and Russell, (2001).

Table 3.1. Preparation of restriction enzyme digestion mixture of the plasmid DNA using *HindIII* and *NheI*.

Components	**Reaction1**	**Reaction1+**	**Reaction2**	**Reaction2+**
Nuclease free water (µl)	34	36	34	36
1X Buffer tank (µl)	9	5	5	5
DNA(µl)	9	9	9	9
***HindIII* (µl)**	1	-	1	-
***NheI* (µl)**	1	-	1	-

3.2.5.5. Agarose gel electrophoresis

An agarose gel was run to confirm if the plasmids contained inserts of the correct size. Agarose gel electrophoretic analysis was done according to Sambrook and Russel, (2001). A gel was made containing 1% agarose in 1 x TAE buffer (Tris-Acetic acid-EDTA, pH 8.2). The gel was cast into a 6 cm x 10 cm x 0.5 cm tray with 10 wells. The O' GeneRuler ladder mix (Life Technologies, Carlsbad, USA) was used in all agarose electrophoretic analysis as the reference of length of DNA in base pairs. Samples were loaded in duplicates, one being a positive control with 6X gel loading buffer (Fermentas; catalogue number R0611). Gel electrophoresis was performed in 1X TAE running buffer in a BioRad PowerPac Basic system at 70 V for 1 hour. DNA in agarose gels was visualised with UV transillumination using Syngene a ChemiGenius Bio-Imaging Gel-documentation system and GeneSnap software (Syngene Vacutech, England). After agarose gel

confirmation a sample of the DNA was sent for sequencing as described in section 3.2.4.to confirm if the gene of interest was still intact.

3.2.6. Expression of the enzyme

Media and buffers

A total volume of 500 ml 20X NPS was prepared containing 0.5 M $(NH_4)_2SO_4$; 1 M KH_2PO_4; 1 M Na_2HPO_4 then filter sterilized with a 0.45 µL syringe filter. A total volume of 50X 5052 was prepared containing 0.139 M glucose, 0.277 M lactose and 2.7 M glycerol then filter sterilized. A total volume of 100 ml of 0.1 M $MgSO_4$ was prepared with H_2O and filtered with a 0.4 µL syringe filter. A total volume of 1 L Zy auto-induction media was prepared containing 1% tryptone and 0.5% yeast extract in water then autoclaved. A total volume of 1L ZYP5052 auto-induction media was prepared from 50 ml (20X NPS), 20 ml (50X 5052), 2 ml ($MgSO_4$) and 928 ml (Zy).

Expression procedure

The transformed BL21(DE3) carrying pET28a(+)/PsVAO was used for expression. The cells were plated on antibiotic selection plates (kanamycin [50 µg/ml]) and incubated overnight at 37°C. A single colony from the overnight incubation was suspended in 10 ml LB broth with kanamycin antibiotic (50 µg/ml) and incubated at 37°C until OD600 reached 0.4-0.8. A total volume of 2 ml solution of that pre-inoculum was inoculated into a 500 mL volumetric flask containing 100 mL of ZYP5052 media and allowed to grow for 36 hours at 20°C with shaking at 200 rpm. Growing the transformed bacteria in this media induces the expression of the protein (Sambrook & Russell, 2001), in this case, vanillyl alcohol oxidase.

3.2.6.1. Sodium dodecyl sulfate polyacrylamide gels

Protein expression and purification steps were monitored by the use of Sodium dodecyl sulfate polyacrylamide gel electrophoresis (SDS-PAGE). The protocol used in this study was adapted from the method described by Sambrook and Russell (2001) and Laemmli (1970). The running gels (12.5% (w/v)) were prepared by mixing 6.25 ml of the monomer solution 30% (w/v) acrylamide (Bio-Rad) and 2.7% (w/v) bisacrylamide (Bio-Rad), 3.75 ml of the 4X running gel buffer (1.5 M TrisCI, pH 8.8), 150 µl of 10% (w/v) SDS (Bio-Rad), 100 µl of 10% (w/v) ammonium persulfate and 4.75 ml nuclease-free H_2O in an Erlenmeyer flask. Prior to use, TEMED was added to a final concentration of 0.05% (v/v). This running gel solution was then poured between the vertical glass plates of the gel casting apparatus (BioRad PowerPac Basic system), up to approximately 3 cm from the top of the glass plates, and overlaid with 1X isopropanol. The gel

was allowed to set at room temperature until an interface between the gel solution and the isopropanol layer could be seen. This took approximately 1 hour. The isopropanol layer was then absorbed by sliding filter paper between the plates. Thereafter, water was added to fill up the space thus washing the remaining solvent. The water was removed the same way with the filter paper.

The stacking gels (4% (w/v)) were prepared by adding 940 µl of the monomer solution (30% (w/v) acrylamide and 2.7% (w/v) bisacrylamide (Bio-Rad)), 1.75 ml of the 4X stacking gel buffer (500m M TrisCI, pH 6.8), 70 µl of 10% SDS (Bio-Rad), 35 µl of 10% (w/v) ammonium persulfate and 4.3 ml nuclease-free H_2O in an Erlenmeyer flask. Prior to use, TEMED was added to a final concentration of 0.1% (v/v). This stacking gel solution was then poured between the vertical glass plates on top of the running gel up to the notch of the glass plates, and a comb was inserted to form the wells. The stacking gel was allowed to set for 30 minutes.
Protein samples were prepared by mixing 15 µl with an equal amount of 4X Dual Color Protein Loading Buffer (Bio-Rad), 2 µl dithiothreitol (reducing agent) and 13 µl nuclease-free water. The samples were boiled for 10 minutes at 98°C, after which they were immediately used for the SDS-PAGE analysis. A volume of 15 µl was loaded onto the gel for electrophoresis. Precision Plus Protein Dual Color Standards (Bio-Rad) (10 kDa to 250 kDa) was used as a molecular size marker, only 5 µl was added to the well.
The gel was then placed in the gel (BioRad PowerPac Basic system) with 1X Tris-glycine-SDS (TGS) buffer (25 mM Tris, 192 mM glycine and 0.1% (v/v) SDS, pH 8.6). For electrophoresis, a constant current of 30 mA was applied for 70 minutes. Thereafter, the gel was removed from the glass plates. For the visualization of the protein bands the gel was placed into a container with Coomassie gel staining solution overnight, with shaking at 50 rpm. For destaining of the gel, it was removed from the Coomassie gel staining solution and rinsed with water to remove excess stain. The gel was resubmerged in a container filled with destaining solution (50% (v/v) methanol, 10% (v/v) acetic acid) with gentle shaking until the blue stain was removed from the gel. The gel images were digitized by scanning (Gel Doc™ XR+ with Image Lab™ Software, Bio-Rad.)

3.2.6.2. Cell harvesting, disruption and enzyme purification

After the expression of the recombinant VAO protein, the protein had to be extracted from the cultured cells. Only one batch of the expressed and purified enzyme was enough for all the subsequent reactions.

Cell harvesting and lysis

After 36hours, the resulting culture was aliquoted into 50 ml falcon tubes, the biomass was harvested through centrifugation (16000 xg, 4°C, 15 minutes). The pellet was kept in a freezer at -20°C until the next step. The frozen pellet was thawed on ice and resuspended in 8 ml of native binding buffer (4 mM Na_2HPO_4, 0.5 M NaCl, 10 mM imidazole). The solution was placed in a beaker with ice and sonicated with the ultrasonic sound probe method. After sonication 8 µl of benzonase was added to the 8 ml solution and incubated on ice for 10 minutes. An aliquot was taken for SDS-PAGE (see section 3.2.6.1) analysis (TGX™ FastCast™ Acrylamide kit, Bio-Rad). The mixture was centrifuged at 16000 xg for 15 minutes and the supernatant was stored as the soluble fraction. An aliquot was taken for SDS-PAGE analysis.

3.2.7. Enzyme purification

Purification of the enzyme was done using Nickel affinity purification using the ProBond™ Purification System (Catalog No. K850-01, Thermo Fisher-scientific) according to the manufacturer's instructions (Thermofisher, 2012). The column was prepared by resuspending the ProBond resin in its bottle by inverting and gently tapping the bottle repeatedly. A volume of 2mL of the resin was pipetted into a 10 ml Purification Column supplied with the kit (ProBond-Thermofisher, 2012). The resin was left to settle completely by gravity for 10 minutes then gently aspirating the supernatant. A volume of 6 ml sterile, distilled water was added to the column and resuspended the resin by inverting and gently tapping the column. The resin was left to settle completely by gravity for 10 minutes then gently aspirating the supernatant.

All the buffers used in purification steps were made from 1X Native Purification Buffer (4 mM Na_2HPO_4, 0.5 M NaCl) and 3M imidazole containing 20 mM sodium phosphate and 500 mM NaCl. A volume of 6 ml Native Binding Buffer (4 mM Na_2HPO_4, 0.5 M NaCl, 10 mM imidazole) was added and resuspended the resin by inverting and gently tapping the column. The resin was left to settle completely by gravity for 10 minutes then gently aspirating the supernatant. The step of Native Binding Buffer was repeated.

The whole 8 mL of lysate prepared under native conditions was added to a prepared Purification Column above. The sample was bound for 45 minutes using gentle agitation thus keeping the resin suspended in the lysate solution. The resin was left to settle completely by gravity for 10 minutes then gently aspirating the supernatant. The supernatant was stored at 4°C for SDS-PAGE analysis. The sample in the column was washed 4X with 8 ml Native Wash Buffer (4 mM Na_2HPO_4, 0.5 M NaCl, 20 mM imidazole) per each run, allowing the resin to settle for 10 minutes and aspirating the supernatant, also stored each supernatant at 4°C for SDS-PAGE analysis. The

column was clamped in a vertical position and snap off the cap on the lower end. The protein was eluted with 8 ml Native Elution Buffer (4 mM Na_2HPO_4, 0.5 M NaCl, 250 mM imidazole), collecting 1 ml fractions and analyze with SDS-PAGE. Samples that showed an enzyme band were pulled together to make one sample and stored the eluted fractions by adding 5% (v/v) glycerol and keep at -80°C. The resin was washed with 0.5 M NaOH for 30 minutes and equilibrated using the Native Binding Buffer, then store at 4°C in 20% ethanol to be able to use the same resin to purify the same recombinant protein.

3.2.8. Enzyme concentration determination

The concentration of the enzyme was determined using the Bicinchoninic Acid (BCA) assay with a linear working range for BSA of 20 to 2000 µg/ml and absorbance at 562 nm for the standard curve (Laboratory protocols mitochondria lab North-west University). A total of six Bovine Serum Albumin (BSA) containing samples were also loaded on the 96 well plate in triplicates covering the range from 20 to 2000 µg/mL Three enzyme samples were prepared, 50X and 71X and one undiluted sample. These samples were also loaded in triplicate of each on the same 96 well plate. The concentration of the enzyme was deduced by relating the concentration of the three enzyme samples to that of the BSA on the standard curve.

3.2.9. Preliminary activity assay to confirm activity of the soluble expressed enzyme.

Relative enzyme activity was measured using the Libra S12 spectrophotometer (Thermo Fisher Scientific). The initial enzyme activity after purification was confirmed using the Libra S12 spectrophotometer.

For the enzyme assays, reaction mixtures were prepared in the form of master mixes. A total volume of 900 µl of the master mixes was prepared, composed of 50 mM potassium phosphate buffer (pH 8) and 1 mM vanillyl alcohol in nuclease-free water. Negative control reactions were set up identically to the positive reactions, but with addition of 100 µl elution buffer instead of enzyme in the samples. Equal amounts (100 µl) of the enzyme (50 µg/ml) samples in triplicates were added to the cuvette, after which 900 µl of the master mix was also added. The reaction mixtures and enzymes were then mixed by briefly shaking the cuvette by hand. The reactions were allowed to proceed for 120 minutes at 25°C and absorbance measurements were taken at 340 nm every 5 minutes.

A vanillin standard curve was prepared for a reference in product quantification. Vanillin has a maximum absorption of light at 340 nm. Samples containing different vanillin concentrations were prepared in a linear working range from 0.000 to 0,025 g/l.

A similar reaction to that of 120 minutes was repeated for 10 hours to determine the initial velocity and the product concentration over a prolonged time in a cuvette.

3.2.10. Optimization of enzyme reaction parameters.

The enzyme reaction time for the plate reader

From the enzyme reactions measured with the spectrophotometer, it was determined that the enzyme reaction reached a plateau after 60 minutes. A series of enzyme reactions were set up to determine the concentration of enzyme that resulted in a linear slope over time.

A vanillin standard curve for the plate reader was prepared in a linear working range from 0.00 to 0.025 g/l. For the enzyme assays, reaction mixtures were prepared in the form of master mixes for the sake of convenience and accuracy. The master mixes were composed of 50 mM phosphate buffer (pH 8), 1 mM (0.154 mg/ml) vanillyl alcohol, variable volumes of elution buffer (0.250 M imidazole, 0.05 M NaH_2PO_4, 0.5 M NaCl) (see table 3.9) with exception of the enzyme sample making a final volume of 210 µl. Negative control reactions were set up identically to the positive reactions, but with the enzyme omitted from the reaction mixture on starting the reaction. The enzyme and the master mix were added to each well of the 96-well plate in triplicates (Table 3.2).

Table 3.2. Enzyme reactions to determine the protein concentration that results in a linear reaction time. Concentration of components added to each well of the 96-well plate for the enzyme reaction with a total volume 210 µl.

Vanillyl alcohol oxidase concentration (µg/ml)	vanillyl alcohol concentration (mg/ml)	Potassium phosphate buffer (mM)	Elution buffer volume (µl)	Total reaction volume (µl)
0	0.15	50	10.5	210
10	0.15	50	8.8	210
20	0.15	50	6.6	210
30	0.15	50	4.4	210

40	0.15	50	2.5	210

The reaction was started by adding the enzyme according to volumes in table 3.2 above. The reaction mixtures and enzymes were then mixed by briefly shaking the plate for 10 seconds. For analysis a BioTek plate reader and accompanying Gen5 software were used. The reactions were allowed to proceed for 60 minutes at 30°C and absorbance measurements were made at 340 nm every 5 minutes.

The temperature of reaction was used according to the plasmid supplier's recommendation (Van Rooyen, 2012).The reaction optimization for substrate concentration was not done practically. However, for the aim of the experiment, only higher substrate to enzyme ratio was required. Therefore, it was shown with the reactions on optimizing enzyme concentration using 1 mM (0.154 mg/ml) of substrate that the substrate was not a limiting factor and therefore considered using 1 mM vanillyl alcohol throughout

3.3. Vanillyl alcohol oxidase reaction in the synthetic HTL aqueous phase

In this section, a detailed list of reagents used for the preparation of reaction mixtures is given (section 3.3.1, Table 3.3). A subsection is compiled of how the synthetic aqueous phase was prepared, section 3.3.2. Vanillyl alcohol substrate was used in the same manner described in section 3.2.10. A concentration of 50 µg/ml enzyme was used see section 3.2.10.

The absorbance of the product (vanillin) was monitored. Before the preparation of the synthetic aqueous phase, the first step was to determine the concentration of each known compound mainly phenolics, sugars and metal ions in the HTL aqueous phase. This was done in another project in the same lab by another MSc student (work not published yet). In their project, they did hydrothermal liquefaction of sewage sludge biomass at 300°C for 20 minutes. Then from the liquefied products thus where the aqueous phase was sourced for this project. Already there were figures from HPLC, and ICP to show the composition of the aqueous phase from this liquefaction process.

3.3.1. Reagents

For the synthetic aqueous phase, commercial reagents were purchased from different companies.

Table 3.3. A detailed list of reagents.

Chemical name	CAS #	Purity (%)	Density (mg/ml)	Supplier
Guaiacol	90-05-1	99	1.129	Merck
Catechol	50-00-0	98	1.09	Sigma Aldrich
Vanillin	121-33-5	99	1.06 g/cm3 (20 °C)	Merck
Vanillyl alcohol (p-VA)	498-00-0	98	Not specified	Sigma Aldrich
Vanillyl alcohol (m-VA)	4383-06-6	98	Not specified	Sigma Aldrich
Phenol	108-95-2	99.5	Not specified	Sigma Aldrich
Vanillic acid	121-34-6	97	Not specified	Sigma Aldrich
Acetic acid				
H_2KPO_4	7778-77-0	99	Not specified	Sigma Aldrich
$HK_2\ PO_4$	7758-11-4	98	Not specified	Sigma Aldrich

3.3.2. Preparation of the synthetic aqueous phase.

In order to determine the effect of the components in the aqueous phase on enzyme activity, a detailed list of the major components of the HTL aqueous phase was compiled with reference to HPLC analysis (Table 3.4).

Table 3.4. Reference concentrations of each component as detected by HPLC in the original aqueous phase from HTL

Component	Aqueous phase concentration (g/l)
Vanillyl alcohol	0.52
Vanillic acid	0.05
catechol	0.01
phenol	0.05
Guaiacol	0.01
Acetic acid	0.91

According to the concentrations from HPLC analysis (Table 3.7), samples were prepared with the same ratio but different compositions using commercial reagents. A synthetic HTL aqueous phase was prepared from commercial reagents because the original sample was too dark so it cannot absorb light on a single wavelength for vanillin only. Furthermore, the aim was also to determine

the effect of individual as well as combinations of the components in the aqueous phase. To make up 1 mM (0.154 g/l) vanillyl alcohol, each of the component concentration in table 3.4 above was diluted 3.4 times (Table 3.5).

Table 3.5. Representation of the concentration of phenolic compounds and acetic acid used to make up synthetic aqueous phase for the enzyme reaction.

Component	Concentration of each component (g/l)
Vanillyl alcohol	0,152
Vanillic acid	0,015
Catechol	0,003
Phenol	0,015
Guaiacol	0,003
Acetic acid	0,266

A total of eleven different reactions in triplicates were set up (Table 3.6). The reactions contained two negative control reactions without the enzyme and one other control with enzyme but no the substrate. The two negative controls only differ in that the other one contains acetic acid and the other does not. The positive control only contained vanillyl alcohol and the enzyme. The rest of the reactions contained both the enzyme and the substrate in similar proportions with customized phenolic compounds and acetic acid per each reaction see table 3.6. The reaction was started by adding the enzyme according to concentrations shown in table 3.6. In each sample a calculated volume of deionized water was added to make up the total volume of 210µl in each well. A spectrophotometer (microplate reader) was set at 30°C and allowed to shake for 10 seconds before addition of the enzyme and starting the A340 absorbance readings (Benen *et al.*, 1998). Readings were taken for 60 minutes with 5 minutes' intervals.

Table 3.6. Representation of the concentrations of the components in each of the eleven enzyme reactions making up to a total volume of 210 µl in each well of the microplate.

	Reaction number										
Components	1	2	3	4	5	6	7	8	9	10	11
Phosphate buffer pH 8 (mM)	50	50	50	50	50	50	50	50	50	50	50
Enzyme (µg/ml)	-	-	50	50	50	50	50	50	50	50	50
Vanillyl alcohol (g/L)	0.152	0.152	-	0.152	0.152	0.152	0.152	0.152	0.152	0.152	0.152
Vanillic acid (g/L)	0,015	0,015	0,0150	-	0,015	-	-	-	-	0,015	0,015
Catechol (g/L)	0,003	0,003	0,003	-	-	0,003	-	-	-	0,003	0,003
Phenol (g/L)	0,015	0,015	0,015	-	-	-	0,015	-	-	0,015	0,015
Guaiacol (g/L)	0,003	0,003	0,003	-	-	-	-	0,003	-	0,003	0,003
Acetic acid (g/L)	-	0,266	-	-	-	-	-	-	0,266	-	0,266
Total volume (µl)	210.00	210.00	210.00	210.00	210.00	210.00	210.00	210.00	210.00	210.00	210.00

CHAPTER FOUR

RESULTS AND DISCUSSION

4.1. Guaiacol conversion to vanillyl alcohol

In this section, the effect of reaction time on the product yield percentage was also observed. Other parameters (methanol content and acid catalyst) were used as described in literature (Cavani *et al.*, 2002). The overall reaction was considered at estimated overall optimum pH and time and used to show the overall yield (w/w) with time. The difference in selectivity of the two major product of the carboxylation of guaiacol (para vanillyl alcohol and meta vanillyl alcohol) was also reported in terms of yield percent by mass. The overall yield by mass, achieved for the para vanillyl alcohol product is also discussed as the para vanillyl alcohol is of main aim to this project. The conversion recorded as yield (%) was calculated from the mass of the products at all times.

4.1.1 The effect of temperature and pH on guaiacol conversion to vanillyl alcohol

Temperature plays a very important role in the conversion of guaiacol to vanillyl alcohol. At ow temperatures, around room temperature, the rate of reaction is almost zero. This is due to limited interactions as the kinetic energy of collision between the guaiacol and the formaldehyde molecules is low (Atkins *et al*., 2017). On the other hand, at very high temperatures above 100°C, it is easy to the formation of byproducts rather than vanillyl alcohol. The formation of these byproducts is due to the instability of water and methanol. At or above their boiling points, the two solvents will exist in the vapor phase thus leading to the change of formalin (stabilized formaldehyde with methanol), into diaryl compounds (Cavani., *et al.*, 2002). A fixed temperature of 80ºC was used with variable pH samples in order to determine the optimum pH (Figure 4.1).

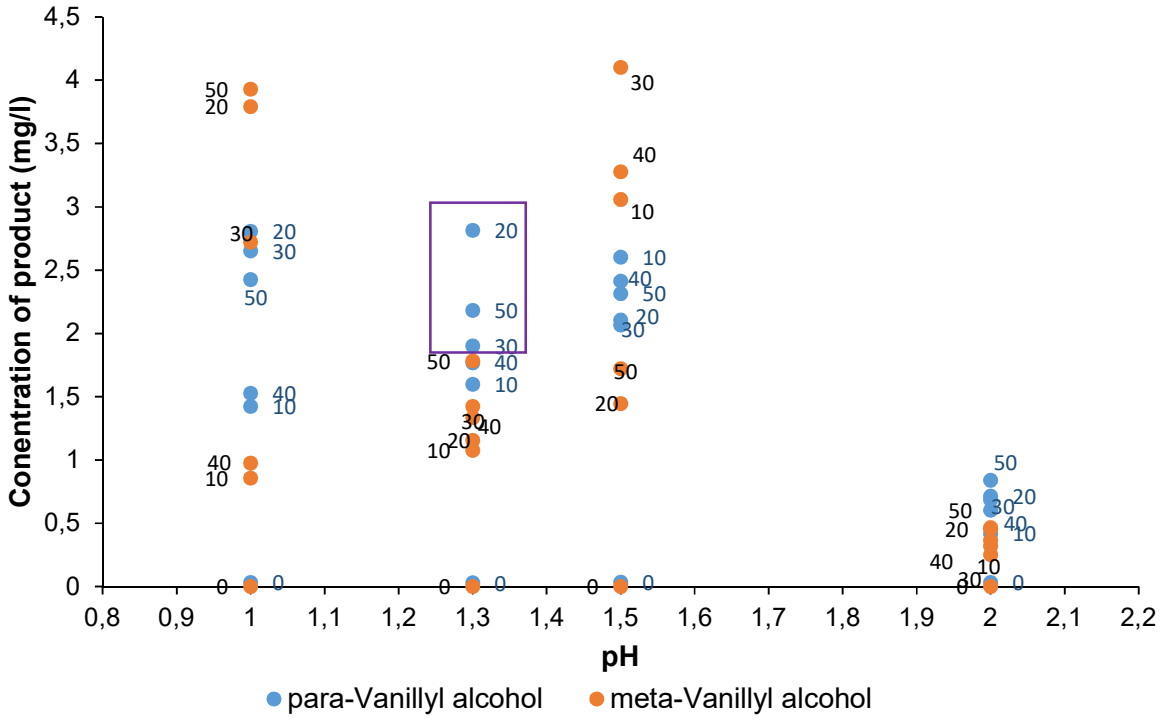

Figure 4.1. Concentration against pH of the para (●) and the meta (●) products at each time interval during the conversion of guaiacol to vanillyl alcohol. Different times per each pH are shown as data labels next to each data point.

From a reaction setup described in chapter three, section 3.1.3, the yield of vanillyl alcohol was recorded as shown in figure 4.1. Vanillyl alcohol can be either para (p-VA), meta (m-VA) and/or ortho (o-VA) according to the position of the CH_2OH group on the phenolic ring (McMurry, 2012). Because of the OCH_3 group on the ortho position chances are close to zero for a single substitution to take place on the other ortho side without the OCH_3 group, therefore only meta and para positions are highly favoured (McMurry, 2012). HPLC analysis was used to determine the p-VA and m-VA product concentration. The results were presented in forms of chromatograms that shows the peak areas. These chromatogram areas were then used together with the calibration curves to calculate the concentration and thereafter the yield.

From figure 4.1, four reactions were set up with only one different parameter from each other, which is pH. In this case, the resulting concentration of the two vanillyl alcohols products was used to plot the graph and deduce the most favorable pH. It is shown on the graph that, at pH 1 comparing the selectivity of para and meta vanillyl alcohol yield from zero to 50 minutes that meta yield is higher than the para overall. This means that during the progress of the reaction there is

more meta substitution than para substitution. Therefore, pH 1 is not ideal for the aim of the reaction. Considering pH 1.3, there is a higher selectivity to p-VA compared to m-VA throughout the 50 minutes of reaction. At pH 1.5, the same trend of higher meta selectivity than para selectivity as pH 1 was observed. At pH 2, the para selectivity is higher (maximum 0.84 mg/ml compared to maximum 0.45 mg/ml for meta). The same trend of higher para selectivity is shown at pH 1.3 (maximum 2.81 mg/ml compared to maximum 1.78 mg/ml for meta). From these four trends, it becomes apparent that there is a marginal difference in selectivity between the para and meta vanillyl alcohols with higher p-VA than m-VA at pH 1.3 (Ardizzi *et al.,* 2005). However, to conclude that pH 1.3 is ideal for the optimized reaction yield, a comparison was done on the optimum concentrations of each reaction. Considering the para products, the highest yield in terms of concentration is observed at 20 minutes (2.81 mg/ml) and 50 minutes (2.18 mg/ml) pH 1.3, this is in line with the selectivity observation. As highlighted in purple on the graph, there is not any meta selectivity above these para data points unlike on all the other treatments where the meta is the highest. Therefore, pH 1.3 was deemed the optimum pH of the reaction at 80°C.

Considering pH 1.3, the optimum temperature for the reaction was investigated. Four different temperatures were chosen considering that a too low temperature will fail to initiate the reaction and a too high temperature will destabilize formalin (Cavani *et al.,* 2002). This was done in a temperature range of 55 to 90°C (Figure 4.2).

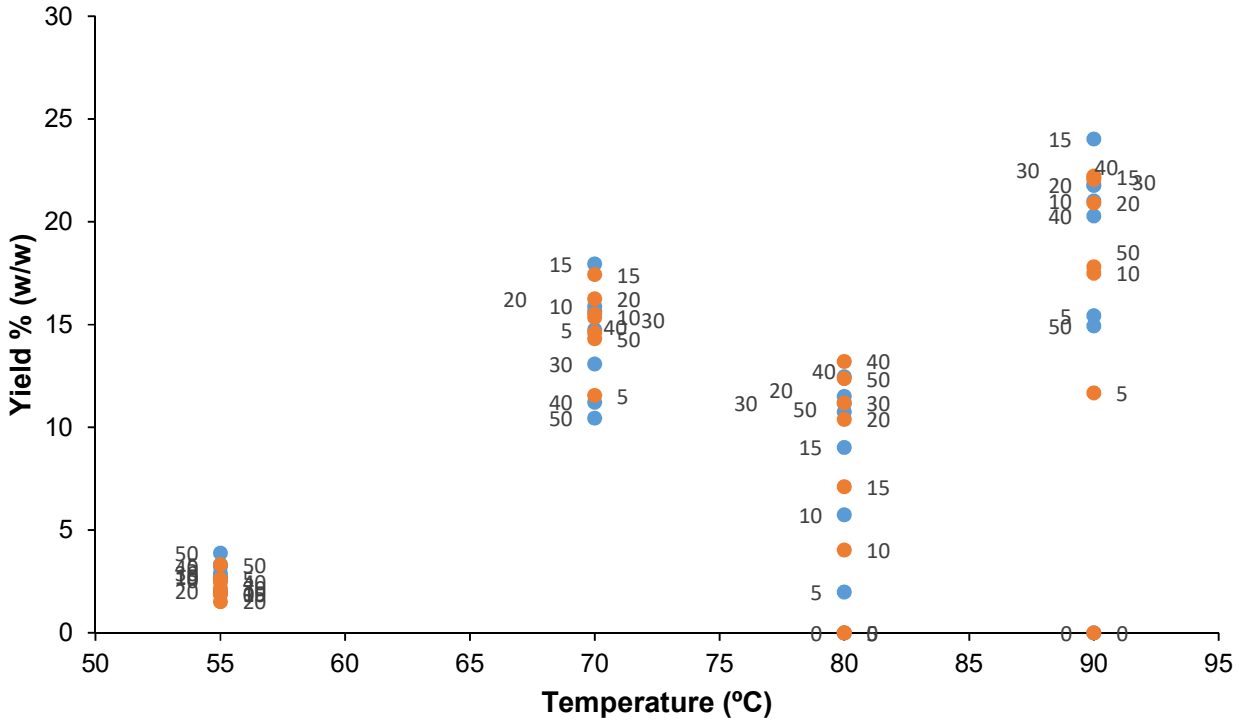

Figure 4.2. The yield percent for each of the vanillyl alcohol para (●) and the meta (●) products at a given temperature during the conversion of guaiacol to vanillyl alcohol. The time of the reaction is given inside the chat in labels (para on the left and meta on the right side of the series) representing temperature in ºC.

Conversion of guaiacol towards para-vanillyl alcohol at temperatures 55, 70, 80 and 90°C was reported as shown in figure 4.2. From figure 4.2, both the meta and the para yield was recorded for each temperature. The same analysis was used as described for figure 4.1. However, in this case it was necessary not only to record the concentration as in figure 4.1 but to consider how much the output in terms of yield percent is. The yield percent was calculated from the converted guaiacol considering the mass converted, the para and meta vanillyl alcohols at each temperature. All the other products were recorded as by-products.

At temperature 55, as shown on the graph, both the meta and p-VA had a maximum yield lower than 5% with a greater para selectivity. At 70°C there is a higher selectivity towards the p-VA in the first 15 minutes then thereafter the m-VA selectivity becomes greater. At this temperature, the p-VA yield increases to an optimum yield of approximately 18% at time 15 minutes then decreases thereafter. At 90°C it is clear that there is the highest optimum yield of approximately 24%.

Therefore, there is a higher selectivity to para up to nearly 30 minutes with an optimum yield at 15 minutes (Figure 4.3).

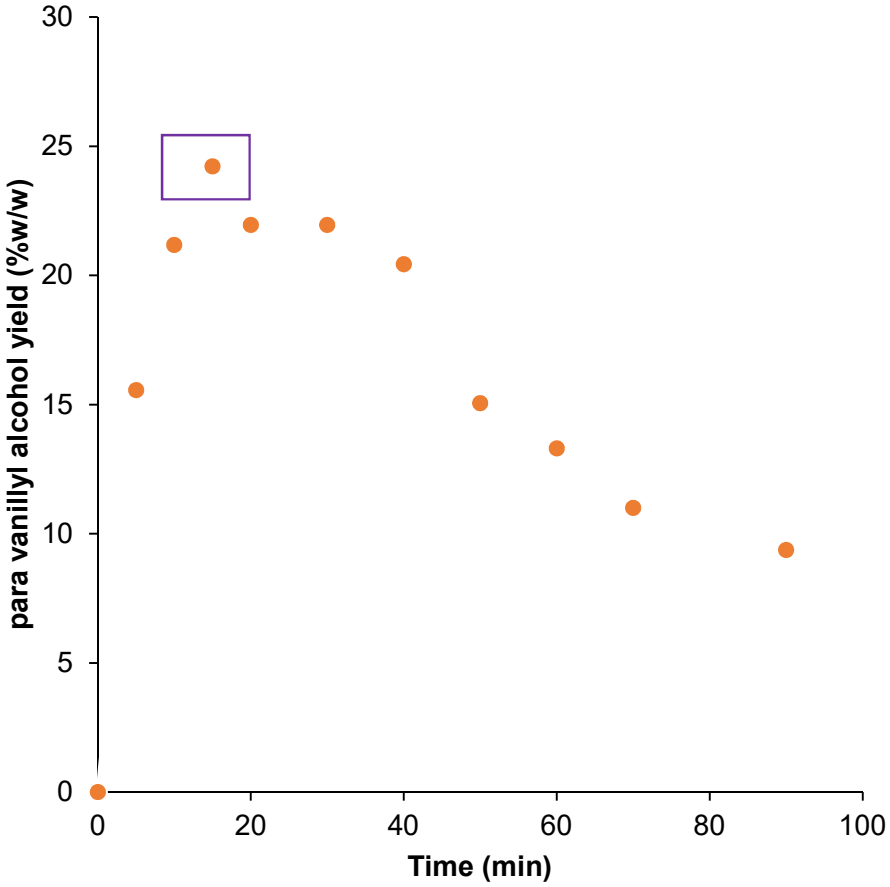

Figure 4.3. Reaction yield of para-Vanillyl alcohol from formaldehyde and guaiacol at optimum temperature (90°C) and pH (1.3) within 90 minutes' reaction time.

A clear extract of optimum pH and temperature graph is presented in figure 4.3 above. It is shown that there is a sharp linear increase in yield in the first 15 minutes. Thereafter the para product formation starts to decrease very slowly for 20 minutes. After 40 minutes there is a sharp decrease from 21% to 15% within 10 minutes, the decrease continued down to 9% in 90 minutes of reaction. The last 20 minutes of the reaction can be recorded as constant as there is only a 2% percent decrease within the 20 minutes. Accounting for the possible factors that lead to product depletion, figure 4.4 was considered.

However, from this experimental data, there is a possibility of error at time 15 minutes. Considering the raw data from the chromatograms in terms of area (see index), there is no

observable possibility of outliers for data used to calculate the average yield. The data point at 15 minutes in terms of observable area on the chromatogram, shows that at 15 minutes there is still an increase to get to 20 minutes. By calculation now for the yield a different case is reported due to changes in volume when an aliquot is removed. Therefore, in this account, the data was considered as it is for discussion purposes, but however a different approach can be used in future experiments to see if there will be any difference.

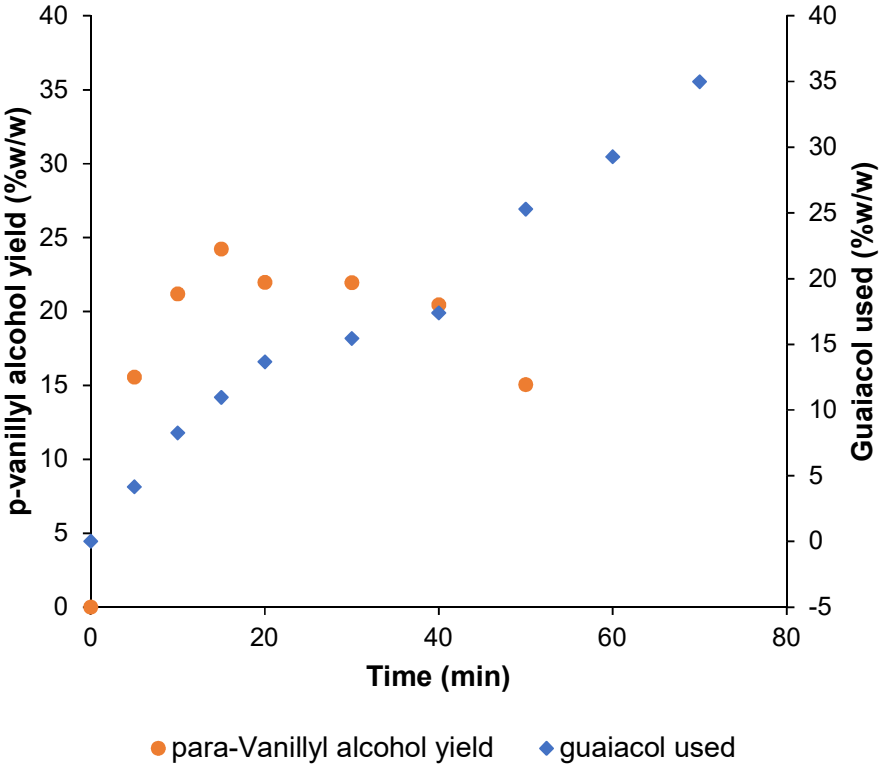

Figure 4.4. Amount of guaiacol used (secondary axis) and para vanillyl alcohol yield as functions of time.

A trend line in yellow shows the behavior of guaiacol within the 70 minutes of reaction. From the above figure, guaiacol used increases with time with approximately 35% guaiacol being converted within the 70 minutes of reaction. The rate of increase of guaiacol used increases sharply in the first 25 minutes, thereafter it started to level off for about 20 minutes. After 45 minutes there is an observable linear sharp increase up to 70 minutes. However, it is of paramount importance to trace how much of the guaiacol is channeled towards our product. A graph of the yield percentage of para vanillyl alcohol, shows that the optimum yield of p-VA is at 15 minutes despite an error if any. Within 15 minutes only approximately 10% of guaiacol have been converted. Therefore, 10%

guaiacol converted has its 24% channeled to p-VA and the other 74% to m-VA and byproducts (reaction scheme figure 4.5).

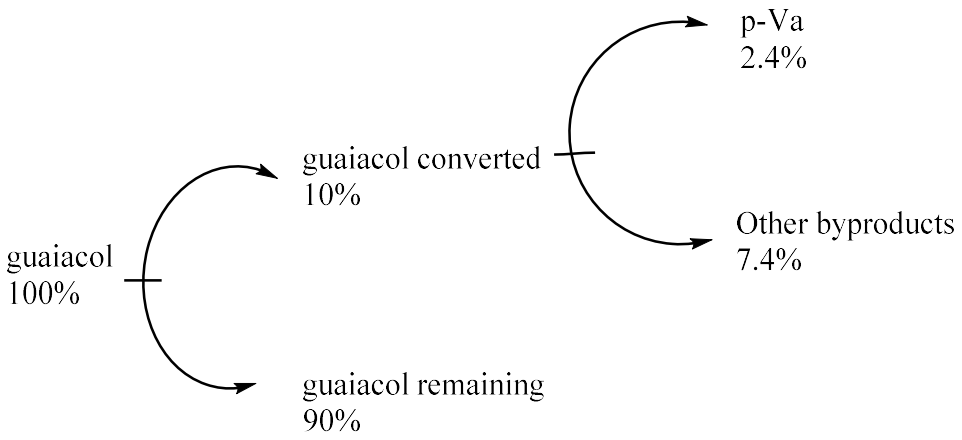

Figure 4.5. Outline of percentage conversions of guaiacol at 15 minutes' reaction time.

Under optimum conditions, at 15 minutes, 24% of para vanillyl alcohol is formed and this relates to the converted 10% guaiacol. From the 10% converted guaiacol thus only 2.4% results in para-vanillyl alcohol as depicted in figure 4.5. About 90% of the guaiacol remain unused at this 15-minute reaction time. However further increase in reaction time, figure 4.4, shows that as guaiacol conversion levels off, also vanillyl alcohol does the same. The sharp increase in guaiacol used and also a sharp decrease in vanillyl alcohol at the same time after a levelling off shows a change in reaction behavior. Possibilities are, when the reaction levels off, the reaction is reaching equilibrium. Therefore, from this point the guaiacol is channeled towards other products depicted as by-products in this reaction data analysis. The fall of the vanillyl alcohol yield in this instance shows that vanillyl alcohol is channeled to other products. However, the degradation of vanillyl alcohol should also favour an equilibrium shift thus guaiacol should start forming vanillyl alcohol to close the gap and therefore vanillyl alcohol remain constant. An assumption can be that there is now limited formaldehyde for vanillyl alcohol formation, therefore, guaiacol cannot compensate for vanillyl alcohol because of this limit.

According to Cavani et al. (2002), methanol stabilizes formaldehyde to remain formalin. In this reaction, there is another possibility of methanol evaporation at 90°C, though in a condensed flask. The methanol might remain all gaseous above the liquid solution thus favouring more the

formation of diaryl compounds from both guaiacol and formaldehyde (Bolognini *et al.*, 2004). The formed product now decreases to meet equilibrium with the guaiacol being converted. A better explanation of equilibrium position is shown in figure 4.4 where the p-VA remains almost constant for 20 minutes from time 20 minutes to 40 minutes then a sharp decrease. But in this case, guaiacol degradation favors byproducts formation, therefore the p-VA will also be converted to by-products with time. Under heterogeneous conditions, long reaction times leads to catalyst deactivation. This results in the irreversible vanillyl alcohol etherification with methanol and the selectivity to p-VA drops quickly (Cavani *et al.,* 2002).

4.2. Enzyme production from DNA

In this section we report the results and discussion of each step of vanillyl alcohol oxidase production and purification. The results and discussion include sequencing of the recombinant pET28a(+)/PsVAO plasmid, agarose gel electrophoresis after restriction enzyme digestion to confirm the PsVAO insert size, transformation of pET28a(+)/PsVAO into *E. coli* BL21(DE3) cells and expression and purification of VAO which was confirmed by SDS-PAGE analysis. The concentration and activity of the purified protein were determined according to protocols in sections 3.2.8 and 3.2.9, respectively.

4.2.1. Sanger sequencing and data analysis of the PsVAO insert

The sequence of amino acids of an enzyme, mainly the active site amino acids is critical for the function of the enzyme. Any alteration of these amino acids due to mutations can lead to the enzyme losing its function. Therefore, the first step prior to transformation of pET28a(+)/PsVAO was to sequence the insert using the T7 promoter and T7 terminator primers. The reference sequence used in this study was VAO: EC 1:1:3:38 (Accession: 5MXU_A, NCBI) (Figure 4.6). The concentration of the pET28a(+)/PsVAO sample which was sent for sequencing was determined to be 98.8 ng/µl after concentration using the SpeedVac (see section 3.2.4).

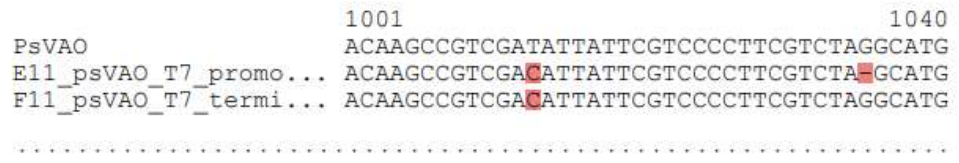

Figure 4.6. The aligned sequences of the PsVAO insert and the sequences generated by the forward and reverse primers. These sequences confirmed that the PsVAO gene was successfully

inserted into the pET28a(+) vector with a mutation at position 1013 bp. (for full alignment see Appendix A).

In order to confirm the effect of the mutation on the amino acid sequence, the translation of the PsVAO nucleotide sequence was compared to that of the reference sequence (Figure 4.7).

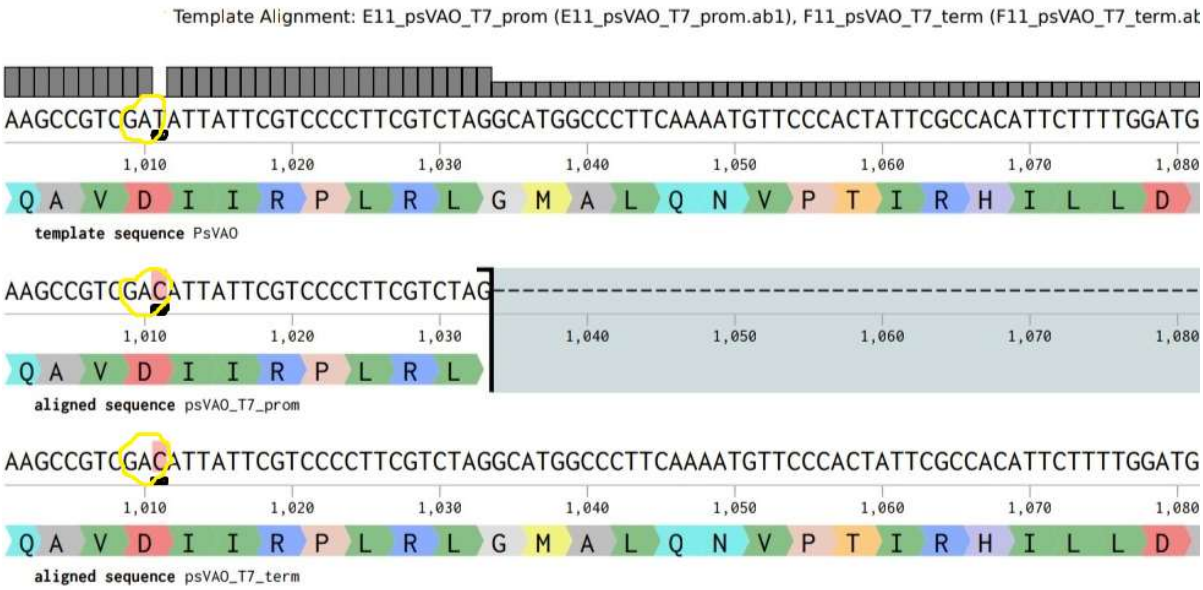

Figure 4.7. A section of the multiple sequence alignment with the corresponding amino acid translation. From the top is the reference sequence, followed by the sequence generated by the T7 promoter primer and then the T7 terminator reverse primer at the bottom.

The sequencing results confirmed a mismatch at nucleotide position 1011bp as shown in figure 4.6. However, translation of the DNA sequence to protein sequence confirmed that the mutation did not result in a change in the amino acid sequence. Both GAC and GAT codons code for the same amino acid asparagine, thus it can be concluded that there is a silent mutation in the gene sequence and this will not affect the structure of the enzyme. The amino acids that are coded by the DNA showed a corresponding match to the amino acid sequence for the *Penicillium simplicissimum* sourced vanillyl alcohol oxidase (PsVAO) gene (accession Y15627.1) with a 100% similarity on protein-protein blast (Madden, 2013).

4.2.2. Transformation of the recombinant pET28a(+)/PsVAO plasmid

Having confirmed that the PsVAO sequence is correct, the next step was the transformation of pET28a(+)/PsVAO into the *E. coli* BL21(DE3) bacterial cells. The process of making competent

BL21(DE3) cells was confirmed by the formation of colonies on a kanamycin plate (Sundar & Sakthivel, 2008). These colonies also show the successful transformation of pET28a(+)/PsVAO. The kanamycin antibiotic resistance gene characteristic of the pET28a(+) helps to identify if the pET28a(+)/PsVAO is successfully transformed into BL21(DE3) bacteria cells. A successful transformation of pET28a(+)/PsVAO is shown by colonies growing in a time frame of 12 to 24 hours. However, this alone cannot give an indication on whether the plasmid transformed contains the PsVAO insert. To confirm if the insert is in the pET28a(+) plasmid, a single colony from the transformation plate was grown in an antibiotic containing LB broth. A positive growth was depicted by an increase in optical density at 600 nm with time. From the resulting culture, the biomass was harvested, lysing the *E. coli* BL21(DE3) cells and isolating the pET28a+/PsVAO using a plasmid extraction midi-prep kit (Section 3.2.5.3). The plasmid was digested using the same restriction enzymes *(HindIII and NheI)* that were used to ligate the gene into the plasmid thus excising the PsVAO gene from the pET28a(+)/PsVAO plasmid. An agarose gel was used to confirm a successful restriction enzyme digestion (Figure 4.7).

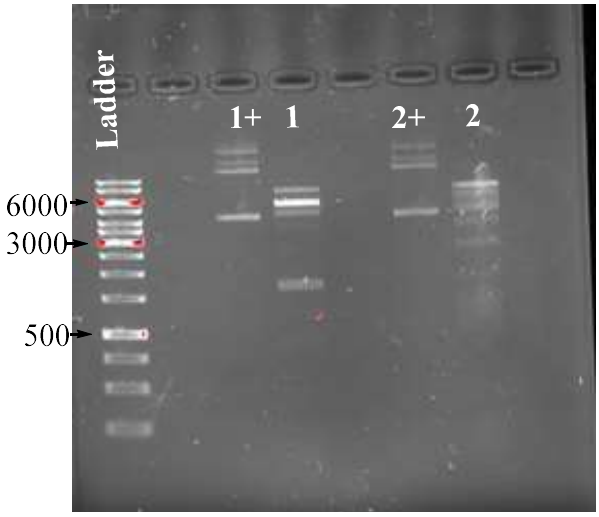

Figure 4.8. Agarose gel (1%) electrophoresis of the *HindIII and NheI* restriction enzyme digestion of pET28(+)/PsVAO. Lanes 1+ and 2+ are the undigested control samples and lanes 1 and 2 contain the plasmid and insert after restriction enzyme digestion.

The recombinant pET28a(+)/PsVAO plasmid has a total of 7000 bp (See Figure 3.3). The length of the ligated PsVAO gene into pET28a(+) is approximately 1695 bp (Benen *et al.*, 1998).Therefore the pET28a(+) linearized plasmid is approximately 5305 bp as shown by the intense white band in lane 1. In figure 4.8 samples labeled sample 1 and sample 2 are the recombinant plasmid after restriction enzymes digestion with *HindIII* and *NheI*. With reference to the DNA ladder and the control samples, sample1+ and sample2+, it is shown that in sample 1, there is a band at approximately 1695 (between 3000 bp and 500bp) bp which corresponds to the expected base pairs of the ligated PsVAO gene.

However, this only showed that an insert of the correct size was present. It was, therefore, still necessary to confirm the PsVAO sequence by Sanger sequencing. The sequencing results corresponded to the alignment reported in figure 4.6 and Appendix A.

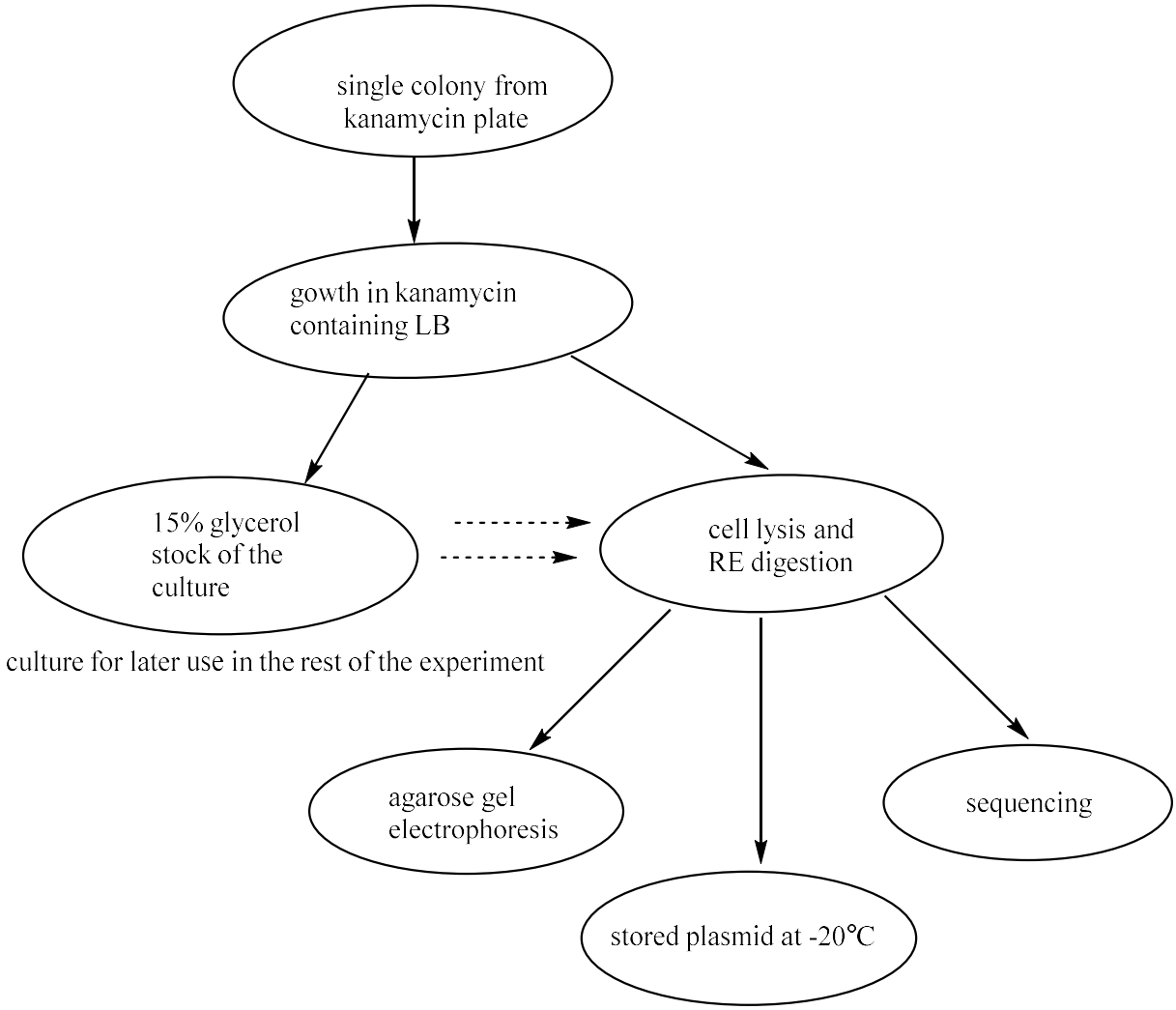

Figure 4.9. Summary of the steps involved in DNA preparation how it was used.

4.2.3. Enzyme expression and purification

Enzyme expression involves the DNA transcription and mRNA translation to amino acids, thus a sequence of peptide bond bound amino acids make up the protein (Crick, 1970). The N terminal His-tagged PsVAO enzyme was expressed in the *E. coli*, BL21(DE3) bacterial cells. The His-tag helps with enzyme purification. Multiple consecutive histidine residues of the proteins allows binding to the nickel column, and the protein will only be released at a higher imidazole gradient (Hochuli *et al.*, 1988).

After ultrasonic sound cell disruption, the total fraction and soluble fraction collected had a negligible difference in band intensities at 65 kDa (figure 4.9). This result shows both successful cell lysis and solubility of the enzyme (McCormick *et al.*, 2014).

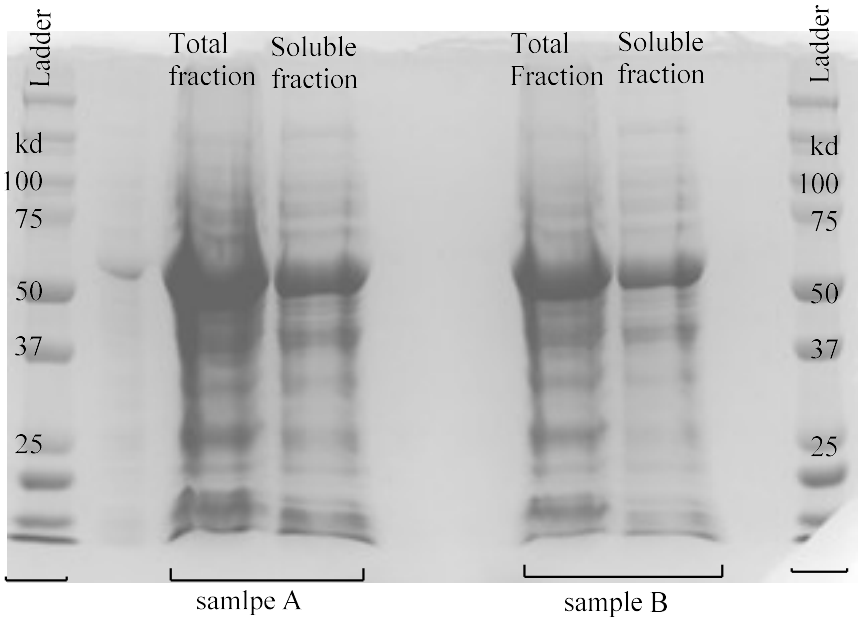

Figure 4.10. Total fraction and soluble fraction of duplicate samples A and B from the same expression after 36 hours using the ultrasonic sound sonication method of cell lysis. The ladder (Precision Plus Protein Dual Color Standards #161-0374 (10 kDa to 250 kDa) act as the reference for the molecular weight of each corresponding band.

Purification was done for ease of quantification and activity determination of the enzyme. The ProBond purification kit was used for purification, where a nickel resin column is used to bind to the six His tag terminal of the protein at low imidazole concentration then eluted at higher concentrations of imidazole (Thermofisher, 2012). Successive wash steps were involved (Figure 4.11a). Washing steps showed no bands at 65 kDa, which confirms that there was no protein lost at this step (Figure 4.10a). The protein elution step resulted in a single, high-intensity band (Figure 4.11b). The single protein band highlight that the protein was pure and the higher intensity highlights a high concentration of the enzyme.

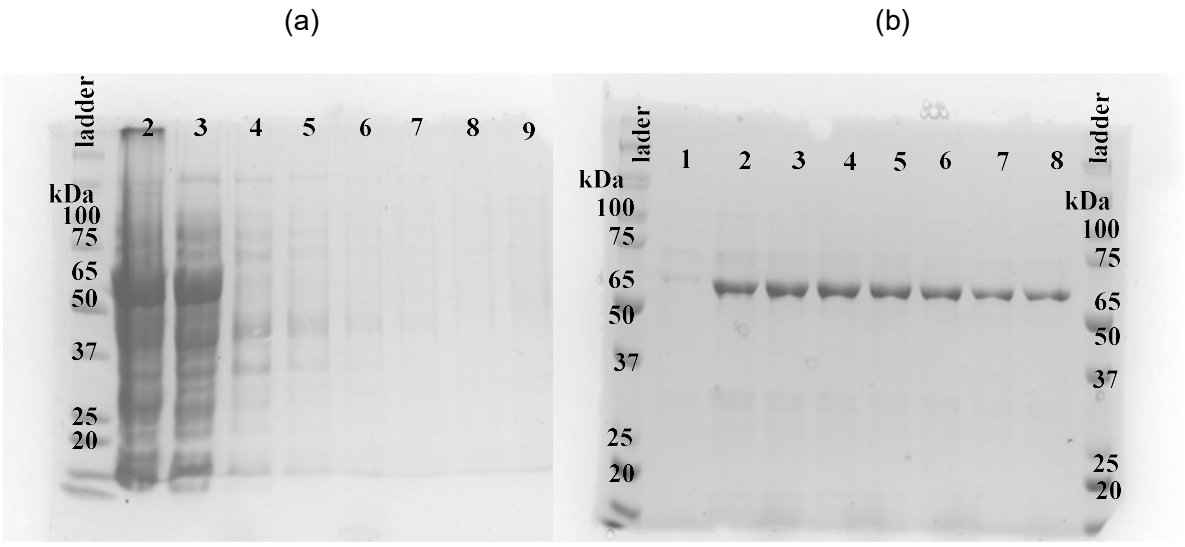

Figure 4.11. (a) A 12,5% SDS-PAGE running gel showing protein bands after purification of the enzyme under native conditions of a small scale (8 ml culture) expressed over 36 hours. Lane 1-ladder; 2-total fraction; 3-soluble fraction; 4-9-wash steps. (b) Lanes 1-8 are elution aliquots.

4.2.4. Enzyme concentration determination using the Bicinchoninic Acid (BCA) method

From the 50 ml culture used for expression, 8 ml of the enzyme was obtained after the purification elution step. The concentration of the enzyme was determined using the BCA assay in a 96 well microplate reader at 562 nm against a Bovine serum albumin (BSA) standard curve (Figure 4.12)

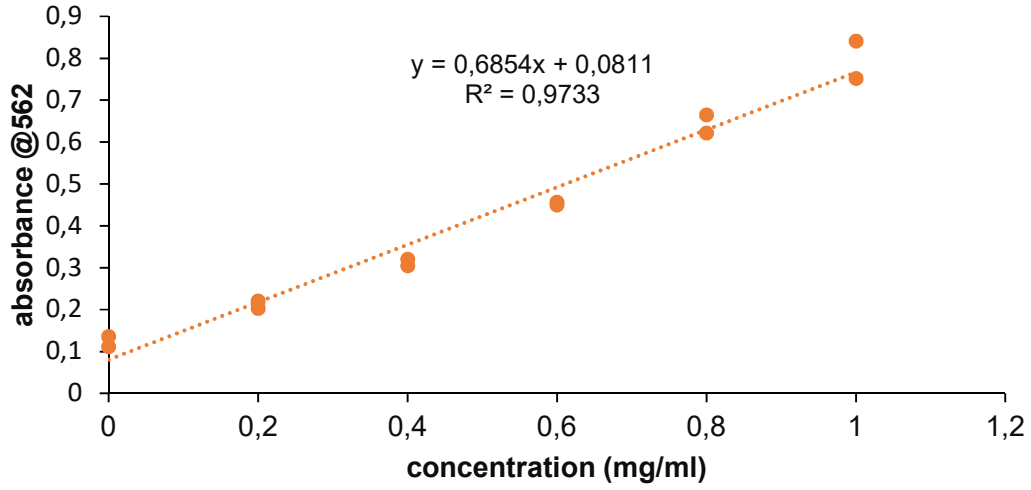

Figure 4.12. BCA standard curve showing the relationship between absorbance and concentration (mg/ml) of the protein. The samples were done in duplicates.

From figure 4.12 the standard curve equation of vanillyl alcohol oxidase obtained from results in is defined by $f(x) = 0.6854x \times 0.0811$ The concentration of the three samples of vanillyl alcohol oxidase was calculated from the standard curve. Three enzyme samples, in triplicates, undiluted (absorbance; 1.656,1.664, 1.599), 50% (absorbance; 0.838, 0.815, 0.837) and 71% (absorbance; 0.514, 0.524, 0.526) diluted gave an average of approximately 2.2 mg/ml of the enzyme.

4.2.5. Preliminary activity assay to confirm activity of the soluble expressed enzyme

The activity of the enzyme was tested using a colorimetric method in a 1 ml cuvette on Libra S3 spectrophotometer. The graph (Figure 4.13) illustrates that there is a linear increase in absorbance with time. This reveals that there is a product formed due to vanillyl alcohol oxidase. A control reaction without enzyme showed a constant absorbance with time. Therefore, these results highlight that a compound absorbing at 340 nm is formed and this is vanillin. The activity assay at this point was only used to confirm that the expressed soluble enzyme was indeed active. No quantification was done at this stage.

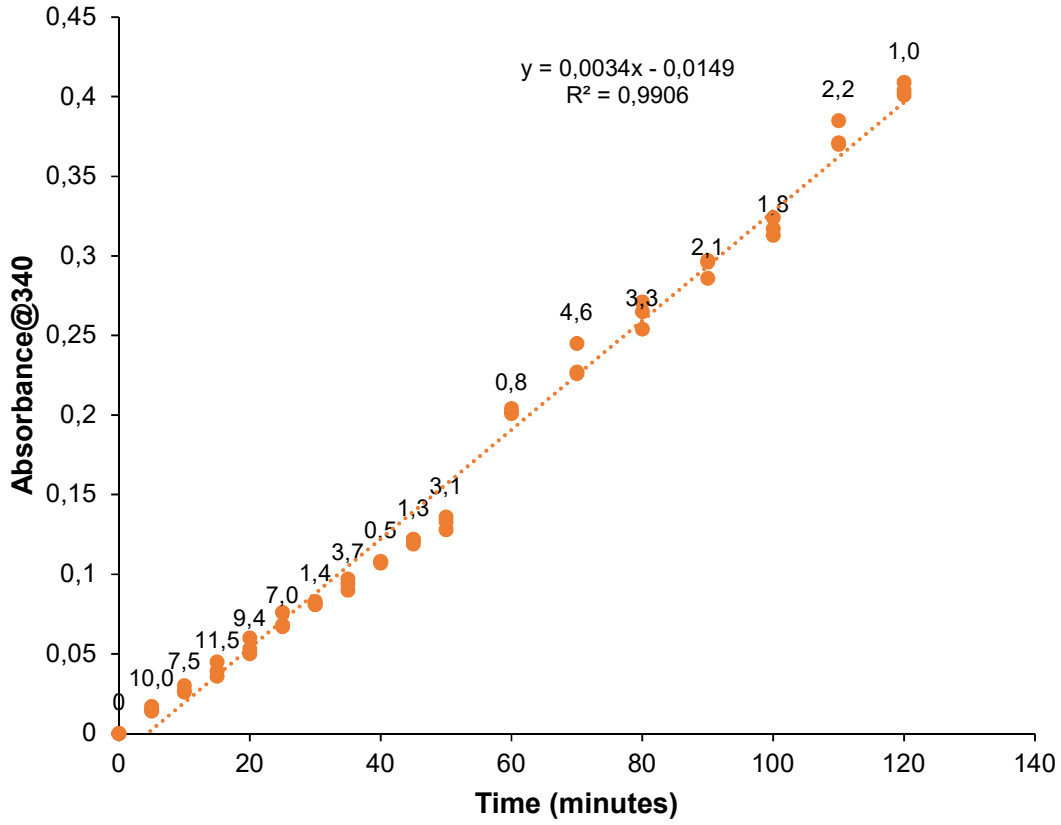

Figure 4.13. Change in absorbance with time of vanillyl alcohol oxidase, an activity test. Each result was done and recorded in triplicates at five minute intervals. The data labels in numbers shows the CV% of each triplicates at a given time.

A vanillin standard curve with a working concentration range from 0 to 0.025 mg/ml was set up to relate absorbance at 340 nm to vanillin concentration using a 1 ml cuvette. This relationship gave the equation of a straight line $y = 122.56x + 0.0163$. (Figure 4.14).

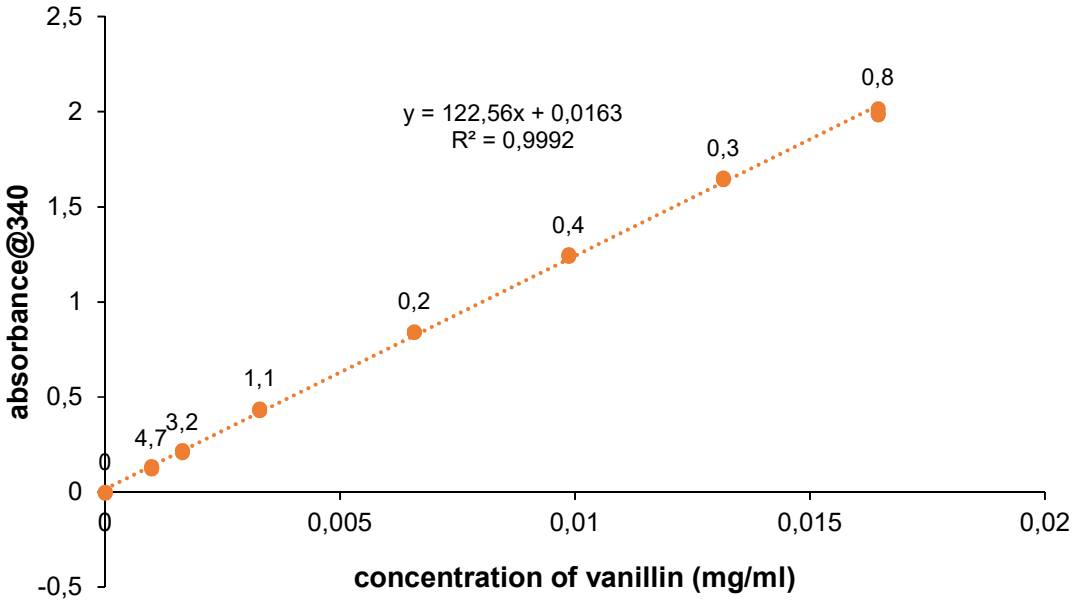

Figure 4.14. Vanillin standard curve using LibraS12 spectrophotometer with 1 ml volume in a cuvette at 340nm. The data is in triplicates and labels above each data point shows the CV%.

In order to determine the initial velocity of the enzyme (Figure 4.15), the enzyme reaction was allowed to proceed for several hours (10 hours) using 1 mM (0.154 mg/ml) vanillyl alcohol and 50 µg/ml of the enzyme Initial velocity is an important parameter in enzyme kinetics, and was used to calculate the enzyme units (IU) of the purified vanillyl alcohol per given volume.

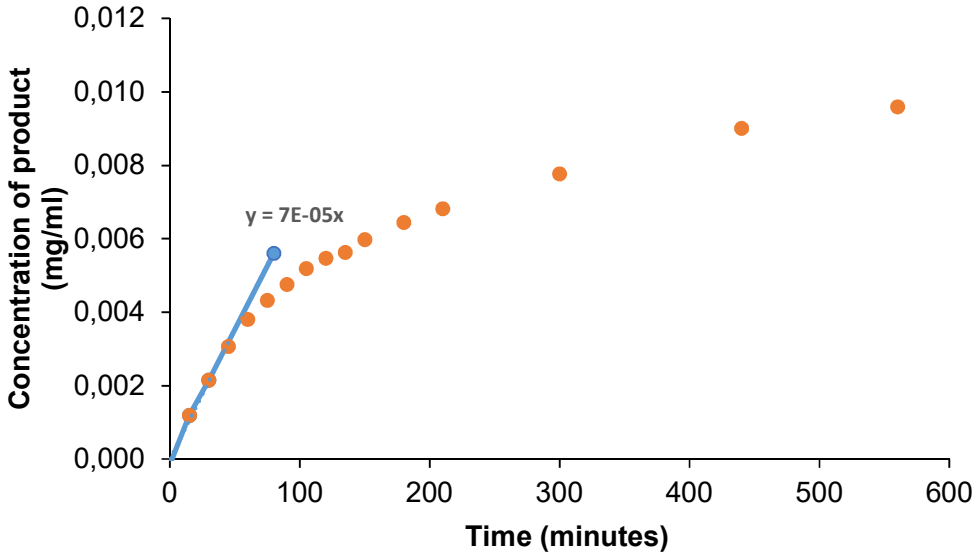

Figure 4.15. A 600-minute vanillyl alcohol oxidase reaction graph illustrating the relationship between concentrations of the product with time. A straight line was also extrapolated on this curve to show the initial velocity.

The graph in figure 4.15 were constructed after converting the absorbance readings to concentration using the standard curve equation $y = 122.56x + 0.0163$ There is a sharp increase in product concentration with time during the first 50 minutes. From this point the concentration of product decreased with time, As the reaction approaches time 400 minutes the concentration of product showed no further increase with time. In other words, the velocity of the reaction decreases and tends towards zero. Any enzyme reaction (change in concentration of product with time) can be described in three phases of the plotted graph. As shown in figure 4.15, the first portion is linear and this tells that the rate of reaction is constant thus the substrate is not a limiting factor. In the second phase, the curved part of the graph shows that the reaction rate has decrease suddenly. Then the last portion the reaction is almost constant i.e.no more product is formed with time. The decrease in the rate of reaction with time may be related to the enzyme losing its activity with time. This might be due to a change in its active site conformation after catalyzing several reactions. There were no experiments done on determining maximum velocity as the substrate uses (1 mM vanillyl alcohol) was enough for the enzyme to operate at its Vmax.

An initial velocity of 0.00007 mg/ml/min was recorded. This in other words means that the enzyme was able to convert 0,00007 mg of the substrate every minute. The initial velocity with known enzyme concentration enables the calculation of the enzyme active units per given mass. In this case, 0.045 enzyme units (IU) i.e. 2.03 mg of enzyme mass is equal to one enzyme unit. Enzyme

unit is defined as the amount of enzyme needed to convert 1 µmol of the substrate in one minute. Enzyme units are an easy way of expressing the enzyme activity as they only account for the active enzyme species, unlike concentration which accounts for both active and inactive protein.

4.2.6. Optimization of enzyme reaction parameters

The optimization of the enzyme reaction parameters is described in this section. The parameters that were optimized include enzyme concentration and reaction time. The time of reaction was deduced from figure 4.17 The reaction at 50 µg/ml VAO shows that within 60 minutes, the rate of increase in product with time is constant. This then acted as a reference in the subsequent reactions to only use 60 minute or less reaction time for the enzyme reaction because of the known linearity.

A standard curve for the plate reader was set up using a linear working range of 0 to 0.25 mM vanillin (Figure 4.16).

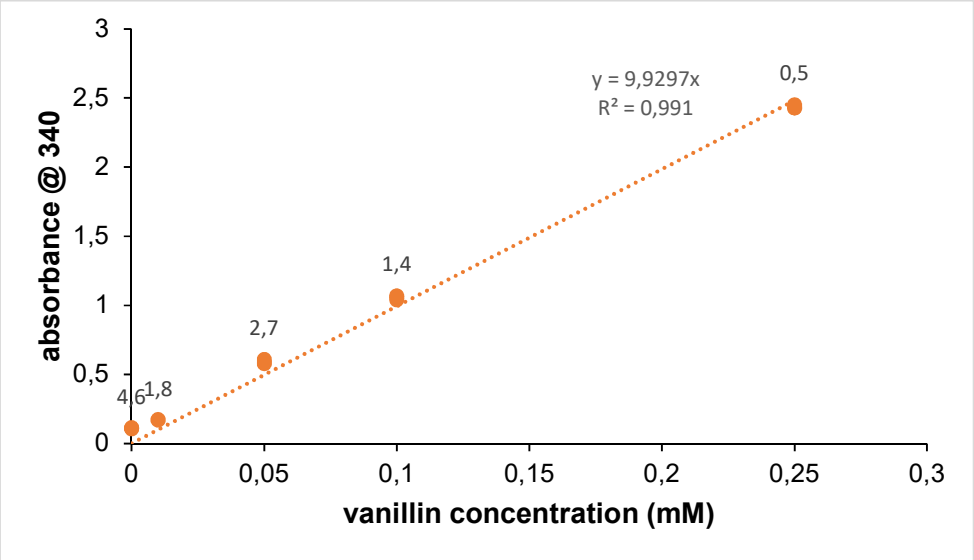

Figure 4.16. Vanillin standard curve for plate reader showing concentration against absorbance of vanillin standard in triplicates. The data labels above each data point shows the CV% of the triplicates

Five different concentration of the enzyme were chosen, 10 to 50 µg/ml for the determination of the working concentration in the subsequent reactions (Figure 4.17)

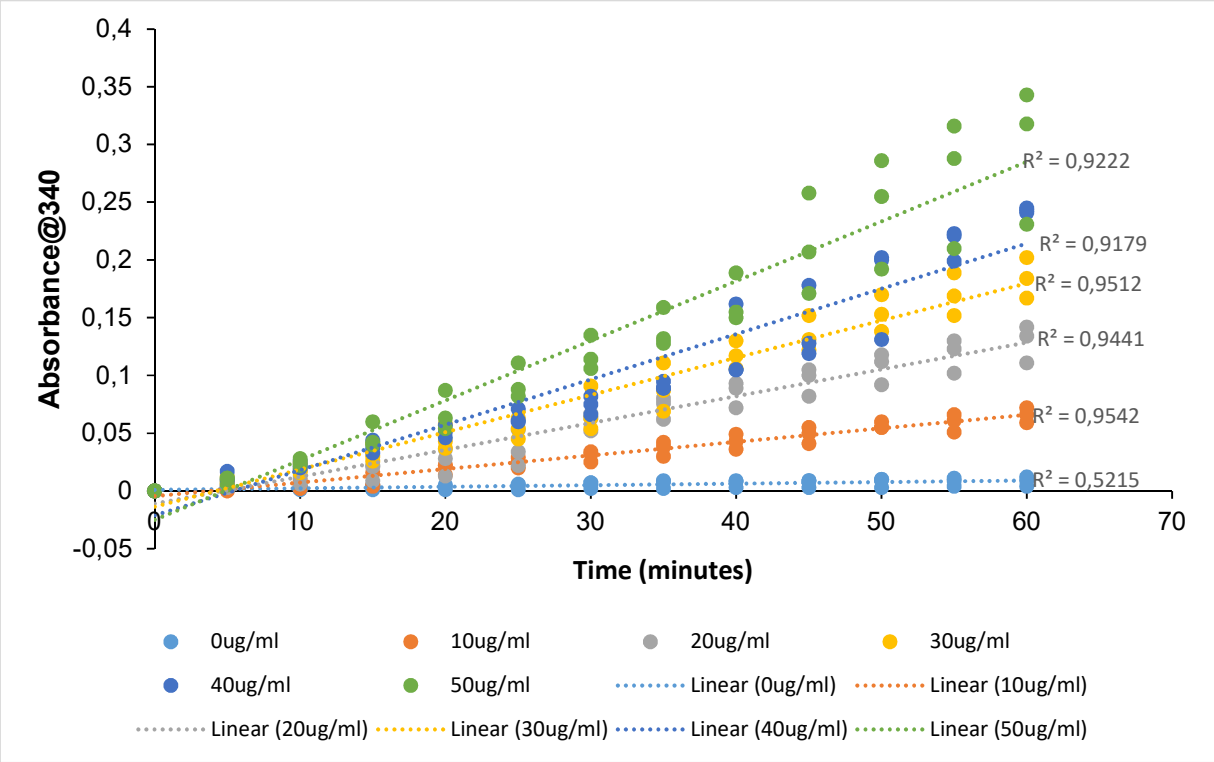

Figure 4.17. Relationship between the absorbance of the product with time at different enzyme concentrations. The reactions were done in triplicates shown by the same colour on the chart. A linear regression plot was used to determine the linear portion of the graph. The series name denotes the concentration of enzyme in each reaction.

The enzyme reaction was done at different enzyme concentrations in phosphate buffer with 1 mM of the substrate. From figure 4.17, there is a linear increase in absorbance with time for the five different concentrations of the enzyme. Therefore, it is apparent that a positive correlation exists between absorbance and enzyme concentration. Comparing the five different concentrations of enzymes, absorbance is highly pronounced at high enzyme concentration and vice versa, i.e., 10 µg/ml has the lowest and 50 µg/ml has the highest rate. These findings suggest that there is somewhat ample of substrate to enzyme ratio at all these concentrations within the 60 minutes' reaction time. Therefore, from this observation, a concentration of 50 µg/ml enzyme and 1 mM substrate was used throughout the whole following experiments. The temperature of 25ºC was used according to the plasmid (Van Rooyen, 2012). There was no temperature optimization reaction. The enzyme was supposed to be always saturated with the substrate. Therefore, a concentration of 1 mM was enough since the reactions in figure 4.15, showed that this amount of a substrate is not a limiting factor at 60 minutes.

Summary of the optimized parameters.

A reaction time of maximum 60 minutes, enzyme concentration of 50 mg/ml, substrate concentration of 1 mM and temperature 25ºC were considered for all the subsequent enzyme reactions.

4.3. Effect of the synthetic HTL aqueous phase on the Vanillyl alcohol oxidase enzyme activity

In order to test the effect of the synthetic aqueous phase on the activity of the vanillyl alcohol oxidase enzyme, different combinations of the components in the aqueous phase were investigated. As described earlier in chapter 3, the HTL aqueous phase was represented by eleven different reactions. These eleven reactions consist of two negative control reactions without an enzyme. On these control reactions the other one has acetic acid but the other one does not, this was for a better comparison for acetic acid reactions as separate. However, there was no much margin between the two negative control reactions as shown on figure 4.18. Another reaction was also set up as a control reaction with enzyme and no substrate. A positive control reaction which had only the known substrate (vanillyl alcohol) and lastly seven reactions with different combinations of the aqueous phase components (Figure 4.18).

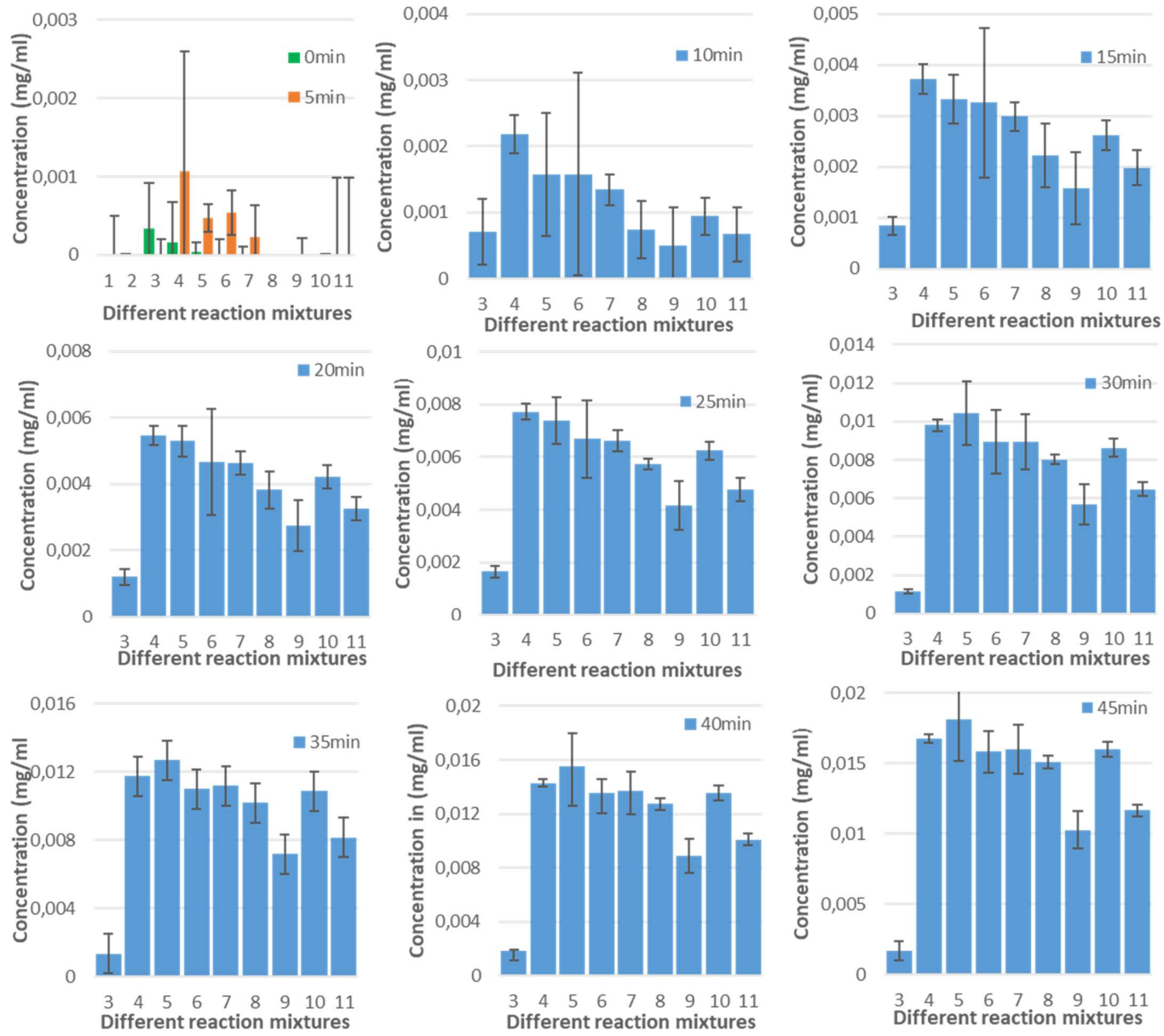

	Key
1	Vanillyl Alcohol+Vanillic Acid+Catechol+Phenol+Guaiacol
2	Vanillyl Alcohol+Vanillic acid+Catechol+Phenol+Guiacol+Acetic acid
3	Enzyme+Vanillic Acid+Catecho+Phenol+Guaiacol
4	Enzyme+Vanillyl Alcohol
5	Enzyme+Vanillyl alcohol+Vanillic Acid
6	Enzyme+Vanillyl Alcohol+Catechol
7	Enzyme+Vanillyl Alcohol+Phenol
8	Enzyme+Vanillyl Alcohol+Guaiacol
9	Enzyme+Vanillyl Alcohol+Acetic acid
10	Enzyme+Vanillyl Alcohol+Vanillic Acid+Catechol+Phenol+Guaiacol
11	Enzyme+Vanillyl Alcohol+Vanillic Acid+Catechol+Phenol+Guaiacol+Acetic acid

Figure 4.18. Each graph shows the concentration of product in each of the eleven reaction mixtures per given time. Error bars represent the standard error at a 95% confidence level. Each one of the graphs has a different scale of concentration for clarity sake, therefore the graphs are

not drawn to scale. The key shows the corresponding concentrations of each number in the x-axis.

The eleven enzyme reactions were followed for 45 minutes. Each time interval was tested for any significant differences. Significant and non-significant differences at 95% confidence level are represented by error bars on the graphs in figure 4.18. If there is a significant difference there is no overlap between the error bars at that particular time interval, and vice versa is true for the non-significant differences. Considering the eight graphs in figure 4.18, it is shown that for each enzyme reaction 4 to 11, the concentration of the product increases every 5 minutes. Reactions 1, 2 (differs in that reaction 2 have additional acetic acid) and 3 are exceptions due to the absence of either the enzyme (in 1 and 2) or the vanillyl alcohol substrate (in 3). The two control reactions without the enzyme, showed no increase in product over time, therefore figure 4.18 mainly shows data from reactions 3 to 11. The only difference between the two reactions' compositions is the presence of acetic acid in reaction 2. It would be expected that these reactions would proceed at a very slow rate or not proceed at all, owing to the absence of the enzymes and was used to account for any background absorbance. Reaction 3 (Enzyme+Vanillic aid+catechol+phenol+guaiacol), without vanillyl alcohol, showed a different behavior discussed in detail below.

From figure 4.18, considering the graph at times 0 and 5 minutes, it is clearly shown by error bars representing the standard error at 95% confidence that, there is no significant difference between the 11 reactions. At time 10 minutes, the graph shows that there is an emerging significant difference of reaction 4 (Vanillyl alcohol+Enzyme), which is also the reference reaction, to all the other reactions except for reaction 5 (Enzyme+Vanillyl alcohol+Vanillic acid) and 6 (Enzyme+vanillyl alcohol+Catechol). However, the reactions 5 to 11 shows no difference between them at 10 minutes at 95% confidence.

At 15 minutes, there is a visible difference in enzyme reaction 3 to the rest of the reactions (4 to 11). Amongst 4 to 11, reaction 4 again showed the same results as those reported above after 10 minutes. The only difference is the concentration of product which is increasing at every time interval. At 15 minutes again, reaction 9 (Enzyme+Vanillyl alcohol+vanillic acid+ Catechol+phenol+guaiacol) showed a significant difference to reactions, 5, 7 and 10 and no difference to reactions 6, 8 and 11. Reaction 9 contains acetic acid and it is known that acids are often used to precipitate proteins out of solution (Jiang *et al.*, 2004; Rajalingam *et al.*, 2009).

From 15 minutes, considering enzyme reaction 3 (Figure 4.19), the product concentration did not increase further and remained very close to zero as the other reactions showed an increase in the product. This depicts that there was little or no product formation with time. However, to determine if the change in product formation was significant, a statistical test was employed at 95% confidence (Figure 4.19).

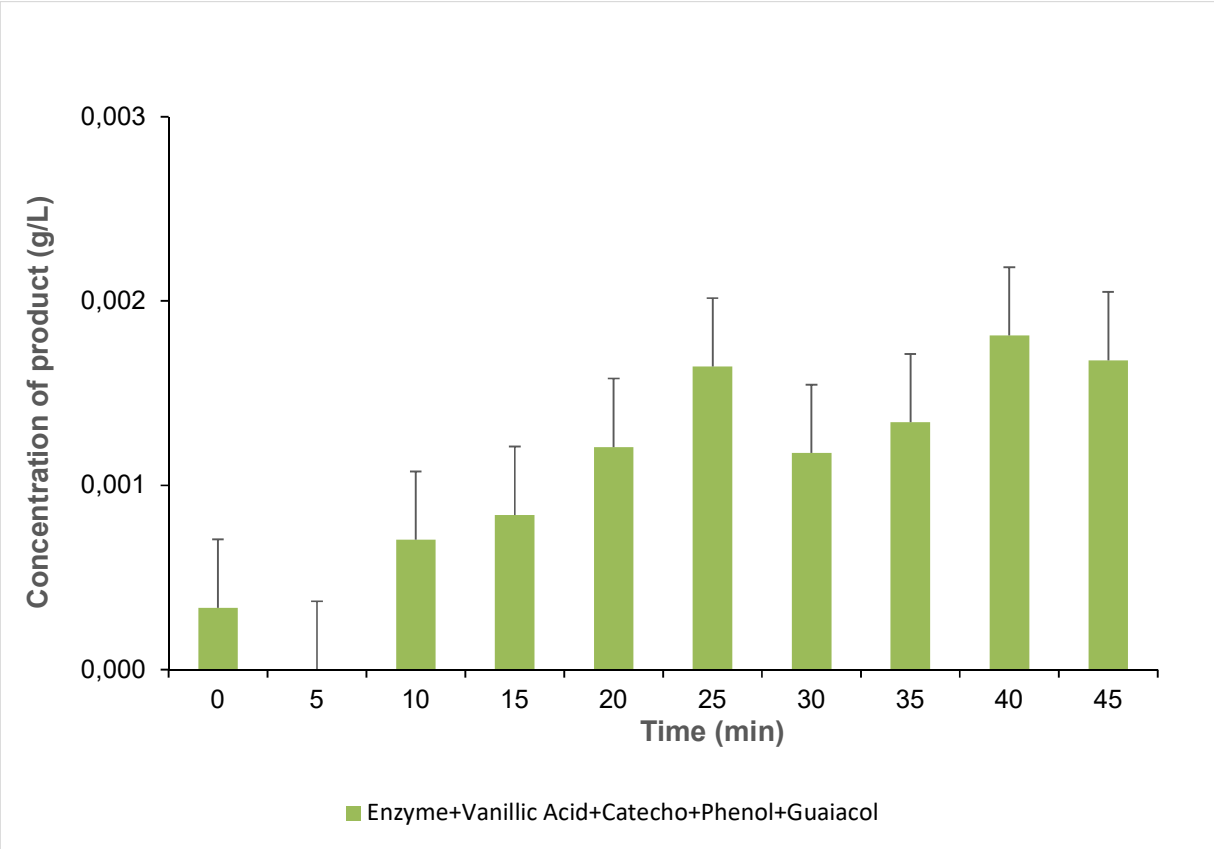

Figure 4.19. A representation of reaction 3 in figure 4.16 with a 95% confidence comparison within the 45 minutes. The error bars show the 95% confidence level calculated from the mean and standard deviation of the 10 data points.

From the graph in figure 4.19 at time zero there is vanillin formed that disappears at time 5 minutes. From 5 minutes to 25 minutes, there is an increase in product which decreases at time 30 minutes and a further increase up to 40 minutes then a decrease again at 45 minutes. This can be ascribed to the fact that there is a product formed and utilized at the same time but at different rates. From the chemical structures of, vanillyl alcohol, vanillin and vanillic acid, they only differ on the functional groups H_2OH, CHO and COOH groups. In an aqueous solution, there is a

possibility of slight dissociation of the COOH group into CHO and/or CH_2OH shown by a reaction scheme (Figure 4.20) (Skoog *et al.,* 1992).

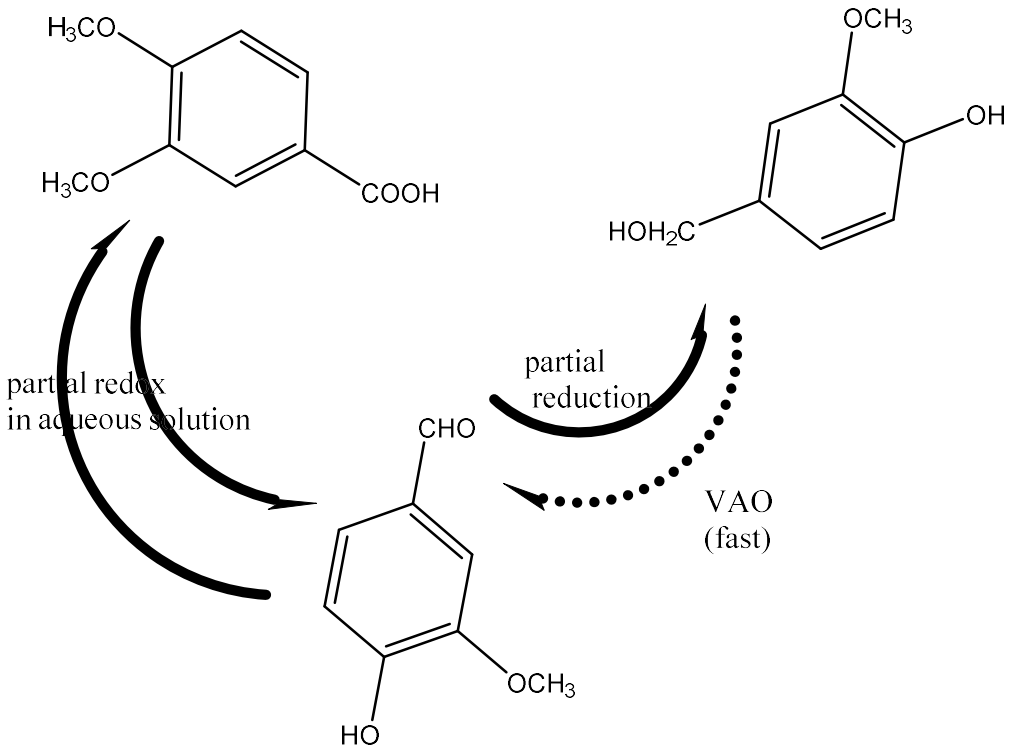

Figure 4.20. Reaction scheme, the behavior of vanillic acid and vanillyl alcohol in aqueous solution and the vanillyl alcohol oxidase pathway.

From the above scheme figure 4.20, vanillic acid dissociates slightly to form vanillin thus the vanillin at zero reaction in figure 4.19. Then because there is no vanillyl alcohol in this reaction the vanillin can be reduced to vanillyl alcohol thus a decrease at 5 minutes. Because there is plenty of vanillyl alcohol oxidase that act on vanillyl alcohol, the vanillyl alcohol is quickly converted to product vanillin. Because the rate of vanillin dissociation is lower than the enzyme conversion, then we will have vanillin accumulating thus to 25 minutes in figure 4.19. As more vanillin accumulates dissociation of vanillic acid stops or decreases to meet equilibrium thus a small drop-down at 30 minutes. This cycle continues but vanillin is increasing very slightly as the rate of increase is higher than the rate of decrease because of the presence of the enzyme.

With the exception of enzyme reactions 1 to 3, reactions 4 (Enzyme+Vanillyl alcohol), 5 (Enzyme +Vanillyl alcohol+Vanillic acid), 6 (Enzyme+Vanillyl acohol+Catechol), 7 (Enzyme+Vanillyl alcohol+Phenol), 8 (Enzyme+Vanillyl alcohol+Guaiacol), 9 (Enzyme+Vanillyl alcohol+Acetic

acid), 10 (Enzyme+Vanillyl alcohol+Vanillic acid+Catechol+Phenol+Guaiacol), and 11 (Enzyme+Vanillyl alcohol+Vanillic acid+Catechol+Phenol+Guaiacol+Acetic acid) where analyed and compared. This was from time 20 to 45 minutes where there was visible difference, i.e. from time 0-15 minutes there was no visible trends. There is a noticeable and statistically significant difference between the acetic acid-containing reaction compared to the ones without acetic acid from time 25 minutes onwards (see Figure 4.18). As depicted by figure 4.18, the acetic acid containing enzyme reactions are significantly lower than the phenolic containing reactions. But interestingly the rate of increase of all the reactions from 4 to 11 is almost constant**.** The two acetic acid reactions 9 and 11 differ in that 11 contains all the phenolic compounds in addition to vanillyl alcohol and acetic acid in 9. Acids tends to precipitate proteins (Jiang ***et al.***, 2004; Rajalingam ***et al.***, 2009), thus in this case vanillyl alcohol may be precipitated outside the solution. But there is no significant difference between the two graphs. This might possibly be due to the effect of vanillic acid as described in the reaction scheme given in figure 4.20.

Considering only the phenolic containing graphs from 20 minutes (Figure 4.21), the positive control reaction with only vanillyl alcohol is denoted reaction 4. Reactions 5, 6, 7 and 8 contains vanillyl alcohol and one other phenolic component, then lastly reaction 10 contains all the phenolic compounds. All the reactions were compared with reference to the positive control reaction 4.

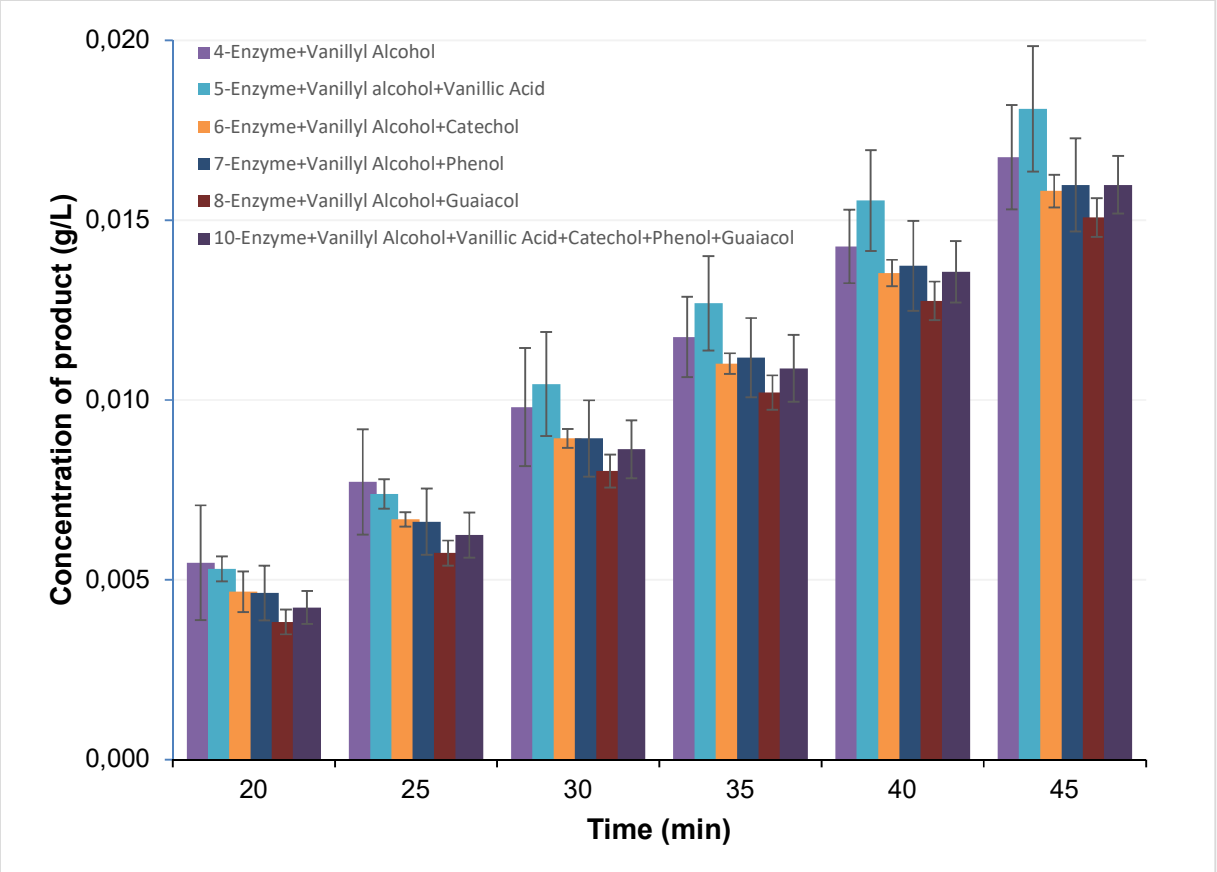

Figure 4.21. An extract of some reactions from figure 4.18, showing only the graphs due to the enzyme, vanillyl alcohol and one or more other phenolic compounds.

Reaction 5 with vanillic acid shows a different behavior to all other phenolic containing treatments. From a time of 30 minutes, it overtook the positive reaction 4, this shows that the rate of increase of reaction 5 is higher than the reference reaction. From this observation, paying attention to the products of the oxidation of vanillyl alcohol to vanillin, hydrogen peroxide is one of the products. Under alkaline conditions, hydrogen peroxide decomposes. Because hydrogen peroxide is produced under alkaline conditions, it quickly decomposes in solution (Elamathi *et al.*, 2018). Hydrogen peroxide at higher amounts in the reaction leads to deep oxidation of vanillin leading to vanillic acid formation. From our reactions as more hydrogen peroxide accumulates with time, vanillin formed may be converted to vanillic acid. But for reaction 5, there is plenty of vanillic acid in solution, therefore, considering the equilibrium laws (Driel & Gräber, 2006), it would be difficult

for hydrogen peroxide to favor the formation of vanillyl alcohol. Thus, the vanillin formed remains constant with time in treatment 5.

Considering reactions 6, 7, 8 and 10 from figure 4.19 above there is no statistically significant difference between the three reaction mixtures 6, 7 and 10 at 25 minutes as shown by the error bars. Reactions 8 is significantly different to 6 and 7 but not to 10 at time 25 minutes. However, after 25 minutes there is no observed differences between the four reactions. Looking at the components of each reaction, the guaiacol containing reactions formed the least amount of product. When comparing the phenol only and catechol only reactions, 6 and 7 to the control reaction 4 there is no significant differences throughout from 25 minutes to 45 minutes at 95% confidence level. A significant difference to the control reaction 4 was observed in guaiacol-containing treatments.

The presence of vanillic acid in treatment 10 has a positive effect that can lead to an increase in vanillin as described earlier for treatment 5. However, guaiacol is also present in treatment 10 and is inhibiting the enzyme reaction. Guaiacol is of the same structure as vanillyl alcohol, the substrate, only differing in that vanillyl alcohol has an additional CH_2OH group. From the reaction mechanism of VAO described in Chapter 2, Section 2.7.2, it is the proton on the OH group attached to the ring that is first attacked by amino acid ASP170 in the enzyme active site. Both guaiacol and vanillyl alcohol has this OH group in similar confirmation, therefore, there is a possibility of guaiacol always delaying the enzyme reaction as it can also enter the active site. So there is an assumption that, when guaiacol enters the active site it can participate in the first step of the reaction but no further reaction will occur as it lacks the para-CH_2OH group.

From the 11 enzyme reactions it can be concluded that acetic acid inhibits the enzyme reaction to a greater extent. Guaiacol also can be deemed an inhibitor but to a lesser extent. Vanillic acid was rather promoting more product formation but with a very little margin. Phenol and catechol showed no significant effect to the reaction.

CHAPTER FIVE

CONCLUSIONS AND RECOMMENDATIONS

Overview

The key outcomes of vanillyl alcohol oxidase activity on the hydrothermal liquefied biomass waste water from sewage sludge are outlined. These outcomes expand from the amount of enzyme produced from a given bacterial culture and its activity units per given mass to the yield of vanillin from vanillyl alcohol. The effect of other aqueous phase components on the enzyme reaction is also summarized in this chapter Section 5.1.1. The recommendations for future studies are given in Section 5.1.2 with regards to the results obtained by this study. The biomass type which is rich in vanillyl alcohol, the substrate, after hydrothermal liquefaction was sourced after getting a lower product yield of 2.5% from the guaiacol formaldehyde reaction described in section 4.1. Therefore, all the conclusions were drawn based on Sections 4.2 and 4.3.

Conclusion

The aim of this study involved the investigation of the feasibility of producing vanillin by using a recombinant expressed and purified vanillyl alcohol oxidase for the easy of separation of phenols from the whole aqueous solution. The key outcomes of the vanillyl alcohol oxidase activity on the liquid of aqueous phase HTL processed sewage sludge are presented. These outcomes expand from the amount of enzyme produced from a given bacterial culture and its activity units per given mass to the yield of vanillin from vanillyl alcohol. To achieve the main goal several objectives were completed, which include the expression and purification of vanillyl alcohol oxidase from a recombinant plasmid (pET28a(+)/PsVAO) transformed into *E. coli* BL21(DE3) as well as the optimization and analyses of the enzyme activity assay.

Initially the synthesis of vanillyl alcohol oxidase from pET28a(+)/PsVAO was successful. This was validated by SDS-PAGE gel and activity assay using the known commercial substrate vanillyl alcohol. The SDS-PAGE results gave a distinct protein band at around 65 kDa which corresponds to vanillyl alcohol oxidase molecular weight. From the obtained purified vanillyl alcohol oxidase concentration, a protein mass of 2.03 mg was related to one enzyme unit which catalyzes 1 µmol of substrate in 1 minute.

In the hydrothermal liquefaction aqueous phase, 50 µg/ml of enzyme was used throughout. To achieve the aim of synthesizing vanillin from vanillyl alcohol, more attention was given on the

trends of enzyme action with time in the presence of HTL aqueous phase components. The sewage sludge aqueous phase contains acetic acid, guaiacol, vanillic acid, catechol, phenol and vanillyl alcohol as major components as reported by ICP and HPLC analyses. The trends show that acetic acid negatively affects the reaction with a greater margin at 95% confidence. Guaiacol, phenol and catechol also have a negative effect on the reaction but to a lesser extent compared to vanillin. Vanillic acid promotes an increase in vanillyl alcohol yield and thus adds to the product yield. This study was concluded only on reporting the trends of the effect of each component, however more work should be done according to recommendations in the next section.

Recommendations

The HTL aqueous phase was analysed through HPLC, which was not fully characterised by the chromatogram peaks, the components existent. So, an urgent need is required to characterise the HTL aqueous phase liquid.

A spectrochemical method was used indirectly to the aqueous phase as the background of the aqueous phase does not allow to zero the spectrophotometer thus giving values above the detection limit. It would be recommended that a method which can allow detection of the products of the enzyme within the aqueous phase should be devised and avoid an indirect analysis method. One method can be by finding adsorbents to either the substrate, product or all the other components that forms the background thus separating the compounds. The high volume of water remained one of the major gaps that makes the sample too dilute. It would be recommended that a method that can concentrate the phenolic components from the vast amount of water should be devised.

The elution buffer imidazole (250 mM) would have affected greatly the enzyme activity, therefore more purification steps of the enzyme are recommended that includes dialysis or gel-filtration chromatography.

For industrial implementation of this type of reactions, all the acidic components like acetic acid should be first removed from the solution before the enzyme reaction.

References

Akhtar, J. & Amin, N.A.S. 2011. A review on process conditions for optimum bio-oil yield in hydrothermal liquefaction of biomass. *Renewable and Sustainable Energy Reviews*. 15(3):1615–1624.

Anastasakis, K., Biller, P., Madsen, R.B., Glasius, M. & Johannsen, I. 2018. Continuous Hydrothermal Liquefaction of Biomass in a Novel Pilot Plant with Heat Recovery and Hydraulic Oscillation. *Energies*. 11(10):2695.

Arun, J., Varshini, P., Prithvinath, P.K., Priyadarshini, V. & Gopinath, K.P. 2018. Enrichment of bio-oil after hydrothermal liquefaction (HTL) of microalgae C. vulgaris grown in wastewater: Bio-char and post HTL wastewater utilization studies. *Bioresource Technology*. 261(1):182–187.

Arun, J., Gopinath, K.P., Sivaramakrishnan, R., Shyam, S., Mayuri, N., … Pugazhendhi, A. 2021. Hydrothermal liquefaction of Prosopis juliflora biomass for the production of ferulic acid and bio-oil. *Bioresource Technology*. 319:124116.

Arya, S.S. 2019. (PDF) Vanilla Farming: The Way Forward. *The Energy and Resources Institute*. 2(3):20–24. https://www.researchgate.net/publication/334576313_Vanilla_Farming_The_Way_Forward.

Asadullah, M., Ab Rasid, N.S., Kadir, S.A.S.A. & Azdarpour, A. 2013. Production and detailed characterization of bio-oil from fast pyrolysis of palm kernel shell. *Biomass and Bioenergy*. 59:316–324.

Asghari, A., Khorrami, M.K. & Kazemi, S.H. 2019. Hierarchical H-ZSM5 zeolites based on natural kaolinite as a high-performance catalyst for methanol to aromatic hydrocarbons conversion. *Scientific Reports*. 9(1):1–9.

Atkins, P., De Paula, J. & Keeler, J. 2017. *Atkin's Physical Chemistry, 11th Ed*. *OUP Oxford*.

Baloch, H.A., Nizamuddin, S., Siddiqui, M.T.H., Riaz, S., Jatoi, A.S., … Griffin, G.J. 2018. Recent advances in production and upgrading of bio-oil from biomass: A critical overview. *Journal of Environmental Chemical Engineering*. 4(8):5101--5118.

Banerjee, G. & Chattopadhyay, P. 2019. Vanillin biotechnology: the perspectives and future. *Journal of the Science of Food and Agriculture*. 99(2):499–506.

Beims, R.F., Hu, Y., Shui, H. & Xu, C. (Charles). 2020. Hydrothermal liquefaction of biomass to fuels and value-added chemicals: Products applications and challenges to develop large-scale operations. *Biomass and Bioenergy*. (135):105–510.

Benen, J.A.E., Sánchez-Torres, P., Wagemaker, M.J.M., Fraaije, M.W., Van Berkel, W.J.H. & Visser, J. 1998. Molecular cloning, sequencing, and heterologous expression of the vaoA gene from Penicillium simplicissimum CBS 170.90 encoding vanillyl-alcohol oxidase. *Journal of Biological Chemistry*. 273(14):7865–7872.

Biller, P., Ross, A.B., Skill, S.C., Lea-Langton, A., Balasundaram, B., … Llewellyn, C.A. 2012. Nutrient recycling of aqueous phase for microalgae cultivation from the hydrothermal liquefaction process. *Algal Research*. 1(1):70–76.

Biswas, B., Kumar, J. & Bhaskar, T. 2019. Advanced hydrothermal liquefaction of biomass for bio-oil production. In: *Biomass, Biofuels, Biochemicals: Biofuels: Alternative Feedstocks and Conversion Processes for the Production of Liquid and Gaseous Biofuels*. pp. 245–266.

Bloom, J. 2017. Natural and Artificial Flavors What ' s the Difference ? Natural and Artificial Flavors. In: *Science and health*. New York: American council on science and health. pp. 1–40. http://www.acsh.org.

Bolognini, M., Cavani, F., Dal Pozzo, L., Maselli, L., Zaccarelli, F., … Garrone, E. 2004. Guaiacol hydroxyalkylation with aqueous formaldehyde: Role of surface properties of H-mordenites on catalytic performance. *Applied Catalysis A: General*. 272(1–2):115–124.

Bosque, I., Magallanes, G., Rigoulet, M., Kärkäs, M.D. & Stephenson, C.R.J. 2017. Redox Catalysis Facilitates Lignin Depolymerization. *ACS Central Science*. 3(6):621–628.

Brindhadevi, K., Anto, S., Rene, E.R., Sekar, M., Mathimani, T., … Pugazhendhi, A. 2021. Effect of reaction temperature on the conversion of algal biomass to bio-oil and biochar through pyrolysis and hydrothermal liquefaction. *Fuel*. 285(1):119106.

Bunzel, M. & Ralph, J. 2006. NMR characterization of lignins isolated from fruit and vegetable insoluble dietary fiber. *Journal of Agricultural and Food Chemistry*. 54(21):8352–8361.

Bunzel, M., Steinhart, H. & Ralph, J. 2007. NMR and DFRC Characterization of Lignins Isolated from Fruit, Vegetable and Cereal Dietary Fiber. In: T.E. Hervé This, ed. *Euro Food Chem XIV (Food Quality, an Issue of Molecule-based Science)*. Paris, France. pp. 29–31.

Calvo-Flores, F.G., José A., D., Isac-García, J. & Martín-Martínez, F.J. 2015. Functional and Spectroscopic Characterisation of Lignins. In: *Lignin and Lignans As Renewable Raw Materials*. John Wiley \& Sons. pp. 145–168.

Cantero-Tubilla, B., Cantero, D.A., Martinez, C.M., Tester, J.W., Walker, L.P. & Posmanik, R. 2018. Characterization of the solid products from hydrothermal liquefaction of waste feedstocks from food and agricultural industries. *Journal of Supercritical Fluids*. 133(1):665–673.

Cao, L., Zhang, C., Chen, H., Tsang, D.C.W., Luo, G., … Chen, J. 2017. Hydrothermal liquefaction of agricultural and forestry wastes: state-of-the-art review and future prospects. *Bioresource Technology*. 245:1184--1193.

Carpio, R., Kuo, C.T., De Leon, R., Schideman, L.C. & Zhang, Y. 2018. Hydrothermal liquefaction of demineralized wastewater algae biomass. *International Journal of Smart Grid and Clean Energy*. 7(1):13–23.

Catallo, W.J., Shupe, T.F., Comeaux, J.L. & Junk, T. 2010. Transformation of glucose to volatile and semi-volatile products in hydrothermal (HT) systems. *Biomass and Bioenergy*. 34(1):1–13.

Cavani, F., Dal Pozzo, L., Maselli, L. & Mezzogori, R. 2002. Hydroxymethylation of 2-methoxyphenol catalyzed by H-mordenite: Analysis of the reaction scheme. *Studies in Surface Science and Catalysis*. 142(1):565–572.

Cavani, F., Corrado, M. & Mezzogori, R. 2002. A note on the role of methanol in the homogeneous and heterogeneous acid-catalyzed hydroxymethylation of guaiacol with aqueous solutions of formaldehyde. *Journal of Molecular Catalysis A: Chemical*. 182–183:447–453.

Cesari, L., Mutelet, F. & Canabady-Rochelle, L. 2019. Antioxidant properties of phenolic surrogates of lignin depolymerisation. *Industrial Crops and Products*. 129(1):480–487.

Cha, J.S., Park, S.H., Jung, S.C., Ryu, C., Jeon, J.K., … Park, Y.K. 2016. Production and

utilization of biochar: A review. *Journal of Industrial and Engineering Chemistry*. 40:1–15.

Chang, S.H. 2014. An overview of empty fruit bunch from oil palm as feedstock for bio-oil production. *Biomass and Bioenergy*. 62:174–181.

Cheetham, P.S.J., Gradley, M.L. & Sime, J.T. 2005. Flavour/aroma materials and their preparation. *Patent WO2000050622 A*. 1:31.

Chen, H., He, Z., Zhang, B., Feng, H., Kandasamy, S. & Wang, B. 2019. Effects of the aqueous phase recycling on bio-oil yield in hydrothermal liquefaction of Spirulina Platensis, A-cellulose, and lignin. *Energy*. 179:1103–1113.

Chen, H., Wan, J., Chen, K., Luo, G., Fan, J., … Zhang, S. 2016. Biogas production from hydrothermal liquefaction wastewater (HTLWW): Focusing on the microbial communities as revealed by high-throughput sequencing of full-length 16S rRNA genes. *Water Research*. 106(1):98–107.

Chen, K., Lyu, H., Hao, S., Luo, G., Zhang, S. & Chen, J. 2015. Separation of phenolic compounds with modified adsorption resin from aqueous phase products of hydrothermal liquefaction of rice straw. *Bioresource Technology*. 182:160–168.

Chen, L., Korányi, T.I. & Hensen, E.J.M. 2016. Transition metal (Ti, Mo, Nb, W) nitride catalysts for lignin depolymerisation. *Chemical Communications*. 52(60):9375--9378.

Chen, W.T., Haque, M.A., Lu, T., Aierzhati, A. & Reimonn, G. 2020. A perspective on hydrothermal processing of sewage sludge. *Current Opinion in Environmental Science and Health*. 14:63–73.

Cherad, R., Onwudili, J.A., Biller, P., Williams, P.T. & Ross, A.B. 2016. Hydrogen production from the catalytic supercritical water gasification of process water generated from hydrothermal liquefaction of microalgae. *Fuel*. 166:24–28.

Cintas, O., Berndes, G., Cowie, A.L., Egnell, G., Holmström, H. & Ågren, G.I. 2016. The climate effect of increased forest bioenergy use in Sweden: Evaluation at different spatial and temporal scales. *Wiley Interdisciplinary Reviews: Energy and Environment*. 5(3):351–369.

Converti, A., Aliakbarian, B., Domínguez, J.M., Vázquez, G.B. & Perego, P. 2010. Microbial production of biovanillin. *Brazilian Journal of Microbiology*. 41(3):519–530.

Crick, F. 1970. Central dogma of molecular biology. *Nature*. 227(5258):561–563.

Cui, Z., Cheng, F., Jarvis, J.M., Brewer, C.E. & Jena, U. 2020. Roles of Co-solvents in hydrothermal liquefaction of low-lipid, high-protein algae. *Bioresource Technology*. 310(1):1234–54.

Das, A. & König, B. 2018. Transition metal- and photoredox-catalyzed valorisation of lignin subunits. *Green Chemistry*. 20(21):4844–4852.

Das, P., Khan, S., AbdulQuadir, M., Thaher, M., Waqas, M., … Al-Jabri, H. 2020. Energy recovery and nutrients recycling from municipal sewage sludge. *Science of the Total Environment*. 715(1):1367–75.

Das, P., Chandramohan, V.P., Mathimani, T. & Pugazhendhi, A. 2021. A comprehensive review on the factors affecting thermochemical conversion efficiency of algal biomass to energy. *Science of the Total Environment*. 766(1):144213.

Day, A., Dehorter, B., Neutelings, G., Czeszak, X., Chabbert, B., … David, H. 2001. Caffeoyl-coenzyme A 3-O-methyltransferase enzyme activity, protein and transcript accumulation in flax (Linum usitatissimum) stem during development. *Physiologia Plantarum*. 113(2):275–284.

Demirbas, A. 2009. Biorefineries: Current activities and future developments. *Energy Conversion and Management*. 50(11):2782–2801.

Demirbas, A. & Fatih Demirbas, M. 2011. Importance of algae oil as a source of biodiesel. *Energy Conversion and Management*. 52(1):163–170.

Demirel, Y. 2017. Lignin for Sustainable Bioproducts and Biofuels. *Journal of Biochemical Engineering & Bioprocess Technology*. 1(1):1–3.

Djandja, O.S., Yin, L., Wang, Z., Guo, Y., Zhang, X. & Duan, P. 2021. Progress in thermochemical conversion of duckweed and upgrading of the bio-oil: A critical review. *Science of the Total Environment*. 769(1):144660.

Driel, J.H. & Gräber, W. 2006. The Teaching and Learning of Chemical Equilibrium. In: *Chemical Education: Towards Research-based Practice*. pp. 271–292.

Drijfhout, F.P., Fraaije, M.W., Jongejan, H., Van Berkel, W.J.H. & Franssen, M.C.R. 1998. Enantioselective hydroxylation of 4-alkylphenols by vanillyl alcohol oxidase. *Biotechnology and Bioengineering*. 59(2):171–177.

Du, X., Li, J. & Lindström, M.E. 2014. Modification of industrial softwood kraft lignin using Mannich reaction with and without phenolation pretreatment. *Industrial Crops and Products*. 52:729–735.

Dunn, K.G. & Hobson, P.A. 2016. Hydrothermal liquefaction of lignin. In: *Sugarcane-based Biofuels and Bioproducts*. pp. 165–206.

Edmundson, S., Huesemann, M., Kruk, R., Lemmon, T., Billing, J., … Anderson, D. 2017. Phosphorus and nitrogen recycle following algal bio-crude production via continuous hydrothermal liquefaction. *Algal Research*. 26(1):415-421`.

Egerland Bueno, B., Américo Soares, L., Quispe-Arpasi, D., Kimiko Sakamoto, I., Zhang, Y., … Tommaso, G. 2020. Anaerobic digestion of aqueous phase from hydrothermal liquefaction of Spirulina using biostimulated sludge. *Bioresource Technology*. 312(1):123552.

Elamathi, P., Kolli, M.K. & Chandrasekar, G. 2018. Catalytic Oxidation of Vanillyl Alcohol Using FeMCM-41 Nanoporous Tubular Reactor. *International Journal of Nanoscience*. 17(01n02):1760010.

Elliott, D.C. 2016. Production of biofuels via bio-oil upgrading and refining. In: *Handbook of Biofuels Production: Processes and Technologies: Second Edition*. pp. 595–613.

ETC Group. 2013. *Vanilla & Synthetic Biology: a case of study*. Vol. 1.

Evstigneyev, E.I. & Shevchenko, S.M. 2020. Lignin valorization and cleavage of arylether bonds in chemical processing of wood: a mini-review. *Wood Science and Technology*. 54(1):787–820.

Ewing, T.A., Fraaije, M.W., Mattevi, A. & van Berkel, W.J.H. 2017. The VAO/PCMH flavoprotein family. *Archives of Biochemistry and Biophysics*. 632:104–117.

Fache, M., Boutevin, B. & Caillol, S. 2016a. Vanillin Production from Lignin and Its Use as a Renewable Chemical. *ACS Sustainable Chemistry and Engineering*. 4(1):35–46.

Fache, M., Boutevin, B. & Caillol, S. 2016b. Epoxy thermosets from model mixtures of the lignin-to-vanillin process. *Green Chemistry*. 18(3):712–725.

Fernandez, S., Srinivas, K., Schmidt, A.J., Swita, M.S. & Ahring, B.K. 2018. Anaerobic digestion of organic fraction from hydrothermal liquefied algae wastewater byproduct. *Bioresource Technology*. 247(1):250–258.

Fraaije, M.W., Van Den Heuvel, R.H.H., Van Berkel, W.J.H. & Mattevi, A. 2000. Structural analysis of flavinylation in vanillyl-alcohol oxidase. *Journal of Biological Chemistry*. 275(49):38654–38658.

Franco, A., De, S., Balu, A.M., Romero, A.A. & Luque, R. 2017. Selective Oxidation of Isoeugenol to Vanillin over Mechanochemically Synthesized Aluminosilicate Supported Transition Metal Catalysts. *ChemistrySelect*. 2(29):9546–9551.

Funkenbusch, L.L.T., Mullins, M.E., Vamling, L., Belkhieri, T., Srettiwat, N., … Rogers, T.N. 2019. Technoeconomic assessment of hydrothermal liquefaction oil from lignin with catalytic upgrading for renewable fuel and chemical production. *Wiley Interdisciplinary Reviews: Energy and Environment*. 8(1):e319.

Furuya, T., Miura, M., Kuroiwa, M. & Kino, K. 2015. High-yield production of vanillin from ferulic acid by a coenzyme-independent decarboxylase/oxygenase two-stage process. *New Biotechnology*. 32(3):335–339.

Gai, C., Zhang, Y., Chen, W.T., Zhou, Y., Schideman, L., … Dong, Y. 2015. Characterization of aqueous phase from the hydrothermal liquefaction of Chlorella pyrenoidosa. *Bioresource Technology*. 184:328–335.

Gallage, N.J. & Møller, B.L. 2015. Vanillin-bioconversion and bioengineering of the most popular plant flavor and its de novo biosynthesis in the vanilla orchid. *Molecular Plant*. 8(1):40–57.

Gellerstedt, G.L.F. & Henriksson, E.G. 2008. Lignins: Major sources, structure and properties. *Monomers, Polymers and Composites from Renewable Resources*. 1:201–224.

Gîlcă, I.A., Căpraru, A.M., Grama, S. & Popa, V.I. 2011. Agents for wood bioprotection based on natural aromatic compounds and their complexes with copper and zinc. *Cellulose Chemistry and Technology*. 45(3–4):227–231.

Gollakota, A.R.K., Kishore, N. & Gu, S. 2018. A review on hydrothermal liquefaction of biomass. *Renewable and Sustainable Energy Reviews*. 81:1378–92.

Goswami, P., Chinnadayyala, S.S.R., Chakraborty, M., Kumar, A.K. & Kakoti, A. 2013. An overview on alcohol oxidases and their potential applications. *Applied Microbiology and Biotechnology*. 97(10):4259–4275.

Goyal, H.B., Seal, D. & Saxena, R.C. 2008. Bio-fuels from thermochemical conversion of renewable resources: A review. *Renewable and Sustainable Energy Reviews*. 12(2):504–517.

Graca, I., Lopes, J.M., Cerqueira, H.S. & Ribeiro, M.F. 2013. Bio-oils upgrading for second generation biofuels. *Industrial and Engineering Chemistry Research*. 52(1):275–287.

Green, M. 2019. Solvay increases natural vanillin production amid heightened market demand. *FOOD INGREDIENTS NEWS* (Fi, Europe). 16 December: 1–2.

De Guzman, C.C. & Zara, R.R. 2012. Vanilla. In: *Vanilla: Handbook of Herbs and spices*. Woodhead publishers. pp. 547–589.

Gygli, G., Lucas, M.F., Guallar, V. & van Berkel, W.J.H. 2017. The ins and outs of vanillyl alcohol oxidase: Identification of ligand migration paths. *PLoS Computational Biology*. 13(10):e1005787.

Gygli, G., de Vries, R.P. & van Berkel, W.J.H. 2018. On the origin of vanillyl alcohol oxidases. *Fungal Genetics and Biology*. 116:24–32.

Haghdan, S., Renneckar, S. & Smith, G.D. 2016. Sources of Lignin. In: *Lignin in Polymer Composites*. pp. 1–11.

Haider, K.M. & Guggenberger, G. 2005. Organic Matter - Genesis and Formation. In: Daniel Hillel, ed. *Encyclopedia of Soils in the Environment*. Elsevier. pp. 93–101.

Han, Y., Hoekman, K., Jena, U. & Das, P. 2019. Use of co-solvents in hydrothermal liquefaction (HTL) of microalgae. *Energies*. 13(1):124.

Han, Y., Hoekman, S.K., Cui, Z., Jena, U. & Das, P. 2019. Hydrothermal liquefaction of marine microalgae biomass using co-solvents. *Algal Research*. 38:101421.

Handayani, K., Krozer, Y. & Filatova, T. 2019. From fossil fuels to renewables: An analysis of long-term scenarios considering technological learning. *Energy Policy*. 127:134–146.

Havkin-Frenkel, D. & Belanger, F.C. 2011. *Handbook of Vanilla Science and Technology*. 2nd ed. *Handbook of Vanilla Science and Technology*. Chichester: Wiley-Blackwell.

Hawkins, K.M. & Smolke, C.D. 2008. Production of benzylisoquinoline alkaloids in Saccharomyces cerevisiae. *Nature Chemical Biology*. 4(9):564–573.

He, L.H., Lin, T.T., Ling, Y.H., Wu, H.J. & Lü, Q.F. 2013. Preparation of polyaniline-lignin nanocomposites and their reducing adsorption for silver ions. *Acta Polymerica Sinica*. 13(3):320–326.

He, Z.W., Lü, Q.F. & Zhang, J.Y. 2012. Facile preparation of hierarchical polyaniline-lignin composite with a reactive silver-ion adsorbability. *ACS Applied Materials and Interfaces*. 4(1):369–74.

van den Heuvel, R.H.H., Fraaije, M.W., Mattevi, A. & van Berkel, W.J.H. 2002. Structure, function and redesign of vanillyl-alcohol oxidase. *International Congress Series*. 1233(C):13–24.

Van Den Heuvel, R.H.H., Fraaije, M.W., Ferrer, M., Mattevi, A. & Van Berkel, W.J.H. 2000. Inversion of stereospecificity of vanillyl-alcohol oxidase. *Proceedings of the National Academy of Sciences of the United States of America*. 97(17):9455–60.

Van Den Heuvel, R.H.H.H., Van Den Berg, W.A.M.M., Rovida, S. & Van Berkel, W.J.H.H. 2004. Laboratory-evolved vanillyl-alcohol oxidase produces natural vanillin. *Journal of Biological Chemistry*. 279(32):33492–33500.

Hochuli, E., Bannwarth, W., Dobeli, H., Gentzi, R. & Stuber, D. 1988. Genetic approach to facilitate purification of recombinant proteins with a novel metal chelate adsorbent. *Bio/Technology*. 6(11):1321–1325.

Hossain, M.A., Phung, T.K., Rahaman, M.S., Tulaphol, S., Jasinski, J.B. & Sathitsuksanoh, N. 2019. Catalytic cleavage of the B-O-4 aryl ether bonds of lignin model compounds by Ru/C catalyst. *Applied Catalysis A: General*. 582:117100.

Huang, Z., Dostal, L. & Rosazza, J.P.N. 1993. Microbial transformations of ferulic acid by Saccharomyces cerevisiae and Pseudomonas fluorescens. *Applied and Environmental*

Microbiology. 59(7):2244–2250.

Huet, M., Roubaud, A., Chirat, C. & Lachenal, D. 2016. Hydrothermal treatment of black liquor for energy and phenolic platform molecules recovery in a pulp mill. *Biomass and Bioenergy*. 89:105–112.

Isola, C., Sieverding, H.L., Numan-Al-Mobin, A.M., Rajappagowda, R., Boakye, E.A., … Stone, J.J. 2018. Vanillin derived from lignin liquefaction: a sustainability evaluation. *International Journal of Life Cycle Assessment*. 23(9):1761–1772.

Jain, A., Balasubramanian, R. & Srinivasan, M.P. 2016. Hydrothermal conversion of biomass waste to activated carbon with high porosity: A review. *Chemical Engineering Journal*. 283:789–805.

Jegers, H.E. & Klein, M.T. 1985. Primary and Secondary Lignin Pyrolysis Reaction Pathways. *Industrial and Engineering Chemistry Process Design and Development*. 24(1):173–183.

Ji, R. & Schäffer, A. 2004. Synthesis of [uniformly ring-14C]-labelled 4-hydroxybenzaldehyde, vanillin, and protocatechualdehyde. *Journal of Labelled Compounds and Radiopharmaceuticals*. 47(4):209–216.

Jiang, L., He, L. & Fountoulakis, M. 2004. Comparison of protein precipitation methods for sample preparation prior to proteomic analysis. *Journal of Chromatography A*. 1023(2):317–320.

José Borges Gomes, F., de Souza, R.E., Brito, E.O. & Costa Lelis, R.C. 2020. A review on lignin sources and uses. *Journal of Applied Biotechnology & Bioengineering*. 7(3):100–105.

Kang, S., Li, X., Fan, J. & Chang, J. 2013. Hydrothermal conversion of lignin: A review. *Renewable and Sustainable Energy Reviews*. 27:546–558.

Kapdan, I.K. & Kargi, F. 2006. Bio-hydrogen production from waste materials. *Enzyme and Microbial Technology*. 38(5):569–582.

Kaprasob, R., Kerdchoechuen, O., Laohakunjit, N., Sarkar, D. & Shetty, K. 2017. Fermentation-based biotransformation of bioactive phenolics and volatile compounds from cashew apple juice by select lactic acid bacteria. *Process Biochemistry*. 59:141–149.

Karakhanov, E.A., Maximov, A.L., Kardasheva, Y.S., Skorkin, V.A., Kardashev, S. V., … Cron,

S.L. 2010. Hydroxylation of phenol by hydrogen peroxide catalyzed by copper(II) and Iron(III) complexes: The structure of the ligand and the selectivity of ortho-hydroxylation. *Industrial and Engineering Chemistry Research*. 49(10):4607–13.

Karnjanakom, S., Suriya-umporn, T., Bayu, A., Kongparakul, S., Samart, C., … Guan, G. 2017. High selectivity and stability of Mg-doped Al-MCM-41 for in-situ catalytic upgrading fast pyrolysis bio-oil. *Energy Conversion and Management*. 142:272–285.

Koçar, G. & Civaş, N. 2013. An overview of biofuels from energy crops: Current status and future prospects. *Renewable and Sustainable Energy Reviews*. 28:900–916.

Krings, U. & Berger, R.G. 1998. Biotechnological production of flavours and fragrances. *Applied Microbiology and Biotechnology*. 49(1):1–8.

Kumar, R., Sharma, P.K. & Mishra, P.S. 2012. A review on the vanillin derivatives showing various biological activities. *International Journal of PharmTech Research*. 4(1):266–279.

Kumar, S., Kikon, K., Upadhyay, A., Kanwar, S.S. & Gupta, R. 2005. Production, purification, and characterization of lipase from thermophilic and alkaliphilic Bacillus coagulans BTS-3. *Protein Expression and Purification*. 41(1):38–44.

Lee, M.E., Aswani, A., Han, A.S., Tomlin, C.J. & Dueber, J.E. 2013. Expression-level optimization of a multi-enzyme pathway in the absence of a high-throughput assay. *Nucleic Acids Research*. 41(22):10668–10678.

Leng, L., Zhang, W., Leng, S., Chen, J., Yang, L., … Huang, H. 2020. Bioenergy recovery from wastewater produced by hydrothermal processing biomass: Progress, challenges, and opportunities. *Science of the Total Environment*. 748:142383.

Leng, L., Li, J., Wen, Z. & Zhou, W. 2018. Use of microalgae to recycle nutrients in aqueous phase derived from hydrothermal liquefaction process. *Bioresource Technology*. 256:259–242.

Lesage-Meessen, L., Delattre, M., Haon, M., Thibault, J.F., Ceccaldi, B.C., … Asther, M. 1996. A two-step bioconversion process for vanillin production from ferulic acid combining Aspergillus niger and Pycnoporus cinnabarinus. *Journal of Biotechnology*. 50(2–3):107–113.

Li, B., Wang, Y., Mahmood, N., Yuan, Z., Schmidt, J. & Xu, C. (Charles). 2017. Preparation of bio-based phenol formaldehyde foams using depolymerized hydrolysis lignin. *Industrial*

Crops and Products. 97:409–416.

Li, C., Chen, C., Wu, X., Tsang, C.-W., Mou, J., … Lin, C.S.K. 2019. Recent advancement in lignin biorefinery: with special focus on enzymatic degradation and valorization. *Bioresource Technology*. 291:121898.

Li, C.Z., Wang, Z.B., Liu, J., Liu, C.T., Gu, D.M. & Han, J.C. 2014. The effect of hydrothermal treatment time and level of carbon coating on the performance of PtRu/C catalysts in a direct methanol fuel cell. *RSC Advances*. 4(109):63922–63932.

Li, H., Wang, M., Wang, X., Zhang, Y., Lu, H., … Liu, Z. 2018. Biogas liquid digestate grown Chlorella sp. for biocrude oil production via hydrothermal liquefaction. *Science of the Total Environment*. 635:70–77.

Li, J., Sun, H., Liu, J. xing, Zhang, J. jie, Li, Z. xing & Fu, Y. 2018. Selective reductive cleavage of C–O bond in lignin model compounds over nitrogen-doped carbon-supported iron catalysts. *Molecular Catalysis*. 452:36–45.

Li, R., Greenchem, /, Renders, T., Cooreman, E., Van Den Bosch, S., … Sels, B.F. 2018. Green Chemistry Cutting-edge research for a greener sustainable future Catalytic lignocellulose biorefining in n-butanol/ water: a one-pot approach toward phenolics, polyols, and cellulose †. *Green Chem*. 20(20):4607–4619.

Li, Y., Leow, S., Fedders, A.C., Sharma, B.K., Guest, J.S. & Strathmann, T.J. 2017. Quantitative multiphase model for hydrothermal liquefaction of algal biomass. *Green Chemistry*. 19(4):1163–1174.

Li, Y.H., Sun, Z.H., Zhao, L.Q. & Xu, Y. 2005. Bioconversion of isoeugenol into vanillin by crude enzyme extracted from soybean. *Applied Biochemistry and Biotechnology - Part A Enzyme Engineering and Biotechnology*. 125(1):1–10.

Lin, X., Zhang, Z., Tan, S., Wang, F., Song, Y., … Pittman, C.U. 2017. In line wood plastic composite pyrolyses and HZSM-5 conversion of the pyrolysis vapors. *Energy Conversion and Management*. 141:206–15.

Lin, Y., Ma, X., Peng, X. & Yu, Z. 2017. Hydrothermal carbonization of typical components of municipal solid waste for deriving hydrochars and their combustion behavior. *Bioresource*

Technology. 243:539–547.

López Barreiro, D., Riede, S., Hornung, U., Kruse, A. & Prins, W. 2015. Hydrothermal liquefaction of microalgae: Effect on the product yields of the addition of an organic solvent to separate the aqueous phase and the biocrude oil. *Algal Research*. 12:206–12.

Loy, D.D. & Lundy, E.L. 2018. Nutritional properties and feeding value of corn and its coproducts. In: *Corn: Chemistry and Technology, 3rd Edition*. pp. 633–659.

Luo, Y.R. 2007. *Comprehensive Handbook of Chemical Bond Energies*. 1st ed. *Comprehensive Handbook of Chemical Bond Energies*. CRC press, Boca Raton, 9 March pp. 1688.

Luziatelli, F., Brunetti, L., Ficca, A.G. & Ruzzi, M. 2019. Maximizing the Efficiency of Vanillin Production by Biocatalyst Enhancement and Process Optimization. *Frontiers in Bioengineering and Biotechnology*. 7:279.

Lyu, H., Chen, K., Yang, X., Younas, R., Zhu, X., … Chen, J. 2015. Two-stage nanofiltration process for high-value chemical production from hydrolysates of lignocellulosic biomass through hydrothermal liquefaction. *Separation and Purification Technology*. 147:276–83.

M. Ardizzi, F. Cavani, L. Dal Pozzo, and L.M. 2005. Hydroxymethylation of 2-Methoxyphenol with Formaldehyde to Yield Vanillic Alcohols: A Comparison Between Homogeneous and Heterogeneous Acid Catalysis. In: J. John R. Sowa, ed. 1st ed. *Catalysts of organic reactions*. Bologna, Italy: CRC Press. pp. 357–361.

Maag, A.R., Paulsen, A.D., Amundsen, T.J., Yelvington, P.E., Tompsett, G.A. & Timko, M.T. 2018. Catalytic hydrothermal liquefaction of food waste using cezrox. *Energies*. 11(3):564.

Madden, T. 2013. The BLAST sequence analysis tool. In: *The NCBI Handbook [Internet]. 2nd edition*. pp. 1–17.

Madsen, R.B., Christensen, P.S., Houlberg, K., Lappa, E., Mørup, A.J., … Glasius, M. 2015. Analysis of organic gas phase compounds formed by hydrothermal liquefaction of Dried Distillers Grains with Solubles. *Bioresource Technology*. 192:826–830.

Marais, H.B., Marx, S. & Venter, R.J. 2019. Valorisation of waste lignin for phenol derivative compounds using hydrothermal liquefaction. In: *27th European Biomass Conference and Exhibition Proceedings*. pp. 1132–1138.

Marx, S. 2016. Glycerol-free biodiesel production through transesterification: A review. *Fuel Processing Technology*. 151:139–147.

Matayeva, A., Bianchi, D., Chiaberge, S., Cavani, F. & Basile, F. 2019. Elucidation of reaction pathways of nitrogenous species by hydrothermal liquefaction process of model compounds. *Fuel*. 240:169–178.

Mathimani, T. & Mallick, N. 2019. A review on the hydrothermal processing of microalgal biomass to bio-oil - Knowledge gaps and recent advances. *Journal of Cleaner Production*. 217:69–84.

Matsumura, Y., Minowa, T., Potic, B., Kersten, S.R.A., Prins, W., … Antal, M.J. 2005. Biomass gasification in near- and super-critical water: Status and prospects. *Biomass and Bioenergy*. 29(4):269–292.

Mattevi, A., Fraaije, M.W., Mozzarelli, A., Olivi, L., Coda, A. & Van Berkel, W.J.H. 1997. Crystal structures and inhibitor binding in the octameric flavoenzyme vanillyl-alcohol oxidase: The shape of the active-site cavity controls substrate specificity. *Structure*. 5(7):907–920.

Mayer, M.. 1995. A new set of useful cloning and expression vectors derived from pBlueScript. *Gene*. 163(1):41–46.

McCormick, A.M., Jarmusik, N.A., Endrizzi, E.J. & Leipzig, N.D. 2014. Expression, isolation, and purification of soluble and insoluble biotinylated proteins for nerve tissue regeneration. *Journal of Visualized Experiments*. (83):1–11.

McMurry, J. 2012. Organic Chemistry, 8th Edition. *Belmont, CA : Brooks Cole/Cengage Learning, 2012.*

Mezzogori, R. & Cavani, F. 2002. Liquid-Phase Hydroxymethylation of 2-Methoxyphenol. In: *CHEMICAL INDUSTRIES-NEW YORK*. pp. 483–490.

Midgett, J.S. & Theegala, C.S. 2007. Improving quality and quantity of oils produced from biomass. In: *ASABE Annual International Meeting, Technical Papers*. pp. 1.

Muheim, A. & Lerch, K. 1999. Towards a high-yield bioconversion of ferulic acid to vanillin. *Applied Microbiology and Biotechnology*. 51(4):456–461.

Mulder, W.J., Gosselink, R.J.A., Vingerhoeds, M.H., Harmsen, P.F.H. & Eastham, D. 2011. Lignin based controlled release coatings. *Industrial Crops and Products*. 34(1):915–920.

Muppaneni, T., Reddy, H.K., Selvaratnam, T., Dandamudi, K.P.R., Dungan, B., … Deng, S. 2017. Hydrothermal liquefaction of Cyanidioschyzon merolae and the influence of catalysts on products. *Bioresource Technology*. 223:91–97.

Nagappan, S., Bhosale, R.R., Nguyen, D.D., Chi, N.T.L., Ponnusamy, V.K., … Kumar, G. 2021. Catalytic hydrothermal liquefaction of biomass into bio-oils and other value-added products – A review. *Fuel*. 285:119053.

Nagaraju, D.H., Rebis, T., Gabrielsson, R., Elfwing, A., Milczarek, G. & Inganäs, O. 2014. Charge storage capacity of renewable biopolymer/conjugated polymer interpenetrating networks enhanced by electroactive dopants. *Advanced Energy Materials*. 4(1):1300443.

Naqi, A. 2018. Conversion of Biomass to Liquid Hydrocarbon Fuels via Anaerobic Digestion: A Feasibility Study. ProQuest Dissertations and Theses.

Naron, D.R., Collard, F.X., Tyhoda, L. & Görgens, J.F. 2019a. Influence of impregnated catalyst on the phenols production from pyrolysis of hardwood, softwood, and herbaceous lignins. *Industrial Crops and Products*. 131:348–356.

Naron, D.R., Collard, F.X., Tyhoda, L. & Görgens, J.F. 2019b. Production of phenols from pyrolysis of sugarcane bagasse lignin: Catalyst screening using thermogravimetric analysis – Thermal desorption – Gas chromatography – Mass spectroscopy. *Journal of Analytical and Applied Pyrolysis*. 138:120–121.

Naylor, A.J., Koukharenko, E., Nandhakumar, I.S. & White, N.M. 2012. Surfactant-mediated electrodeposition of bismuth telluride films and its effect on microstructural properties. *Langmuir*. 28(22):8296–8299.

Neuman, R.C. 2013. Substituent Effects. In: *Organic Chemistry; University of California: Riverside, CA, USA*. pp. 1–35.

Oliveira, C.F. de, Paim, T.G. da S., Reiter, K.C., Rieger, A. & D'azevedo, P.A. 2014. Evaluation of four different DNA extraction methods in coagulase-negative Staphylococci clinical isolates. *Revista do Instituto de Medicina Tropical de São Paulo*. 56(1):29–33.

Omar, Y. 2021. Lignin Conversion to Value-Added Small-Molecule Chemicals : Towards Integrated Forest Bioref ineries. Lund University.

Overhage, J., Steinbüchel, A. & Priefert, H. 2003. Highly Efficient Biotransformation of Eugenol to Ferulic Acid and Further Conversion to Vanillin in Recombinant Strains of Escherichia coli. *Applied and Environmental Microbiology*. 69(11):6569–6576.

van Parijs, F.R.D., Morreel, K., Ralph, J., Boerjan, W. & Merks, R.M.H. 2010. Modeling lignin polymerization. I. Simulation model of dehydrogenation polymers. *Plant Physiology*. 153(3):1332–1344.

Paschalidou, A., Tsatiris, M. & Kitikidou, K. 2016. Energy crops for biofuel production or for food? - SWOT analysis (case study: Greece). *Renewable Energy*. 93:636–647.

Paul, T., Baskaran, D., Pakshirajan, K., Pugazhenthi, G. & Rajamanickam, R. 2021. Bio-oil production by hydrothermal liquefaction of Rhodococcus opacus biomass utilizing refinery wastewater: Biomass valorization and process optimization. *Environmental Technology and Innovation*. 21:101326.

Peterson, A.A., Vogel, F., Lachance, R.P., Fröling, M., Antal, M.J. & Tester, J.W. 2008. Thermochemical biofuel production in hydrothermal media: A review of sub- and supercritical water technologies. *Energy and Environmental Science*. 1(1):32–65.

Pineda, A. & Lee, A.F. 2016. Heterogeneously catalyzed lignin depolymerization. *Applied Petrochemical Research*. 6(3):243–256.

Pinkert, A., Goeke, D.F., Marsh, K.N. & Pang, S. 2011. Extracting wood lignin without dissolving or degrading cellulose: Investigations on the use of food additive-derived ionic liquids. *Green Chemistry*. 13(11):3124–3136.

Pirwitz, K., Rihko-Struckmann, L. & Sundmacher, K. 2016. Valorization of the aqueous phase obtained from hydrothermally treated Dunaliella salina remnant biomass. *Bioresource Technology*. 219:64–71.

Popp, J., Lakner, Z., Harangi-Rákos, M. & Fári, M. 2014. The effect of bioenergy expansion: Food, energy, and environment. *Renewable and Sustainable Energy Reviews*. 32:559–578.

Posmanik, R., Labatut, R.A., Kim, A.H., Usack, J.G., Tester, J.W. & Angenent, L.T. 2017.

Coupling hydrothermal liquefaction and anaerobic digestion for energy valorization from model biomass feedstocks. *Bioresource Technology*. 233:134–143.

Posmanik, R., Martinez, C.M., Cantero-Tubilla, B., Cantero, D.A., Sills, D.L., … Tester, J.W. 2018. Acid and Alkali Catalyzed Hydrothermal Liquefaction of Dairy Manure Digestate and Food Waste. *ACS Sustainable Chemistry and Engineering*. 6(2):2724–2732.

Rajalingam, D., Loftis, C., Xu, J.J. & Kumar, T.K.S. 2009. Trichloroacetic acid-induced protein precipitation involves the reversible association of a stable partially structured intermediate. *Protein science : a publication of the Protein Society*. 18(5):980–993.

Ramachandra Rao, S. & Ravishankar, G. 2000. Vanilla flavour: production by conventional and biotechnological routes. *Journal of the Science of Food and Agriculture*. 80(3):289–304.

Ramola, B., Kumar, V., Nanda, M., Mishra, Y., Tyagi, T., … Sharma, N. 2019. Evaluation, comparison of different solvent extraction, cell disruption methods and hydrothermal liquefaction of Oedogonium macroalgae for biofuel production. *Biotechnology Reports*. 22:e00340.

Ratshomo, K. & Nembahe, R. 2018. *2018 South African Energy Sector Report*. http://www.energy.gov.za.

Remón, J., Randall, J., Budarin, V.L. & Clark, J.H. 2019. Production of bio-fuels and chemicals by microwave-assisted, catalytic, hydrothermal liquefaction (MAC-HTL) of a mixture of pine and spruce biomass. *Green Chemistry*. 21(2):284–299.

Renders, T., Van den Bossche, G., Vangeel, T., Van Aelst, K. & Sels, B. 2019. Reductive catalytic fractionation: state of the art of the lignin-first biorefinery. *Current Opinion in Biotechnology*. 56:293–201.

Renders, T., Cooreman, E., Van Den Bosch, S., Schutyser, W., Koelewijn, S.F., … Sels, B.F. 2018. Catalytic lignocellulose biorefining in n -butanol/water: A one-pot approach toward phenolics, polyols, and cellulose. *Green Chemistry*. 20(20):4607–4619.

Rensburg, G. Van, Kruger, R. & Marx, S. 2018. Effect of Operating Parameters on Hydrothermal Liquefaction of Sugarcane Bagasse. In: *10th Int'l Conference on Advances in Science, Engineering, Technology & Healthcare (ASETH-18) Nov*. pp. 259–264.

Reza, M.T., Andert, J., Wirth, B., Busch, D., Pielert, J., … Mumme, J. 2014. Hydrothermal Carbonization of Biomass for Energy and Crop Production. *Applied Bioenergy*. 1(1):11–29.

Del Río, J.C., Rencoret, J., Gutiérrez, A., Nieto, L., Jiménez-Barbero, J. & Martínez, Á.T. 2011. Structural characterization of guaiacyl-rich lignins in flax (Linum usitatissimum) fibers and shives. *Journal of Agricultural and Food Chemistry*. 59(20):11088–11099.

Van Rooyen, N. 2012. Identification, cloning and heterologous expression of fungal vanillyl-alcohol oxidases. http://etd.uovs.ac.za/ETD-db//theses/available/etd-08162012-112452/unrestricted/VanRooyenN.pdf.

Rosendahl, L. 2017. *Direct thermochemical liquefaction for energy applications*. Woodhead Publishing.

Rutherford, D.W., Wershaw, R.L., Rostad, C.E. & Kelly, C.N. 2012. Effect of formation conditions on biochars: Compositional and structural properties of cellulose, lignin, and pine biochars. *Biomass and Bioenergy*. 46:693–701.

Růžičková, J., Kucbel, M., Raclavská, H., Švédová, B., Raclavský, K. & Juchelková, D. 2019. Comparison of organic compounds in char and soot from the combustion of biomass in boilers of various emission classes. *Journal of Environmental Management*. 236:769–783.

Saber, M., Golzary, A., Hosseinpour, M., Takahashi, F. & Yoshikawa, K. 2016. Catalytic hydrothermal liquefaction of microalgae using nanocatalyst. *Applied Energy*. 183:566–576.

Sadhu, S and Maiti, T.K. 2013. Cellulase Production by Bacteria: A Review. *Microbiology Research Journal International*. 3(3):235–258.

Sambrook, J. & Russell, D.W. 2001. *Molecular Cloning: A Laboratory Manual, Third Edition*. 3rd ed ed. New York: Cold Spring Harbor Laboratory Press.

Sambrook, J., Fritsch, E.F., Maniatis, T. & others. 1989. *Molecular cloning: a laboratory manual.* Cold spring harbor laboratory press.

Sangjan, A., Ngamsiri, P., Klomkliang, N., Wu, K.C.W., Matsagar, B.M., … Sakdaronnarong, C. 2020. Effect of microwave-assisted wet torrefaction on liquefaction of biomass from palm oil and sugarcane wastes to bio-oil and carbon nanodots/nanoflakes by hydrothermolysis and solvothermolysis. *Renewable Energy*. 154:1204–1217.

Santos, B. S. L. dos, Gomes, A. F. S., Franciscon, E. G., Oliveira, J. M. de, & Baffi, M.A. 2018. HIDRÓLISE ENZIMÁTICA, FERMENTAÇÃO E PRODUÇÃO DE BIOCOMBUSTÍVEIS ATRAVÉS DA COROA DE Ananas comosus TT - ENZYMATIC HYDROLYSIS, FERMENTATION AND BIOFUELS PRODUCTION FROM ANANAS COMOSUS CROWN. *Química Nova*. 41(10):1127–1131.

Scarsella, M., de Caprariis, B., Damizia, M. & De Filippis, P. 2020. Heterogeneous catalysts for hydrothermal liquefaction of lignocellulosic biomass: A review. *Biomass and Bioenergy*. 140:105662.

Schmidt, R.J. 2005. Industrial catalytic processes - Phenol production. *Applied Catalysis A: General*. 280(1):89–103.

Schuler, J., Hornung, U., Kruse, A., Dahmen, N. & Sauer, J. 2017. Hydrothermal Liquefaction of Lignin. *Journal of Biomaterials and Nanobiotechnology*. 08(01):96–108.

Schuler, J., Hornung, U., Dahmen, N. & Sauer, J. 2019. Lignin from bark as a resource for aromatics production by hydrothermal liquefaction. *GCB Bioenergy*. 11(1):218–229.

Schutyser, W., Renders, T., Van Den Bosch, S., Koelewijn, S.F., Beckham, G.T. & Sels, B.F. 2018. Chemicals from lignin: An interplay of lignocellulose fractionation, depolymerisation, and upgrading. *Chemical Society Reviews*. 47(3):852–908.

Scientific, T. 2007. *BCA ™ Protein Assay Kit*.

Seyedi, S., Venkiteshwaran, K. & Zitomer, D. 2020. Current status of biomethane production using aqueous liquid from pyrolysis and hydrothermal liquefaction of sewage sludge and similar biomass. *Reviews in Environmental Science and Biotechnology*. 20:237–235.

Shamaei, L., Khorshidi, B., Islam, M.A. & Sadrzadeh, M. 2020. Industrial waste lignin as an antifouling coating for the treatment of oily wastewater: Creating wealth from waste. *Journal of Cleaner Production*.

Shanmugam, S.R., Adhikari, S., Wang, Z. & Shakya, R. 2017. Treatment of aqueous phase of bio-oil by granular activated carbon and evaluation of biogas production. *Bioresource Technology*. 223:115–120.

Sheldon, R.A. & Van Bekkum, H. 2007. *Fine Chemicals through Heterogeneous Catalysis*. Wiley-

VCH Verlag.

Shelke, P.S., Sakhare, N.M. & Lahane, S. 2016. Investigation of Combustion Characteristics of a Cottonseed Biodiesel Fuelled Diesel Engine. *Procedia Technology*. 25:1049–1055.

Shraddha, Shekher, R., Sehgal, S., Kamthania, M. & Kumar, A. 2011. Laccase: Microbial sources, production, purification, and potential biotechnological applications. In: *Enzyme Research*. pp. 11.

Si, B., Li, J., Zhu, Z., Shen, M., Lu, J., … Liu, Z. 2018. Inhibitors degradation and microbial response during continuous anaerobic conversion of hydrothermal liquefaction wastewater. *Science of the Total Environment*. 630:1124–1132.

Sinha, A.K., Sharma, U.K. & Sharma, N. 2008. A comprehensive review on vanilla flavor: Extraction, isolation and quantification of vanillin and others constituents. *International Journal of Food Sciences and Nutrition*. 59(4):299–326.

Skoog, Douglas A.; West, Donald M.; Hollar, J.F. 1992. *Fundamentals of Analytical Chemistry.* Sixth ed. N.Y: Colege Publishing.

Soares-Castro, P., Soares, F. & Santos, P.M. 2021. Current Advances in the Bacterial Toolbox for the Biotechnological Production of Monoterpene-Based Aroma Compounds. *Molecules (Basel, Switzerland)*. 26(1):91.

Song, C., Zhang, C., Zhang, S., Lin, H., Kim, Y., … Barceló, Damià. 2020. Thermochemical liquefaction of agricultural and forestry wastes into biofuels and chemicals from circular economy perspectives. *Science of the Total Environment*. 749:141972.

Stafford, W.H.L., Lotter, G.A., von Maltitz, G.P. & Brent, A.C. 2019. Biofuels technology development in Southern Africa. *Development Southern Africa*. 36(2):155–174.

Sun, X.F., Sun, R.C., Fowler, P. & Baird, M.S. 2005. Extraction and characterization of original lignin and hemicelluloses from wheat straw. *Journal of Agricultural and Food Chemistry*. 53(4):860–70.

Sundar, I.K. & Sakthivel, N. 2008. Advances in selectable marker genes for plant transformation. *Journal of Plant Physiology*. 165(16):1698–1716.

Sweeney, W.A. & Bryan, P.F. 2007. BTX Processing. In: *Encyclopedic Dictionary of Named Processes in Chemical Technology*. pp. 1–49.

Swinehart, D.F. 1962. The beer-lambert law. *Journal of chemical education*. 39(7):333.

Taghipour, A., Ramirez, J.A., Brown, R.J. & Rainey, T.J. 2019. A review of fractional distillation to improve hydrothermal liquefaction biocrude characteristics; future outlook and prospects. *Renewable and Sustainable Energy Reviews*. 115:1093–55.

Theegala, C.S. & Midgett, J.S. 2012. Hydrothermal liquefaction of separated dairy manure for production of bio-oils with simultaneous waste treatment. *Bioresource Technology*. 107:456–63.

Thermofisher. 2012. *ProBond ™ Purification System For purification of polyhistidine-containing recombinant proteins*. https://assets.thermofisher.com/TFS-Assets/LSG/manuals/xprpur_man.pdf.

Tommaso, G., Chen, W.T., Li, P., Schideman, L. & Zhang, Y. 2015. Chemical characterization and anaerobic biodegradability of hydrothermal liquefaction aqueous products from mixed-culture wastewater algae. *Bioresource Technology*. 178:139–146.

Toor, S.S., Conti, F., Shah, A.A., Seehar, T.H. & Rosendahl, L.A. 2019. Hydrothermal Liquefaction: A Sustainable Solution to the Sewage Sludge Disposal Problem. In: *Advances in Waste-to-Energy Technologies*. crc press. pp. 143–163.

Toor, S.S., Rosendahl, L. & Rudolf, A. 2011. Hydrothermal liquefaction of biomass: A review of subcritical water technologies. *Energy*. 36(5):2328–2342.

Trejo-Machin, A., Adjaoud, A., Puchot, L., Dieden, R. & Verge, P. 2020. Elucidating the thermal and polymerization behaviours of benzoxazines from lignin derivatives. *European Polymer Journal*. 124:109468.

Trivedi, J., Aila, M., Bangwal, D.P., Kaul, S. & Garg, M.O. 2015. Algae based biorefinery - How to make sense? *Renewable and Sustainable Energy Reviews*. 47:295–307.

Tzanetis, K.F., Posada, J.A. & Ramirez, A. 2017. Analysis of biomass hydrothermal liquefaction and biocrude-oil upgrading for renewable jet fuel production: The impact of reaction conditions on production costs and GHG emissions performance. *Renewable Energy*.

113:1388–98.

Usman, M., Hao, S., Chen, H., Ren, S., Tsang, D.C.W., … Zhang, S. 2019. Molecular and microbial insights towards understanding the anaerobic digestion of the wastewater from hydrothermal liquefaction of sewage sludge facilitated by granular activated carbon (GAC). *Environment International*. 133:105257.

Varanasi, P., Singh, P., Auer, M., Adams, P.D., Simmons, B.A. & Singh, S. 2013. Survey of renewable chemicals produced from lignocellulosic biomass during ionic liquid pretreatment. *Biotechnology for Biofuels*. 6(1):1–9.

Vardon, D.R., Sharma, B.K., Scott, J., Yu, G., Wang, Z., … Strathmann, T.J. 2011. Chemical properties of biocrude oil from the hydrothermal liquefaction of Spirulina algae, swine manure, and digested anaerobic sludge. *Bioresource Technology*. 102(17):8295–303.

Villadsen, S.R., Dithmer, L., Forsberg, R., Becker, J., Rudolf, A., … Glasius, M. 2012. Development and application of chemical analysis methods for investigation of bio-oils and aqueous phase from hydrothermal liquefaction of biomass. *Energy and Fuels*. 26(11):6988–98.

Wang, X. & Zhao, J. 2013. Encapsulation of the herbicide picloram by using polyelectrolyte biopolymers as layer-by-layer materials. *Journal of Agricultural and Food Chemistry*. 61(16):3789–96.

Wang, Z., Watson, J., Wang, T., Yi, S., Si, B. & Zhang, Y. 2021. Enhancing energy recovery via two stage co-fermentation of hydrothermal liquefaction aqueous phase and crude glycerol. *Energy Conversion and Management*. 231:113855.

Wang, Z.B., Li, C.Z., Gu, D.M. & Yin, G.P. 2013. Carbon riveted PtRu/C catalyst from glucose in-situ carbonization through hydrothermal method for direct methanol fuel cell. *Journal of Power Sources*. 238:283–9.

Watanabe, M., Kanaguri, Y. & Smith, R.L. 2018. Hydrothermal separation of lignin from bark of Japanese cedar. *Journal of Supercritical Fluids*. 133:696–703.

Watson, J., Wang, T., Si, B., Chen, W.T., Aierzhati, A. & Zhang, Y. 2020. Valorization of hydrothermal liquefaction aqueous phase: pathways towards commercial viability. *Progress*

in Energy and Combustion Science. 77:1008–19.

Wielligh, J. Von, Schabort, C.J., Venter, R. & Marx, S. 2018. The Evaluation of Spent Coffee Grounds as Feedstock for Continuous Hydrothermal Liquefaction. In: *10th Int'l Conference on Advances in Science, Engineering, Technology & Healthcare (ASETH-18) Nov*. pp. 246–253.

Wong, J. 2012. Technological, Commercial, Organizational, and Social Uncertainties of a Novel Process for Vanillin Production From Lignin. SIMON FRASER UNIVERSITY.

Wu, Y.T., Feng, M., Ding, W.W., Tang, X.Y., Zhong, Y.H. & Xiao, Z.Y. 2008. Preparation of vanillin by bioconversion in a silicon rubber membrane bioreactor. *Biochemical Engineering Journal*. 41(2):193–7.

Wynberg, H. 1954. Some Observations on the Mechanism of the Reimer-Tiemann Reaction. *Journal of the American Chemical Society*. 76(19):4998–9.

Xing, W., Yuan, H., Zhang, P., Yang, H., Song, L. & Hu, Y. 2013. Functionalized lignin for halogen-free flame retardant rigid polyurethane foam: Preparation, thermal stability, fire performance and mechanical properties. *Journal of Polymer Research*. 20(9):1–12.

Xiu, S. & Shahbazi, A. 2012. Bio-oil production and upgrading research: A review. *Renewable and Sustainable Energy Reviews*. 16(7):4406–4414.

Xu, D. & Savage, P.E. 2017. Effect of temperature, water loading, and Ru/C catalyst on water-insoluble and water-soluble biocrude fractions from hydrothermal liquefaction of algae. *Bioresource Technology*. 239:1–6.

Yamada, M., Okada, Y., Yoshida, T. & Nagasawa, T. 2008. Vanillin production using Escherichia coli cells over-expressing isoeugenol monooxygenase of Pseudomonas putida. *Biotechnology Letters*. 30(4):665–70.

Yang, J., He, Q. (Sophia), Corscadden, K. & Niu, H. 2018. The impact of downstream processing methods on the yield and physiochemical properties of hydrothermal liquefaction bio-oil. *Fuel Processing Technology*. 178:353–61.

Yang, S.K., Xu, Y.P. & Duan, P.G. 2018. Data on characterization of crude bio-oils, gaseous products, and process water produced from hydrothermal liquefaction of eight different

algae. *Data in Brief*. 19:1257–1265.

Yu, G., Zhang, Y., Schideman, L., Funk, T.L. & Wang, Z. 2011a. Hydrothermal liquefaction of low lipid content microalgae into bio-crude oil. *Transactions of the ASABE*. 54(1):239–46.

Yu, G., Zhang, Y., Schideman, L., Funk, T. & Wang, Z. 2011b. Distributions of carbon and nitrogen in the products from hydrothermal liquefaction of low-lipid microalgae. *Energy and Environmental Science*. 4(11):4587–95.

Zabeti, M., Baltrusaitis, J. & Seshan, K. 2016. Chemical routes to hydrocarbons from pyrolysis of lignocellulose using Cs promoted amorphous silica alumina catalyst. *Catalysis Today*. 269(1):156–165.

Zamzuri, N.A. & Abd-Aziz, S. 2012. Biovanillin from agro wastes as an alternative food flavour. *Journal of the Science of Food and Agriculture*. 93(3):429–438.

Zastrow, D.J. & Jennings, P.A. 2013. Hydrothermal Liquefaction of Food Waste and Model Food. In: *2013 AIChE Annual Meeting Online Proceedings*. pp. 3–8.

Zhang, J., Chen, W.T., Zhang, P., Luo, Z. & Zhang, Y. 2013. Hydrothermal liquefaction of Chlorella pyrenoidosa in sub- and supercritical ethanol with heterogeneous catalysts. *Bioresource Technology*. 133(1):389–397.

Zhang, S., Yang, X., Zhang, H., Chu, C., Zheng, K., … Liu, L. 2019. Liquefaction of biomass and upgrading of bio-oil: A review. *Molecules*. 24(12):2250.

Zhang, S., Yan, Y., Li, T. & Ren, Z. 2005. Upgrading of liquid fuel from the pyrolysis of biomass. *Bioresource Technology*. 96(5):545–550.

Zhang, S., Yang, X., Liu, L., Ju, M. & Zheng, K. 2018. Adsorption behavior of selective recognition functionalized biochar to Cd(II) in wastewater. *Materials*. 11(2):299.

Zhang, X., Scott, J., Sharma, B.K. & Rajagopalan, N. 2018. Advanced treatment of hydrothermal liquefaction wastewater with nanofiltration to recover carboxylic acids. *Environmental Science: Water Research and Technology*. 4(4):520–528.

Zhao, L.Q., Sun, Z.H., Zheng, P. & He, J.Y. 2006. Biotransformation of isoeugenol to vanillin by Bacillus fusiformis CGMCC1347 with the addition of resin HD-8. *Process Biochemistry*.

41(7):1673–6.

Zhao, Y., Mao, X., Li, W., Gu, X. & Wang, G. 2017. Study on extraction phenol from coal tar with high flux centrifugal extractor. *International Journal of Coal Science and Technology*. 4(4):333–341.

Zhou, X.F. 2014. Conversion of kraft lignin under hydrothermal conditions. *Bioresource Technology*. 170:583–586.

Zhou, Y., Schideman, L., Zheng, M., Martin-Ryals, A., Li, P., … Zhang, Y. 2015. Anaerobic digestion of post-hydrothermal liquefaction wastewater for improved energy efficiency of hydrothermal bioenergy processes. *Water Science and Technology*. 72(12):2139--2147.

Zhu, X., Liu, Y., Zhou, C., Luo, G., Zhang, S. & Chen, J. 2014. A novel porous carbon derived from hydrothermal carbon for efficient adsorption of tetracycline. *Carbon*. 77(1):627–636.

Zhu, X., Qian, F., Liu, Y., Matera, D., Wu, G., … Chen, J. 2016. Controllable synthesis of magnetic carbon composites with high porosity and strong acid resistance from hydrochar for efficient removal of organic pollutants: An overlooked influence. *Carbon*. 99(1):338–347.

Zhu, Y., Biddy, M.J., Jones, S.B., Elliott, D.C. & Schmidt, A.J. 2014. Techno-economic analysis of liquid fuel production from woody biomass via hydrothermal liquefaction (HTL) and upgrading. *Applied Energy*. 129(1):384–394.

Zhu, Z., Rosendahl, L., Toor, S.S., Yu, D. & Chen, G. 2015a. Hydrothermal liquefaction of barley straw to bio-crude oil: Effects of reaction temperature and aqueous phase recirculation. *Applied Energy*. 137(1):183–192.

Zhu, Z., Rosendahl, L., Toor, S.S., Yu, D. & Chen, G. 2015b. Hydrothermal liquefaction of barley straw to bio-crude oil: Effects of reaction temperature and aqueous phase recirculation. *Applied Energy*. 137(1):183–192.

APPENDIX

Appendix A- Recipes of solutions and buffers

Potassium Phosphate pH 8, 100 mM, 100 ml

- 80 mL of dH2O in a 100ml reagent bottle.
- Add 1.628 g of K2HPO4, 0.089 g of KH2PO4
- Add dH2O until volume is 100ml.

Kanamycin, 50 mg/ml

- Weigh 500mg kanamycin solid
- Add 10ml water

Lysogeny Broth media (LB)

- weigh 10 g Peptone 140,
- weigh 5 g Yeast Extract
- weigh 5 g Sodium Chloride
- add dH_2O to 1 L

  With agar, add 15 capsules to LB above, ***Autoclave***

Glycerol 80%, 100 ml

- 20 ml water
- 80 ml glycerol 100 %

Phenolic compounds stock solutions

- A certain mass (mg) was weighed and dissolved in 1 ml dH_2O in an Eppendorf tube, thus concentration in mg/ml of stock solution
- Molarity was given by $\frac{concentration\left(\frac{mg}{ml}\right)}{Molecuar\ weight}$ in mM.

Appendix B1- High Performance Liquid Chromatography (HPLC) Calibration curves

HPLC calibration curve 2019

STOCK SOLUTION						Detection lin	Quantif. Limit				
Compone	Mass (mg)	olume (m	Conc (g/L)	t Time (mi	k-value	ug/L	ug/L				
Guaiacol	30.5	100	0.305	4.965	2.7062						
p-VA	30.5	100.5	0.303483	1.927	0.3692						
m-VA	30.2	100.4	0.300797	3.267	4.8145						
Vanillic ac	30.8	100	0.308	2.928	1.5905						
Vanillin	30.8	101	0.30495	3.944	0.8059						
Ethanol (in Gallic acid)											
			Conc g/L								
Gallic acid	12.215	mg	0.4886			2) 5 mL etoh and 20 mL water as solvent for the gallic acid					
Ethanol	3.945	g in25 mL	0.1578	0.958							
		g in 25 mL		1.54							
		g/mL									

HPLC calibration curve 2020

Component	Mass (mg)	Volume (ml)	Conc (g/L)	t Time (m	k-value	Area	Area ratio	Calc conc	Verskil
Gallic acid prepared in 25ml with 5ml Ethanol	**12.664**	**25**	**0.507**	**4.2**		3883.54			
Hydroquinone	36.536	100	0.3654	4.47	0.2233	666.46	0.172	0.389	6.553
Vanillyl alchol (p-VA)	29.956	100	0.2996	4.544	0.3112	688.82	0.177	0.289	3.620
Resorcinol	32.171	100	0.3217	4.921	0.3013	776.24	0.200	0.336	4.456
Vanillic acid	32.715	100	0.3272	5.133	0.5936	1548.23	0.399	0.340	3.991
Catechol	117.5	100	1.1750	7.5065	0.3107	2825.6	0.728	1.186	0.957
3-Hydroxy-2Methoxy Benzyl Aclhol	155.9	100	1.5590	8.245	0.1581	1957.08	0.504	1.615	3.570
Vanillin	29.754	100	0.2975	10.258	0.7525	1747.2	0.450	0.303	1.787
Phenol	29.987	100	0.2999	11.527	0.168	398.51	0.103	0.309	3.181
Guiacol	41.56	100	0.4156	12.364	0.2149	696.53	0.179	0.423	1.726
Syringol	106.4	100	1.0640	12.193	0.0629	514.09	0.132	1.066	0.196
4-Nitrophenol	33.325	100	0.3333	13.665	0.2717	735.45	0.189	0.353	5.949
p-Cresol	34.5	100	0.3450	14.677	0.1749	509.06	0.131	0.380	10.043
o-Cresol	39.142	100	0.3914	15.255	0.1753	567	0.146	0.422	7.786
2-Nitrophenol	30.744	100	0.3074	17.223	0.4532	1134	0.292	0.326	6.161
2-Naphthol	38.408	100	0.3841	22.203	0.3226	992.38	0.256	0.401	4.471

Appendix B2- High Performance Liquid Chromatography

optimum temperature.

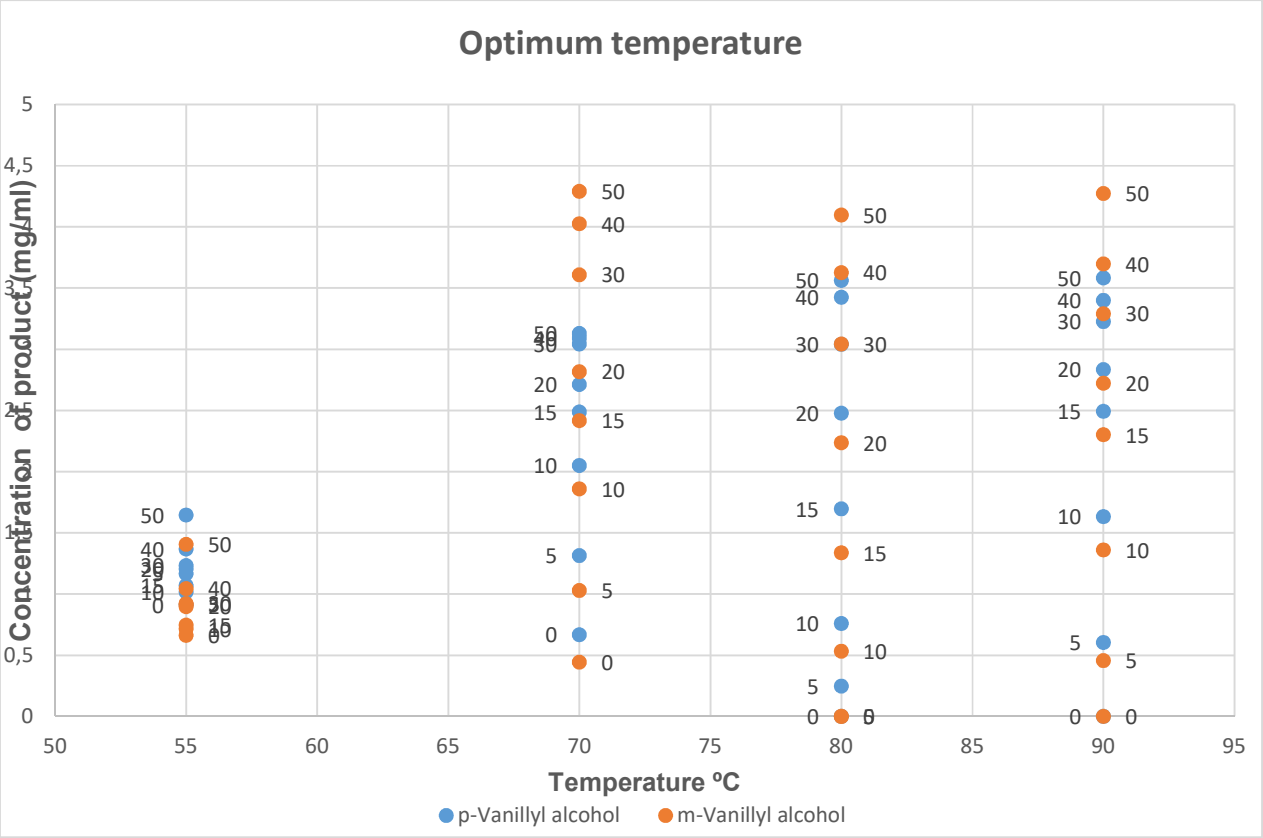

Appendix C- Ultraviolet spectroscopy

Reactions in 1 ml cuvette

The graphs listed in this section shows the vanillyl alcohol oxidase reaction in 1 ml cuvette. Standard curve for vanillin and the relationship of the concertation and absorbance in the enzyme reaction.

concentration of reaction substra		0.154	mg/ml=	1mM
Stock solutions of vanillyl alcohol (mM)			1	100
Stock solutions of vanillyl alcohol (mg/ml)			0.154	15.4
Stock solution of avnillin (mg/ml			0.152	15.2
Preparation of vanillin standard curve				
water	water+500ml buffer	Vanillin volume	concentration of vanillin Mm	concntration of vanillin mg/ml
500.0	1000.0	0.0	0	0.0000
493.5	993.5	6.5	0.015	0.0987
489.2	989.2	10.8	0.025	0.1645
478.4	978.4	21.6	0.05	0.3289
456.7	956.7	43.3	0.1	0.6579
435.1	935.1	64.9	0.15	0.9868
413.4	913.4	86.6	0.2	1.3158
391.8	891.8	108.2	0.25	1.6447

vanillin std curve absorbance data

mg/ml	1	2	3	average	stdev
0.0000	-0.007	-0.002	-0.002	-0.00367	0.002887
0.0010	0.122	0.134	0.128	0.128	0.006
0.0016	0.206	0.219	0.216	0.213667	0.006807
0.0033	0.437	0.431	0.428	0.432	0.004583
0.0066	0.843	0.841	0.84	0.841333	0.001528
0.0099	1.239	1.244	1.249	1.244	0.005
0.0132	1.642	1.649	1.652	1.647667	0.005132
0.0164	2.015	1.983	1.993	1.997	0.016371

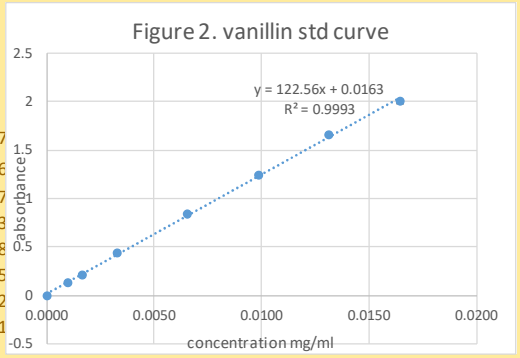

std curve equation

x	y	122.56	0.0163
-0.0001	0.0000		
0.0012	0.1627		
0.0022	0.2803		
0.0031	0.3927		
0.0038	0.4827		
0.0043	0.5457		
0.0048	0.5993		
0.0052	0.6527		
0.0055	0.6863		
0.0056	0.7067		
0.0060	0.7490		
0.0064	0.8057		
0.0068	0.8513		
0.0078	0.9680		
0.0090	1.1197		
0.0096	1.1917		

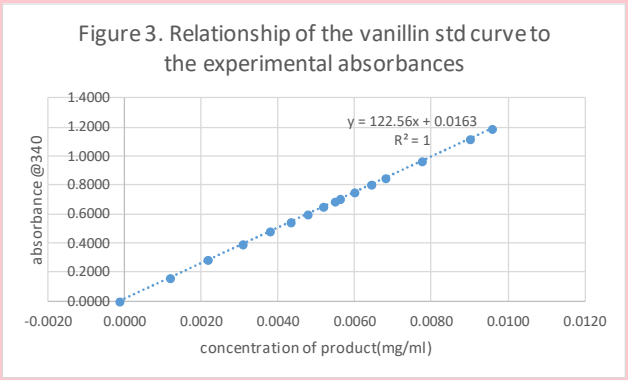

Absorbance agaist concentration of vanillin equation

Curve Name	Curve Formula	A	B	R2
abs/conc	Y=A*X+B	122.56	0.0163	1

Total reaction volume	**30 ml**
Volume of 2.2mg/ml enzyme	**1.257 ml**
Vanillyl alcohol volume	**0.3 ml**
1mM Phosphate buffer	**15 ml**
water (ml)	**13.443 ml**

Data of absorbance and time of reaction

aliquote	Clock	minutes	hours	volume re	triplicates absorbance 1	2	3	average o	stdev
1	1258	0	0	0.5	0	0	0	0	0
2	1313	15		0.5	0.161	0.162	0.165	0.162667	0.002082
3	1328	30		0.5	0.28	0.281	0.28	0.280333	0.000577
4	1343	45		0.5	0.394	0.393	0.391	0.392667	0.001528
5	1358	60	1hr	0.5	0.485	0.482	0.481	0.482667	0.002082
6	1413	75		0.5	0.545	0.547	0.545	0.545667	0.001155
7	1428	90		0.5	0.6	0.599	0.599	0.599333	0.000577
8	1443	105		0.5	0.654	0.652	0.652	0.652667	0.001155
9	1458	120	2hr	0.5	0.686	0.687	0.686	0.686333	0.000577
10	1513	135		0.5	0.708	0.709	0.703		0.003215
11	1528	150	2hr30	0.5	0.749	0.751	0.747	0.749	0.002
12	1558	180	3hrs	0.5	0.805	0.806	0.806	0.805667	0.000577
13	1628	210	3hr30	0.5	0.851	0.852	0.851	0.851333	0.000577
14	1758	300	5	0.5	0.966	0.968	0.97	0.968	0.002
15	2018	440	7hrs 20	0.5	1.123	1.119	1.117	1.119667	0.003055
16	2137	560		0.5	1.186	1.192	1.197	1.191667	0.005508

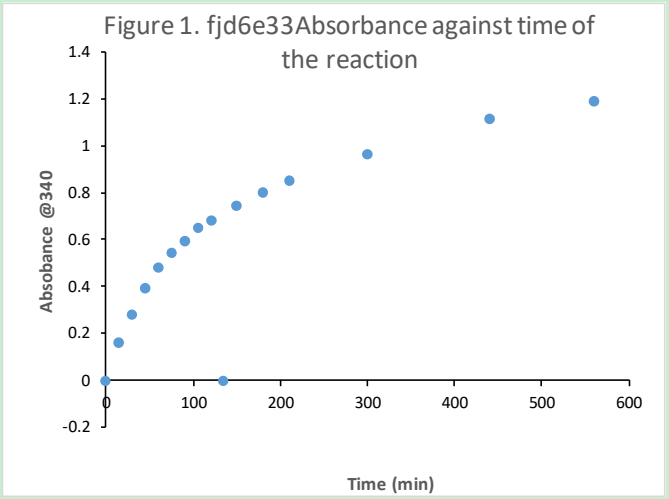

r

Reaction at different enzyme concentrations.

The absorbance readings at 340nm of vanillin standard curve triplicates (blue) and different enzyme concentrations triplicates (black) from the plate reader spectrophotometer at 5minutes intervals.

	1	2	3	4	5	6	7	8	
A	0.105	0.168	0.608	1.069	2.452	3.778	3.904	OVRFLW	340 Read#1
B	0.111	0.174	0.577	1.057	2.429	3.897	OVRFLW	OVRFLW	340 Read#1
C	0.115	0.343	0.588	1.04	2.429	3.786	3.868	3.919	340 Read#1
D	0.118	0.122	0.116	0.128	0.116	0.126			340 Read#1
E	0.121	0.225	0.118	0.117	0.12	0.145			340 Read#1
F	0.13	0.128	0.142	0.19	0.118	0.125			340 Read#1
	1	2	3	4	5	6	7	8	
A	0.112	0.173	0.615	1.082	2.501	3.885	OVRFLW	OVRFLW	340 Read#2
B	0.107	0.175	0.584	1.067	2.457	3.845	OVRFLW	OVRFLW	340 Read#2
C	0.117	0.342	0.594	1.049	2.451	3.909	OVRFLW	OVRFLW	340 Read#2
D	0.119	0.122	0.119	0.135	0.125	0.131			340 Read#2
E	0.122	0.227	0.123	0.125	0.137	0.156			340 Read#2
F	0.132	0.132	0.148	0.202	0.128	0.136			340 Read#2
	1	2	3	4	5	6	7	8	
A	0.112	0.174	0.62	1.088	2.516	3.794	OVRFLW	OVRFLW	340 Read#3
B	0.107	0.181	0.59	1.074	2.474	3.881	OVRFLW	OVRFLW	340 Read#3
C	0.12	0.35	0.596	1.055	2.467	3.9	OVRFLW	OVRFLW	340 Read#3
D	0.123	0.124	0.122	0.144	0.136	0.148			340 Read#3
E	0.122	0.228	0.13	0.135	0.146	0.173			340 Read#3
F	0.132	0.137	0.16	0.214	0.14	0.15			340 Read#3
	1	2	3	4	5	6	7	8	
A	0.114	0.173	0.623	1.092	2.524	3.81	OVRFLW	OVRFLW	340 Read#4
B	0.11	0.179	0.592	1.08	2.486	OVRFLW	OVRFLW	OVRFLW	340 Read#4
C	0.115	0.351	0.599	1.059	2.477	3.856	OVRFLW	OVRFLW	340 Read#4
D	0.123	0.127	0.125	0.154	0.149	0.168			340 Read#4
E	0.122	0.229	0.139	0.147	0.164	0.205			340 Read#4
F	0.134	0.144	0.164	0.231	0.155	0.165			340 Read#4
	1	2	3	4	5	6	7	8	
A	0.114	0.174	0.625	1.095	2.531	3.864	OVRFLW	OVRFLW	340 Read#5
B	0.11	0.177	0.592	1.083	2.491	3.845	3.908	OVRFLW	340 Read#5
C	0.113	0.348	0.601	1.062	2.485	3.812	OVRFLW	OVRFLW	340 Read#5
D	0.123	0.136	0.129	0.165	0.162	0.189			340 Read#5
E	0.122	0.247	0.146	0.16	0.177	0.232			340 Read#5
F	0.134	0.15	0.178	0.248	0.169	0.179			340 Read#5
	1	2	3	4	5	6	7	8	
A	0.113	0.174	0.626	1.096	2.532	OVRFLW	OVRFLW	OVRFLW	340 Read#6
B	0.11	0.179	0.596	1.085	2.495	OVRFLW	OVRFLW	OVRFLW	340 Read#6
C	0.132	0.344	0.602	1.064	2.493	3.93	OVRFLW	OVRFLW	340 Read#6
D	0.123	0.142	0.138	0.173	0.176	0.214			340 Read#6
E	0.122	0.25	0.152	0.171	0.191	0.256			340 Read#6
F	0.136	0.157	0.195	0.253	0.179	0.207			340 Read#6

The absorbance readings at 340nm of vanillin standard curve triplicates (blue) and different enzyme concentrations triplicates (black) from the plate reader spectrophotometer at 5minutes intervals continued…

	1	2	3	4	5	6	7	8	
A	0.11	0.173	0.626	1.096	2.53	3.828	OVRFLW	OVRFLW	340 Read#7
B	0.109	0.178	0.595	1.089	2.503	3.81	OVRFLW	OVRFLW	340 Read#7
C	0.131	0.344	0.602	1.065	2.494	3.825	OVRFLW	OVRFLW	340 Read#7
D	0.125	0.147	0.168	0.182	0.191	0.24			340 Read#7
E	0.123	0.257	0.181	0.18	0.202	0.28			340 Read#7
F	0.137	0.162	0.209	0.281	0.184	0.231			340 Read#7
	1	2	3	4	5	6	7	8	
A	0.108	0.175	0.627	1.097	2.528	3.863	OVRFLW	OVRFLW	340 Read#8
B	0.112	0.177	0.595	1.09	2.509	3.884	3.95	OVRFLW	340 Read#8
C	0.114	0.347	0.602	1.066	2.495	3.929	OVRFLW	OVRFLW	340 Read#8
D	0.127	0.152	0.178	0.215	0.205	0.258			340 Read#8
E	0.123	0.263	0.194	0.186	0.215	0.304			340 Read#8
F	0.138	0.17	0.222	0.301	0.207	0.253			340 Read#8
	1	2	3	4	5	6	7	8	
A	0.108	0.175	0.627	1.097	2.529	3.79	OVRFLW	OVRFLW	340 Read#9
B	0.108	0.183	0.595	1.084	2.51	3.89	OVRFLW	OVRFLW	340 Read#9
C	0.116	0.344	0.603	1.066	2.496	3.89	3.942	OVRFLW	340 Read#9
D	0.127	0.158	0.188	0.234	0.221	0.281			340 Read#9
E	0.124	0.268	0.207	0.234	0.225	0.334			340 Read#9
F	0.138	0.177	0.235	0.32	0.28	0.275			340 Read#9
	1	2	3	4	5	6	7	8	
A	0.108	0.175	0.627	1.097	2.529	3.79	OVRFLW	OVRFLW	340 Read#9
B	0.108	0.183	0.595	1.084	2.51	3.89	OVRFLW	OVRFLW	340 Read#9
C	0.116	0.344	0.603	1.066	2.496	3.89	3.942	OVRFLW	340 Read#9
D	0.127	0.158	0.188	0.234	0.221	0.281			340 Read#9
E	0.124	0.268	0.207	0.234	0.225	0.334			340 Read#9
F	0.138	0.177	0.235	0.32	0.28	0.275			340 Read#9
	1	2	3	4	5	6	7	8	
A	0.108	0.174	0.628	1.096	2.534	OVRFLW	OVRFLW	OVRFLW	340 Read# 10
B	0.109	0.178	0.594	1.09	2.51	3.911	OVRFLW	OVRFLW	340 Read# 10
C	0.115	0.344	0.603	1.068	2.497	OVRFLW	OVRFLW	OVRFLW	340 Read# 10
D	0.127	0.163	0.198	0.25	0.235	0.333			340 Read# 10
E	0.124	0.275	0.218	0.248	0.248	0.403			340 Read# 10
F	0.139	0.183	0.247	0.342	0.296	0.296			340 Read# 10
	1	2	3	4	5	6	7	8	
A	0.108	0.174	0.627	1.096	2.522	3.892	OVRFLW	OVRFLW	340 Read# 11
B	0.11	0.182	0.598	1.086	2.512	3.873	OVRFLW	OVRFLW	340 Read# 11
C	0.126	0.346	0.603	1.067	2.496	3.915	OVRFLW	OVRFLW	340 Read# 11
D	0.128	0.177	0.208	0.266	0.247	0.381			340 Read# 11
E	0.124	0.28	0.23	0.27	0.322	0.431			340 Read# 11
F	0.14	0.188	0.26	0.36	0.318	0.317			340 Read# 11
	1	2	3	4	5	6	7	8	
A	0.109	0.173	0.627	1.095	2.529	3.904	OVRFLW	OVRFLW	340 Read# 12
B	0.108	0.177	0.596	1.084	2.51	OVRFLW	OVRFLW	OVRFLW	340 Read# 12
C	0.117	0.344	0.602	1.067	2.493	OVRFLW	OVRFLW	OVRFLW	340 Read# 12
D	0.127	0.173	0.218	0.28	0.315	0.414			340 Read# 12
E	0.125	0.286	0.241	0.286	0.343	0.461			340 Read# 12
F	0.141	0.194	0.272	0.379	0.339	0.335			340 Read# 12
	1	2	3	4	5	6	7	8	
A	0.109	0.173	0.627	1.095	2.517	3.831	OVRFLW	OVRFLW	340 Read# 13
B	0.111	0.177	0.598	1.087	2.508	3.863	3.889	OVRFLW	340 Read# 13
C	0.123	0.345	0.602	1.067	2.491	3.789	3.951	OVRFLW	340 Read# 13
D	0.127	0.181	0.227	0.295	0.359	0.444			340 Read# 13
E	0.125	0.291	0.252	0.301	0.365	0.488			340 Read# 13
F	0.142	0.2	0.284	0.392	0.359	0.356			340 Read# 13

Calculated mean, and errors

	Absorbance with the blank reaction						absorbance less blank reaction					
Time	0ug/ml	10ug/ml	20ug/ml	30ug/ml	40ug/ml	50ug/ml	0ug/ml	10ug/ml	20ug/ml	30ug/ml	40ug/ml	50ug/ml
0	0.118	0.122	0.116	0.128	0.116	0.126	0	0	0	0	0	0
0	0.121	0.225	0.118	0.117	0.12	0.145	0	0	0	0	0	0
0	0.13	0.128	0.142	0.19	0.118	0.125	0	0	0	0	0	0
5	0.119	0.122	0.119	0.135	0.125	0.131	0.001	0	0.003	0.007	0.009	0.005
5	0.122	0.227	0.123	0.125	0.137	0.156	0.001	0.002	0.005	0.008	0.017	0.011
5	0.132	0.132	0.148	0.202	0.128	0.136	0.002	0.004	0.006	0.012	0.01	0.011
10	0.123	0.124	0.122	0.144	0.136	0.148	0.005	0.002	0.006	0.016	0.02	0.022
10	0.122	0.228	0.13	0.135	0.146	0.173	0.001	0.003	0.012	0.018	0.026	0.028
10	0.132	0.137	0.16	0.214	0.14	0.15	0.002	0.009	0.018	0.024	0.022	0.025
15	0.123	0.127	0.125	0.154	0.149	0.168	0.005	0.005	0.009	0.026	0.033	0.042
15	0.122	0.229	0.139	0.147	0.164	0.205	0.001	0.004	0.021	0.03	0.044	0.06
15	0.134	0.144	0.164	0.231	0.155	0.165	0.004	0.016	0.022	0.041	0.037	0.04
20	0.123	0.136	0.129	0.165	0.162	0.189	0.005	0.014	0.013	0.037	0.046	0.063
20	0.122	0.247	0.146	0.16	0.177	0.232	0.001	0.022	0.028	0.043	0.057	0.087
20	0.134	0.15	0.178	0.248	0.169	0.179	0.004	0.022	0.036	0.058	0.051	0.054
25	0.123	0.142	0.138	0.173	0.176	0.214	0.005	0.02	0.022	0.045	0.06	0.088
25	0.122	0.25	0.152	0.171	0.191	0.256	0.001	0.025	0.034	0.054	0.071	0.111
25	0.136	0.157	0.195	0.253	0.179	0.207	0.006	0.029	0.053	0.063	0.061	0.082
30	0.125	0.147	0.168	0.182	0.191	0.24	0.007	0.025	0.052	0.054	0.075	0.114
30	0.123	0.257	0.181	0.18	0.202	0.28	0.002	0.032	0.063	0.063	0.082	0.135
30	0.137	0.162	0.209	0.281	0.184	0.231	0.007	0.034	0.067	0.091	0.066	0.106
35	0.127	0.152	0.178	0.215	0.205	0.258	0.009	0.03	0.062	0.087	0.089	0.132
35	0.123	0.263	0.194	0.186	0.215	0.304	0.002	0.038	0.076	0.069	0.095	0.159
35	0.138	0.17	0.222	0.301	0.207	0.253	0.008	0.042	0.08	0.111	0.089	0.128
40	0.127	0.158	0.188	0.234	0.221	0.281	0.009	0.036	0.072	0.106	0.105	0.155
40	0.124	0.268	0.207	0.234	0.225	0.334	0.003	0.043	0.089	0.117	0.105	0.189
40	0.138	0.177	0.235	0.32	0.28	0.275	0.008	0.049	0.093	0.13	0.162	0.15
45	0.127	0.163	0.198	0.25	0.235	0.333	0.009	0.041	0.082	0.122	0.119	0.207
45	0.124	0.275	0.218	0.248	0.248	0.403	0.003	0.05	0.1	0.131	0.128	0.258
45	0.139	0.183	0.247	0.342	0.296	0.296	0.009	0.055	0.105	0.152	0.178	0.171
50	0.128	0.177	0.208	0.266	0.247	0.381	0.01	0.055	0.092	0.138	0.131	0.255
50	0.124	0.28	0.23	0.27	0.322	0.431	0.003	0.055	0.112	0.153	0.202	0.286
50	0.14	0.188	0.26	0.36	0.318	0.317	0.01	0.06	0.118	0.17	0.2	0.192
55	0.127	0.173	0.218	0.28	0.315	0.414	0.009	0.051	0.102	0.152	0.199	0.288
55	0.125	0.286	0.241	0.286	0.343	0.461	0.004	0.061	0.123	0.169	0.223	0.316
55	0.141	0.194	0.272	0.379	0.339	0.335	0.011	0.066	0.13	0.189	0.221	0.21
60	0.127	0.181	0.227	0.295	0.359	0.444	0.009	0.059	0.111	0.167	0.243	0.318
60	0.125	0.291	0.252	0.301	0.365	0.488	0.004	0.066	0.134	0.184	0.245	0.343
60	0.142	0.2	0.284	0.392	0.359	0.356	0.012	0.072	0.142	0.202	0.241	0.231

Calculated mean absorbance and errors continued…

	Average absorbance						standard deviation						standard error					
	0ug/ml	10ug/ml	20ug/ml	30ug/ml	40ug/ml	50ug/ml	0ug/ml	10ug/ml	20ug/ml	30ug/ml	40ug/ml	50ug/ml	0ug/ml	10ug/ml	20ug/ml	30ug/ml	40ug/ml	50ug/ml
0	0	0	0	0	0	0	0	0	0	0	0	0	0	0	0	0	0	0
5	0.001333	0.002	0.004667	0.009	0.012	0.009	0.00057735	0.002	0.001528	0.002646	0.004359	0.003464	0.000333	0.001155	0.000882	0.001528	0.002517	0.002
10	0.002667	0.004667	0.012	0.019333	0.022667	0.025	0.002081666	0.003786	0.006	0.004163	0.003055	0.003	0.001202	0.002186	0.003464	0.002404	0.001764	0.001732
15	0.003333	0.008333	0.017333	0.032333	0.038	0.047333	0.002081666	0.006658	0.007234	0.007767	0.005568	0.011015	0.001202	0.003844	0.004177	0.004485	0.003215	0.00636
20	0.003333	0.019333	0.025667	0.046	0.051333	0.068	0.002081666	0.004619	0.011676	0.010817	0.005508	0.017059	0.001202	0.002667	0.006741	0.006245	0.00318	0.009849
25	0.004	0.024667	0.036333	0.054	0.064	0.093667	0.002645751	0.004509	0.015631	0.009	0.006083	0.015308	0.001528	0.002603	0.009025	0.005196	0.003512	0.008838
30	0.005333	0.030333	0.060667	0.069333	0.074333	0.118333	0.002886751	0.004726	0.007767	0.019296	0.008021	0.014978	0.001667	0.002728	0.004485	0.011141	0.004631	0.008647
35	0.006333	0.036667	0.072667	0.089	0.091	0.139667	0.003785939	0.00611	0.009452	0.021071	0.003464	0.016862	0.002186	0.003528	0.005457	0.012166	0.002	0.009735
40	0.006667	0.042667	0.084667	0.117667	0.124	0.164667	0.00321455	0.006506	0.01115	0.012014	0.032909	0.021221	0.001856	0.003756	0.006438	0.006936	0.019	0.012252
45	0.007	0.048667	0.095667	0.135	0.141667	0.212	0.003464102	0.007095	0.012097	0.015395	0.031786	0.043715	0.002	0.004096	0.006984	0.008888	0.018352	0.025239
50	0.007667	0.056667	0.107333	0.153667	0.177667	0.244333	0.004041452	0.002887	0.013614	0.01601	0.040427	0.047899	0.002333	0.001667	0.00786	0.009244	0.02334	0.027655
55	0.008	0.059333	0.118333	0.17	0.214333	0.271333	0.003605551	0.007638	0.014572	0.01852	0.013317	0.05493	0.002082	0.00441	0.008413	0.010693	0.007688	0.031714
60	0.008333	0.065667	0.129	0.184333	0.243	0.297333	0.004041452	0.006506	0.016093	0.017502	0.002	0.058791	0.002333	0.003756	0.009292	0.010105	0.001155	0.033943

Reaction of the 11 different synthetic reactions

Plate reader values for each reaction from time zero at 5minutes intervals.

	1	2	3	4	5	6	7	8	9	10	11	
A	0.114	0.114	0.123	0.116	0.115	0.112	0.115	0.111	0.109	0.111	0.124	340 Read#1
B	0.114	0.111	0.116	0.12	0.115	0.113	0.111	0.11	0.108	0.11	0.107	340 Read#1
C	0.114	0.109	0.113	0.111	0.113	0.116	0.112	0.109	0.109	0.112	0.108	340 Read#1
	1	2	3	4	5	6	7	8	9	10	11	
A	0.114	0.114	0.118	0.122	0.123	0.125	0.123	0.116	0.119	0.117	0.127	340 Read#2
B	0.115	0.111	0.118	0.143	0.122	0.12	0.116	0.115	0.112	0.115	0.111	340 Read#2
C	0.122	0.109	0.115	0.118	0.12	0.122	0.119	0.114	0.114	0.116	0.113	340 Read#2
	1	2	3	4	5	6	7	8	9	10	11	
A	0.114	0.114	0.126	0.133	0.135	0.137	0.135	0.127	0.126	0.128	0.134	340 Read#3
B	0.115	0.111	0.131	0.154	0.132	0.13	0.125	0.124	0.119	0.124	0.117	340 Read#3
C	0.122	0.109	0.115	0.129	0.131	0.131	0.131	0.122	0.121	0.127	0.12	340 Read#3
	1	2	3	4	5	6	7	8	9	10	11	
A	0.114	0.114	0.125	0.147	0.151	0.154	0.15	0.14	0.134	0.143	0.146	340 Read#4
B	0.115	0.111	0.127	0.167	0.146	0.145	0.138	0.137	0.128	0.139	0.127	340 Read#4
C	0.117	0.109	0.119	0.143	0.148	0.144	0.147	0.135	0.131	0.142	0.132	340 Read#4
	1	2	3	4	5	6	7	8	9	10	11	
A	0.114	0.114	0.13	0.164	0.171	0.167	0.166	0.157	0.146	0.162	0.159	340 Read#5
B	0.115	0.111	0.123	0.186	0.165	0.162	0.154	0.153	0.14	0.157	0.139	340 Read#5
C	0.118	0.109	0.13	0.16	0.169	0.157	0.165	0.151	0.143	0.154	0.146	340 Read#5
	1	2	3	4	5	6	7	8	9	10	11	
A	0.114	0.114	0.136	0.183	0.193	0.183	0.186	0.176	0.161	0.183	0.175	340 Read#6
B	0.115	0.112	0.123	0.207	0.186	0.183	0.172	0.172	0.153	0.178	0.153	340 Read#6
C	0.118	0.109	0.137	0.187	0.188	0.18	0.186	0.17	0.157	0.172	0.161	340 Read#6
	1	2	3	4	5	6	7	8	9	10	11	
A	0.114	0.114	0.143	0.204	0.233	0.205	0.208	0.199	0.174	0.207	0.191	340 Read#7
B	0.115	0.112	0.122	0.229	0.209	0.205	0.193	0.194	0.168	0.202	0.169	340 Read#7
C	0.116	0.109	0.115	0.204	0.214	0.201	0.21	0.191	0.172	0.193	0.178	340 Read#7
	1	2	3	4	5	6	7	8	9	10	11	
A	0.114	0.114	0.15	0.227	0.255	0.225	0.231	0.222	0.191	0.231	0.209	340 Read#8
B	0.115	0.111	0.123	0.244	0.233	0.228	0.216	0.216	0.183	0.226	0.185	340 Read#8
C	0.119	0.109	0.115	0.227	0.238	0.223	0.234	0.214	0.188	0.215	0.197	340 Read#8
	1	2	3	4	5	6	7	8	9	10	11	
A	0.114	0.114	0.157	0.251	0.283	0.247	0.255	0.247	0.207	0.257	0.227	340 Read#9
B	0.115	0.111	0.127	0.267	0.259	0.253	0.239	0.24	0.199	0.25	0.202	340 Read#9
C	0.116	0.109	0.115	0.252	0.266	0.248	0.26	0.238	0.204	0.242	0.215	340 Read#9
	1	2	3	4	5	6	7	8	9	10	11	
A	0.114	0.114	0.164	0.276	0.315	0.271	0.28	0.273	0.222	0.284	0.246	340 Read#10
B	0.115	0.112	0.125	0.299	0.286	0.279	0.264	0.266	0.216	0.276	0.22	340 Read#10
C	0.125	0.109	0.115	0.278	0.292	0.275	0.286	0.264	0.222	0.27	0.235	340 Read#10

Appendix D- Errors and calculations.

Calculated mean and errors

The mean is given by

$$\frac{Total\ sum\ of\ triplicates}{3}$$

	Mean values										
Time	1	2	3	4	5	6	7	8	9	10	11
0	0.01148	0.01121	0.01182	0.01165	0.01151	0.01145	0.01135	0.01108	0.01094	0.01118	0.01138
5	0.01178	0.01121	0.01178	0.01286	0.01225	0.01232	0.01202	0.01158	0.01158	0.01168	0.01178
10	0.01178	0.01121	0.01249	0.01396	0.01336	0.01336	0.01313	0.01252	0.01229	0.01272	0.01245
15	0.01161	0.01121	0.01245	0.01534	0.01494	0.01487	0.01460	0.01383	0.01319	0.01423	0.01360
20	0.01165	0.01121	0.01286	0.01712	0.01695	0.01631	0.01628	0.01548	0.01440	0.01588	0.01490
25	0.01165	0.01125	0.01329	0.01937	0.01903	0.01833	0.01826	0.01739	0.01581	0.01789	0.01642
30	0.01158	0.01125	0.01276	0.02138	0.02202	0.02051	0.02051	0.01960	0.01725	0.02021	0.01806
35	0.01168	0.01121	0.01302	0.02343	0.02437	0.02269	0.02286	0.02189	0.01887	0.02256	0.01984
40	0.01158	0.01121	0.01339	0.02585	0.02712	0.02511	0.02531	0.02434	0.02048	0.02514	0.02162
45	0.01188	0.01125	0.01356	0.02863	0.02998	0.02769	0.02786	0.02696	0.02216	0.02786	0.02353

Calculated mean and errors continued…

	mean less blank									
Time	1	2	3	4	5	6	7	8	9	10
0	0.00000	-0.00027	0.00034	0.00017	0.00003	-0.00003	-0.00013	-0.00040	-0.00054	-0.00030
5	0.00000	-0.00057	0.00000	0.00107	0.00047	0.00054	0.00023	-0.00020	-0.00020	-0.00010
10	0.00000	-0.00057	0.00070	0.00218	0.00158	0.00158	0.00134	0.00074	0.00050	0.00094
15	0.00000	-0.00040	0.00084	0.00373	0.00332	0.00326	0.00299	0.00222	0.00158	0.00262
20	0.00000	-0.00044	0.00121	0.00547	0.00530	0.00467	0.00463	0.00383	0.00275	0.00423
25	0.00000	-0.00040	0.00164	0.00772	0.00739	0.00668	0.00661	0.00574	0.00416	0.00624
30	0.00000	-0.00034	0.00117	0.00980	0.01044	0.00893	0.00893	0.00802	0.00567	0.00863
35	0.00000	-0.00047	0.00134	0.01175	0.01269	0.01101	0.01118	0.01021	0.00718	0.01088
40	0.00000	-0.00037	0.00181	0.01427	0.01554	0.01353	0.01373	0.01276	0.00890	0.01356
45	0.00000	-0.00064	0.00168	0.01675	0.01809	0.01581	0.01598	0.01507	0.01027	0.01598

Calculated mean and errors continued…

Standard deviation was calculated directly from excel formulas.

	standard deviation										
Time	1	2	3	4	5	6	7	8	9	10	11
0	0.00000	0.00025	0.00052	0.00045	0.00012	0.00021	0.00021	0.00010	0.00006	0.00010	0.00096
5	0.00044	0.00025	0.00017	0.00135	0.00015	0.00025	0.00035	0.00010	0.00036	0.00010	0.00088
10	0.00044	0.00025	0.00082	0.00135	0.00021	0.00038	0.00051	0.00025	0.00036	0.00021	0.00091
15	0.00015	0.00025	0.00042	0.00129	0.00025	0.00055	0.00063	0.00025	0.00030	0.00021	0.00099
20	0.00021	0.00025	0.00041	0.00141	0.00031	0.00050	0.00067	0.00031	0.00030	0.00041	0.00102
25	0.00021	0.00025	0.00079	0.00129	0.00036	0.00017	0.00081	0.00031	0.00040	0.00055	0.00112
30	0.00010	0.00025	0.00147	0.00145	0.00128	0.00023	0.00094	0.00041	0.00031	0.00071	0.00111
35	0.00027	0.00025	0.00185	0.00099	0.00116	0.00025	0.00097	0.00042	0.00041	0.00082	0.00121
40	0.00010	0.00025	0.00218	0.00090	0.00124	0.00032	0.00110	0.00048	0.00041	0.00076	0.00126
45	0.00061	0.00025	0.00261	0.00128	0.00154	0.00040	0.00115	0.00048	0.00035	0.00071	0.00131

Calculated mean and errors continued…

Standard error of the mean is given by

$$\frac{standarddeviation(\sigma)}{\sqrt{3}}$$

	Standard error of the mean										
Time	1	2	3	4	5	6	7	8	9	10	11
0	0	0.000146	0.000298	0.000262	6.71387E-05	0.000121	0.000121	5.81E-05	3.36E-05	5.81E-05	0.000555
5	0.000253	0.000146	0.000101	0.000781	8.88161E-05	0.000146	0.000204	5.81E-05	0.00021	5.81E-05	0.000507
10	0.000253	0.000146	0.000476	0.000781	0.000121036	0.00022	0.000293	0.000146	0.00021	0.000121	0.000528
15	8.88E-05	0.000146	0.000242	0.000748	0.000146325	0.00032	0.000363	0.000146	0.000174	0.000121	0.000573
20	0.000121	0.000146	0.000235	0.000814	0.000177632	0.000291	0.000387	0.000178	0.000174	0.000235	0.00059
25	0.000121	0.000146	0.000454	0.000748	0.00020964	0.000101	0.00047	0.000178	0.000233	0.00032	0.000647
30	5.81E-05	0.000146	0.000847	0.000839	0.000736233	0.000134	0.00054	0.000235	0.000178	0.000413	0.000643
35	0.000154	0.000146	0.001066	0.000571	0.000670547	0.000146	0.000561	0.000242	0.000235	0.000476	0.000698
40	5.81E-05	0.000146	0.001258	0.000521	0.00071763	0.000187	0.000638	0.000275	0.000235	0.000436	0.000727
45	0.000354	0.000146	0.001505	0.000741	0.000890062	0.000233	0.000661	0.000275	0.000201	0.000408	0.000759

Calculated mean and errors continued…

The error at 95% level is given by

$$\pm 1.96(standard\ error)$$

From the 11 values of error at each time, the LSD was calculated by

$$\frac{total\ sum}{11}$$

	Error at 95% confidence level											
Time	1	2	3	4	5	6	7	8	9	10	11	**LSD**
0	0	0.000287	0.000585	0.000514	0.000132	0.000237	0.000237	0.000114	6.58E-05	0.000114	0.001087	0.000307
5	0.000497	0.000287	0.000197	0.00153	0.000174	0.000287	0.0004	0.000114	0.000411	0.000114	0.000993	0.000455
10	0.000497	0.000287	0.000933	0.00153	0.000237	0.000431	0.000574	0.000287	0.000411	0.000237	0.001034	0.000587
15	0.000174	0.000287	0.000474	0.001465	0.000287	0.000628	0.000712	0.000287	0.000342	0.000237	0.001122	0.000547
20	0.000237	0.000287	0.000461	0.001595	0.000348	0.00057	0.000759	0.000348	0.000342	0.000461	0.001157	0.000597
25	0.000237	0.000287	0.00089	0.001465	0.000411	0.000197	0.000921	0.000348	0.000456	0.000628	0.001269	0.000646
30	0.000114	0.000287	0.001661	0.001645	0.001443	0.000263	0.001059	0.000461	0.000348	0.000809	0.00126	0.00085
35	0.000302	0.000287	0.00209	0.001119	0.001314	0.000287	0.001099	0.000474	0.000461	0.000933	0.001368	0.000885
40	0.000114	0.000287	0.002465	0.001021	0.001407	0.000366	0.00125	0.000539	0.000461	0.000855	0.001425	0.000926
45	0.000693	0.000287	0.002951	0.001452	0.001745	0.000456	0.001296	0.000539	0.000395	0.0008	0.001487	0.0011

Sequence alignment of PsVAO gene promoter and terminator sequences (mega multiple alignment tool)

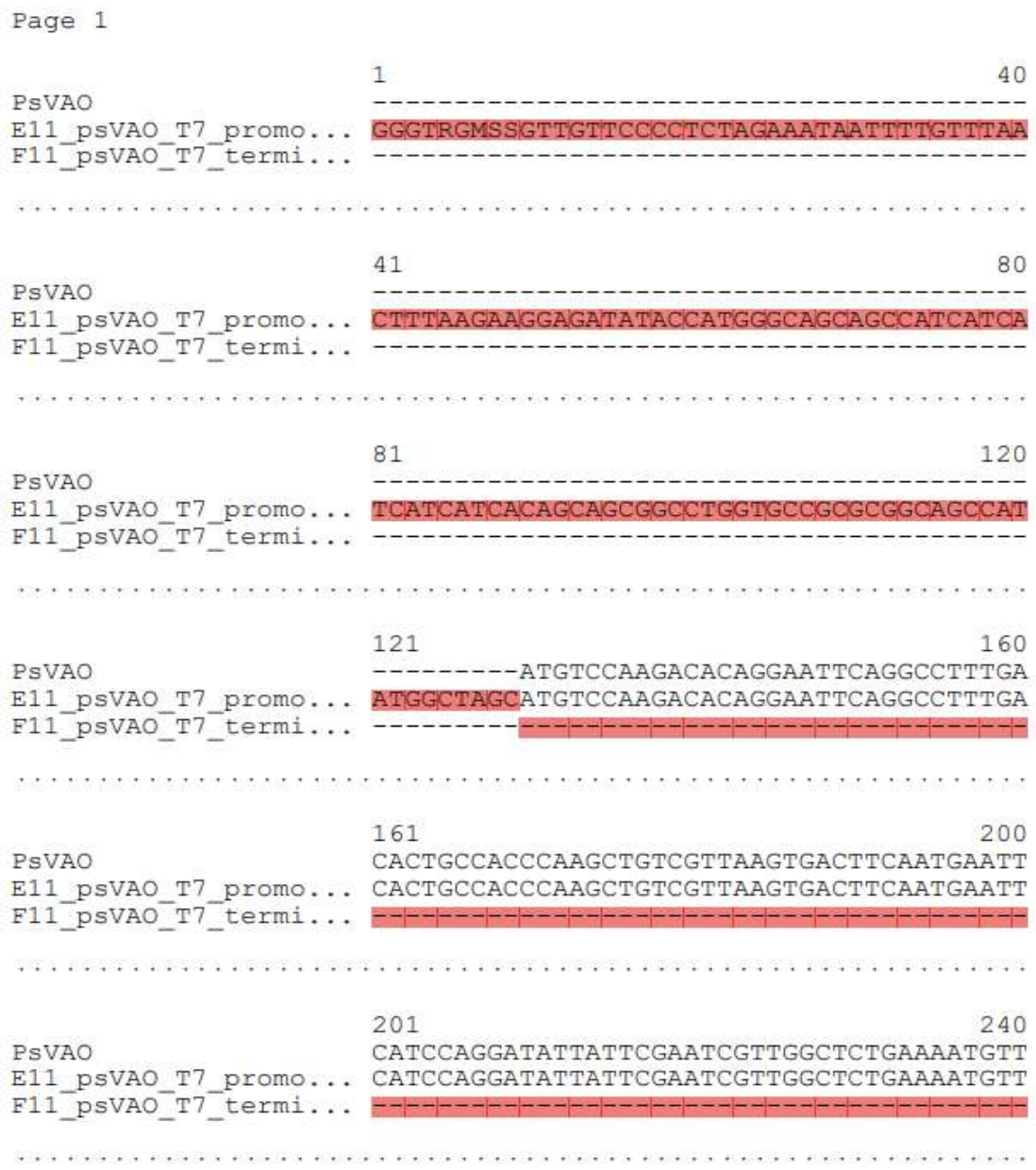

Page 2

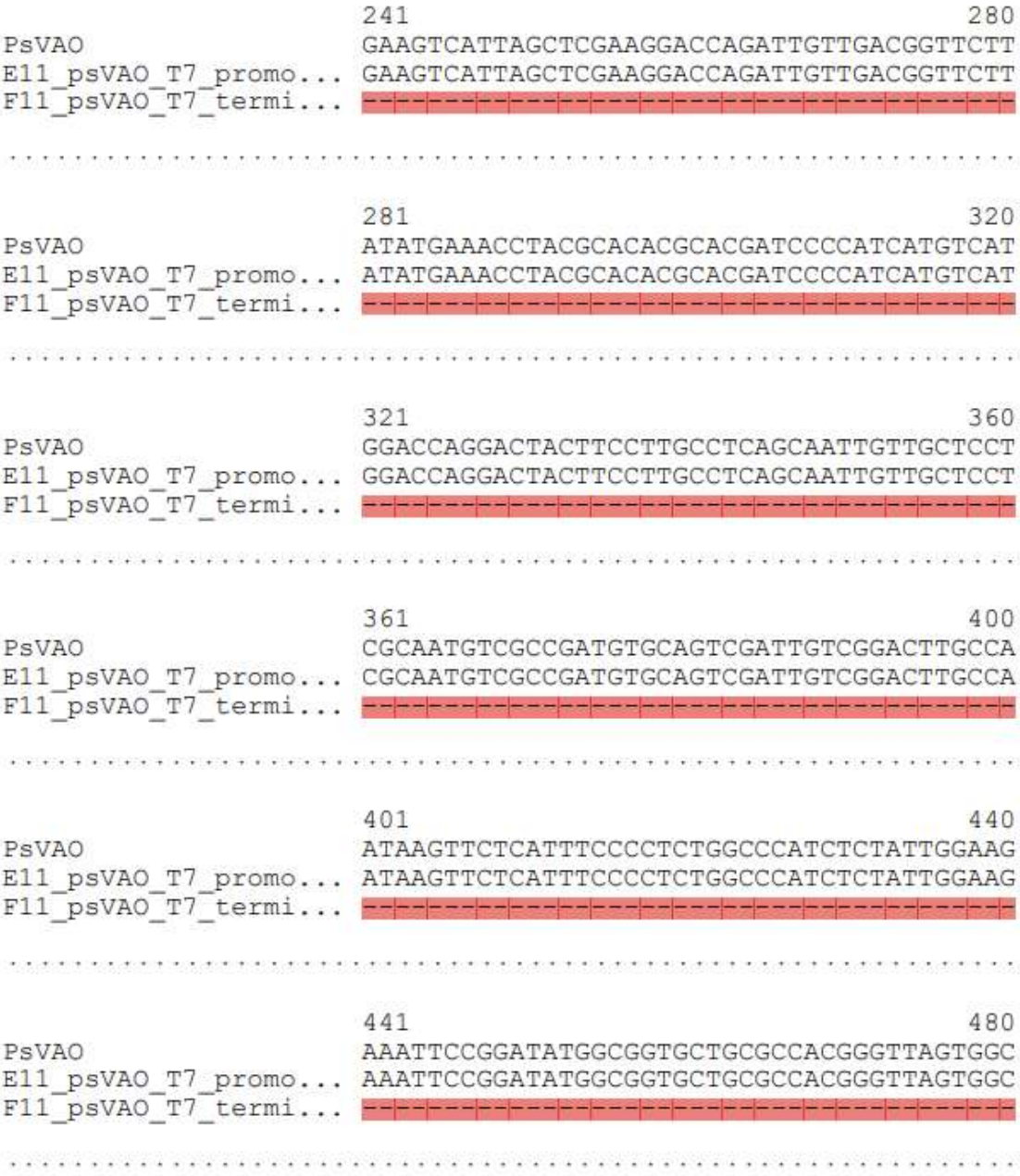
241 280
PsVAO GAAGTCATTAGCTCGAAGGACCAGATTGTTGACGGTTCTT
E11_psVAO_T7_promo... GAAGTCATTAGCTCGAAGGACCAGATTGTTGACGGTTCTT
F11_psVAO_T7_termi...
281 320
PsVAO ATATGAAACCTACGCACACGCACGATCCCCATCATGTCAT
E11_psVAO_T7_promo... ATATGAAACCTACGCACACGCACGATCCCCATCATGTCAT
F11_psVAO_T7_termi...
321 360
PsVAO GGACCAGGACTACTTCCTTGCCTCAGCAATTGTTGCTCCT
E11_psVAO_T7_promo... GGACCAGGACTACTTCCTTGCCTCAGCAATTGTTGCTCCT
F11_psVAO_T7_termi...
361 400
PsVAO CGCAATGTCGCCGATGTGCAGTCGATTGTCGGACTTGCCA
E11_psVAO_T7_promo... CGCAATGTCGCCGATGTGCAGTCGATTGTCGGACTTGCCA
F11_psVAO_T7_termi...
401 440
PsVAO ATAAGTTCTCATTTCCCCTCTGGCCCATCTCTATTGGAAG
E11_psVAO_T7_promo... ATAAGTTCTCATTTCCCCTCTGGCCCATCTCTATTGGAAG
F11_psVAO_T7_termi...
441 480
PsVAO AAATTCCGGATATGGCGGTGCTGCGCCACGGGTTAGTGGC
E11_psVAO_T7_promo... AAATTCCGGATATGGCGGTGCTGCGCCACGGGTTAGTGGC
F11_psVAO_T7_termi...

```
                     481                                                 520
PsVAO                AGTGTCGTGCTGGACATGGGAAAGAATATGAACAGAGTTC
E11_psVAO_T7_promo... AGTGTCGTGCTGGACATGGGAAAGAATATGAACAGAGTTC
F11_psVAO_T7_termi... ----------------------------------------

.....................................................................

                     521                                                 560
PsVAO                TAGAAGTGAACGTGGAAGGCGCATATTGCGTGGTGGAGCC
E11_psVAO_T7_promo... TAGAAGTGAACGTGGAAGGCGCATATTGCGTGGTGGAGCC
F11_psVAO_T7_termi... ----------------------------------------

.....................................................................

                     561                                                 600
PsVAO                CGGTGTAACTTACCACGACTTGCATAATTACCTTGAGGCG
E11_psVAO_T7_promo... CGGTGTAACTTACCACGACTTGCATAATTACCTTGAGGCG
F11_psVAO_T7_termi... ----------------------------------------AGTCG

.....................................................................

                     601                                                 640
PsVAO                AACAATCTTCGAGACAAATTATGGCTTGATGTACCGGATC
E11_psVAO_T7_promo... AACAATCTTCGAGACAAATTATGGCTTGATGTACCGGATC
F11_psVAO_T7_termi... AACGGTT-------------------------------------

.....................................................................

                     641                                                 680
PsVAO                TTGGTGGCGGTTCTGTTCTCGGC-AATGCCGTTGAGAGAG
E11_psVAO_T7_promo... TTGGTGGCGGTTCTGTTCTCGGC-AATGCCGTTGAGAGAG
F11_psVAO_T7_termi... ---------TCCKGTTCTCCGCGAATGGCAGTTCRAGAC

.....................................................................

                     681                                                 720
PsVAO                GTGTGGGCTATACGCCTTACGGAGATCATTGGATGATGCA
E11_psVAO_T7_promo... GTGTGGGCTATACGCCTTACGGAGATCATTGGATGATGCA
F11_psVAO_T7_termi... GTTAGGCCTA---GCCTTAC-GARATCAT--GATGATGCA

.....................................................................
```

```
                     721                                         760
PsVAO                CAGTGGGATGGAAGTCGTCCTTGCGAATGGCGAGCTTCTT
E11_psVAO_T7_promo... CAGTGGGATGGAAGTCGTCCTTGCGAATGGCGAGCTTCTT
F11_psVAO_T7_termi... CAGTGGAATGAG------T-TCGTCTGCGATGCGRGCTTC

.....................................................................

                     761                                         800
PsVAO                AGGACTGGCATGGGGGCTCTACCTGATCCTAAACGTCCCG
E11_psVAO_T7_promo... AGGACTGGCATGGGGGCTCTACCTGATCCTAAACGTCCCG
F11_psVAO_T7_termi... TAGACTGGCATGRGGGCTCTACTGA--T-TCTAACGTCCCG

.....................................................................

                     801                                         840
PsVAO                AAACGATGGGGCTAAAGCCAGAAGACCAGCCATGGA-GCA
E11_psVAO_T7_promo... AAACGATGGGGCTAAAGCCAGAAGACCAGCCATGGA-GCA
F11_psVAO_T7_termi... AAACGATGGRGCT-AAGCCAGAAGACCAGCCATGGAGGCA

.....................................................................

                     841                                         880
PsVAO                AAATCGCTCATCTGTTTCCTTATGGCTTCGGTCCCTATAT
E11_psVAO_T7_promo... AAATCGCTCATCTGTTTCCTTATGGCTTCGGTCCCTATAT
F11_psVAO_T7_termi... AAATCGCTCATCTGTTT-CTTATGRCTTCGGTCCCTATAT

.....................................................................

                     881                                         920
PsVAO                AGATGGGCTATTCAGCCAATCGAATATGGGAATTGTTACC
E11_psVAO_T7_promo... AGATGGGCTATTCAGCCAATCGAATATGGGAATTGTTACC
F11_psVAO_T7_termi... AGATGGGCTA-TCAGCCCATCGAATATGGGAATTGTTACC

.....................................................................

                     921                                         960
PsVAO                AAGATCGGGATCTGGTTAATGCCCAATCCAGGGGGTTATC
E11_psVAO_T7_promo... AAGATCGGGATCTGGTTAATGCCCAATCCAGGGGGTTATC
F11_psVAO_T7_termi... AAGATCGGGATCTGGTTAATGCCCAATCCAGGGGGTTATC

.....................................................................
```

```
                     961                                       1000
PsVAO                AATCCTACTTGATCACACTACCCAAAGATGGTGATTTAAA
E11_psVAO_T7_promo... AATCCTACTTGATCACACTACCCAAAGATGGTGATTTAAA
F11_psVAO_T7_termi... AATCCTACTTGATCACACTACCCAAAGATGGTGATTTAAA

.....................................................................

                     1001                                      1040
PsVAO                ACAAGCCGTCGATATTATTCGTCCCCTTCGTCTAGGCATG
E11_psVAO_T7_promo... ACAAGCCGTCGACATTATTCGTCCCCTTCGTCTA-GCATG
F11_psVAO_T7_termi... ACAAGCCGTCGACATTATTCGTCCCCTTCGTCTAGGCATG

.....................................................................

                     1041                                      1080
PsVAO                GCCCTTCAAAATGTTCCCACTATTCGCCACATTCTTTTGG
E11_psVAO_T7_promo... GCCCTTC-AAATGTTCCCACTATTCGCCACATTC-TTTGG
F11_psVAO_T7_termi... GCCCTTCAAAATGTTCCCACTATTCGCCACATTCTTTTGG

.....................................................................

                     1081                                      1120
PsVAO                ATGCAGCGGTGCTCGGTGACAAGCGATCTTATTCATCCAA
E11_psVAO_T7_promo... ATGCAGC-GTGCTCGGTGACAG---+---+-CGATCTATTCAT
F11_psVAO_T7_termi... ATGCAGCGGTGCTCGGTGACAAGCGATCTTATTCATCCAA

.....................................................................

                     1121                                      1160
PsVAO                GACCGAACCCCTCTCCGACGAGGAATTAGACAAGATCGCG
E11_psVAO_T7_promo... CAGACGACCCCTCCTCGACGAGATA---+--GACAGATCGCG
F11_psVAO_T7_termi... GACCGAACCCCTCTCYGACGAGGAATTAGACAAGATCGCG

.....................................................................

                     1161                                      1200
PsVAO                AAACAGCTCAACTTGGGACGATGGAACTTTTACGGGGCGC
E11_psVAO_T7_promo... -AACAGCTCA---+-CTGGACGATGGA--CTTTACGGGGC-+-
F11_psVAO_T7_termi... AAACAGCTCAACTTGGGACGATGGAACTTTTACGGGGCGC

.....................................................................
```

```
                     1201                                        1240
PsVAO                TCTATGGACCTGAGCCGATTCGAAGGGTTCTCTGGGAAAC
E11_psVAO_T7_promo... -CTATGACCTGAA--CGATTCGAGG---TTYCTGGCAAC
F11_psVAO_T7_termi... TCTATGGACCTGAGCCGATTCGAAGGGTTCTCTGGGAAAC

.....................................................................

                     1241                                        1280
PsVAO                GATTAAAGACGCATTCTCGGCGATCCCAGGCGTCAAGTTT
E11_psVAO_T7_promo... GATTARGACSGCATTTCG-----------------------
F11_psVAO_T7_termi... GATTAAAGACGCATTCTCGGCGATCCCAGGCGTCAAGTTT

.....................................................................

                     1281                                        1320
PsVAO                TATTTTCCGGAGGACACTCCTGAAAACTCCGTTCTCCGCG
E11_psVAO_T7_promo... ------------------------------------------
F11_psVAO_T7_termi... TATTTTCCGGAGGACACTCCTGAAAACTCCGTTCTCCGCG

.....................................................................

                     1321                                        1360
PsVAO                TGCGTGATAAGACTATGCAAGGCATTCCAACTTACGACGA
E11_psVAO_T7_promo... ------------------------------------------
F11_psVAO_T7_termi... TGCGTGATAAGACTATGCAAGGCATTCCAACTTACGACGA

.....................................................................

                     1361                                        1400
PsVAO                GCTAAAGTGGATCGATTGGCTCCCTAATGGTGCGCATCTG
E11_psVAO_T7_promo... ------------------------------------------
F11_psVAO_T7_termi... GCTAAAGTGGATCGATTGGCTCCCTAATGGTGCGCATCTG

.....................................................................

                     1401                                        1440
PsVAO                TTCTTCTCTCCTATTGCGAAGGTATCTGGTGAAGATGCAA
E11_psVAO_T7_promo... ------------------------------------------
F11_psVAO_T7_termi... TTCTTCTCTCCTATTGCGAAGGTATCTGGTGAAGATGCAA

.....................................................................
```

```
                      1441                                        1480
PsVAO                 TGATGCAATACGCAGTCACCAAGAAAAGGTGTCAGGAGGC
E11_psVAO_T7_promo... ----------------------------------------
F11_psVAO_T7_termi... TGATGCAATACGCAGTCACCAAGAAAAGGTGTCAGGAGGC

.....................................................................

                      1481                                        1520
PsVAO                 TGGGTTAGATTTTATCGGCACTTTCACAGTCGGTATGAGA
E11_psVAO_T7_promo... ----------------------------------------
F11_psVAO_T7_termi... TGGGTTAGATTTTATCGGCACTTTCACAGTCGGTATGAGA

.....................................................................

                      1521                                        1560
PsVAO                 GAGATGCATCATATCGTTTGTATTGTGTTCAACAAGAAGG
E11_psVAO_T7_promo... ----------------------------------------
F11_psVAO_T7_termi... GAGATGCATCATATCGTTTGTATTGTGTTCAACAAGAAGG

.....................................................................

                      1561                                        1600
PsVAO                 ACCTAATACAAAAGAGAAAAGTACAGTGGCTGATGAGAAC
E11_psVAO_T7_promo... ----------------------------------------
F11_psVAO_T7_termi... ACCTAATACAAAAGAGAAAAGTACAGTGGCTGATGAGAAC

.....................................................................

                      1601                                        1640
PsVAO                 CCTTATTGATGACTGTGCTGCAAATGGATGGGGCGAATAT
E11_psVAO_T7_promo... ----------------------------------------
F11_psVAO_T7_termi... CCTTATTGATGACTGTGCTGCAAATGGATGGGGCGAATAT

.....................................................................

                      1641                                        1680
PsVAO                 CGAACCCATCTGGCCTTCATGGACCAAATTATGGAAACCT
E11_psVAO_T7_promo... ----------------------------------------
F11_psVAO_T7_termi... CGAACCCATCTGGCCTTCATGGACCAAATTATGGAAACCT

.....................................................................
```

```
                      1681                                      1720
PsVAO                 ACAACTGGAACAACAGCAGCTTCCTAAGGTTCAATGAGGT
E11_psVAO_T7_promo... ----------------------------------------
F11_psVAO_T7_termi... ACAACTGGAACAACAGCAGCTTCCTAAGGTTCAATGAGGT

.....................................................................

                      1721                                      1760
PsVAO                 CCTCAAGAATGCGGTGGATCCTAATGGCATCATTGCCCCG
E11_psVAO_T7_promo... ----------------------------------------
F11_psVAO_T7_termi... CCTCAAGAATGCGGTGGATCCTAATGGCATCATTGCCCCG

.....................................................................

                      1761                                      1800
PsVAO                 GGAAAGTCTGGTGTTTGGCCGAGTCAATACAGTCATGTTA
E11_psVAO_T7_promo... ----------------------------------------
F11_psVAO_T7_termi... GGAAAGTCTGGTGTTTGGCCGAGTCAATACAGTCATGTTA

.....................................................................

                      1801                                      1840
PsVAO                 CTTGGAAACTGTAA--------------------------
E11_psVAO_T7_promo... ----------------------------------------
F11_psVAO_T7_termi... CTTGGAAACTGTAAAAGCTTGCGGCCGCACTCGAGCACCA

.....................................................................

                      1841                                      1880
PsVAO                 ----------------------------------------
E11_psVAO_T7_promo... ----------------------------------------
F11_psVAO_T7_termi... CCACCACCACCACTGAGATCCGGCTGCTAACAAAGCCCGA

.....................................................................

                      1881           1899
PsVAO                 -------------------
E11_psVAO_T7_promo... -------------------
F11_psVAO_T7_termi... AAGAAGCKKWGKKYCCCGA
```